Phenotypic characterization of Urocortin 3 in the paraventricular nucleus of the hypothalamus

Christine van Hover

Annapolis, MD

Bachelor of Science, University of Maryland 2009

A Dissertation presented to the Graduate Faculty of the University of Virginia in Candidacy for the Degree of Doctor of Philosophy

Neuroscience Graduate Program

University of Virginia

May 2015

Chien Li, PhD (Dissertation advisor)

Ignacio Provencio, PhD (Executive committee member)

Patrice Guyenet, PhD

Edward Perez-Reyes, PhD

Craig Nunemaker, PhD

Abstract

Regulation of food intake and energy expenditure is crucial to maintain a stable body weight. Excessive energy intake combined with inadequate energy expenditure leads to obesity, which is co-morbid with many devastating diseases such as cancer, cardiovascular diseases, and infertility. The hypothalamus plays a pivotal role in the regulation of energy balance. It integrates signals from both the external environment and internal milieu to modulate feeding and energy expenditure to maintain energy homeostasis. Neuropeptides are critical molecular mediators underlying many important energy homeostatic functions of the hypothalamus. Thus, a detailed knowledge of the role of hypothalamic peptides and their receptors in controlling feeding, metabolism, and energy expenditure is essential to understand the causes of obesity and related metabolic disorders. Urocortin 3 (Ucn 3) is a member of the corticotropin-releasing factor (CRF) family of peptides. The CRF family plays a critical role in coordinating aspects of the stress response including stimulation of the hypothalamic-pituitary-adrenal axis, behavioral arousal, and energy adaptation through suppression of feeding and promotion of energy mobilization. Centrally-injected Ucn 3 suppresses feeding, elevates blood glucose concentration and body temperature, and stimulates the hypothalamic-pituitary-adrenal axis, indicating that central Ucn 3 may be involved in regulating energy homeostasis and the stress response. Cell bodies of neurons expressing Ucn 3 are located in the hypothalamus and medial amygdala. Direct injection of Ucn 3 into the ventromedial hypothalamus (VMH) has been shown to potently suppress feeding and rapidly elevate blood glucose levels. Anatomical studies revealed that Ucn 3 neurons in the anterior parvicellular part of the paraventricular nucleus of the hypothalamus

(PVHap) provide the major Ucn 3 afferent input into the VMH, therefore it is conceivable that the Ucn 3 PVHap-VMH pathway may play a critical role in modulating energy homeostasis in response to stress. Currently, little is known about the Ucn 3 neurons in the PVHap. In my thesis studies, I combined functional and anatomical approaches to characterize these neurons in great detail. I first showed that acute stress rapidly stimulates Ucn 3 expression in the PVHap. A functional neuroanatomical tracing study identified a number of brain areas that provide stress-activated input into the PVHap area. In the forebrain, the bed nucleus of the stria terminalis, lateral septal nucleus, the medial amygdala, and a number of nuclei in the hypothalamus including the VMH, the arcuate nucleus, the posterior nucleus, and the ventral premammillary nucleus provide stress-activated input into the PVHap. In the brainstem, stress-sensitive input originates from the periaqueductal gray, the nucleus of the solitary tract, and the ventrolateral medulla. These areas are potentially important in mediating the stress-induced activation of Ucn 3 neurons in the PVHap. I then determined that Ucn 3 neurons in the PVHap do not express oxytocin, CRF, or vasopressin, major neuropeptides expressed in the PVH that have been shown to play an important role in regulating energy balance. A conditional viral tracing study then confirmed that Ucn 3 neurons in the PVHap project prominently to the VMH, an area important for feeding and sympathetic outflow. I also determined that the PVHap Ucn 3 cells project to the external zone of the median eminence where neuropeptides are released from nerve terminals into the portal blood system to influence release of hormones from the pituitary gland, raising the possibility that PVHap Ucn 3 cells may be involved in neuroendocrine regulation of pituitary function. Finally, I attempted to test the hypothesis that enhanced Ucn 3 input

into the VMH from the PVHap can recapitulate energy adaptation induced by stress. I found that enhanced Ucn 3 expression in the PVHap resulted in suppression of basal feeding and elevation of circulating glycerol, indicative of enhanced lipolysis. In conclusion, these studies thoroughly characterized Ucn 3 neurons in the PVHap and provide significant insight into the hypothalamic Ucn 3 neurocircuit in regulating stress-associated energy adaptation.

Dedications

The following studies would not be possible without the help and support of a large group of wonderful people. My mentor, Dr. Chien Li, has patiently taught me everything from the location of the hypothalamus in a fresh mouse brain, to connecting a computer network printer, to pulling the ideal micrometer diameter of a glass pipette for central microinjections. He has always been available and supportive and the following studies would simply not exist if not for him. If it takes a village to raise a child, then it takes a lab to create a dissertation, and the invaluable help of Dr. Peilin Chen and an army of intelligent and vibrant undergrads, among them Alex Fletcher-Jones, Adrienne Doebrich, and Catherine Jones has been essential for my work.

My committee members have helped me well above and beyond the call of committee duty. Dr. Iggy Provencio, official committee head honcho since qualifying exam days, always improves my work with excellent suggestions. Dr. Ed Perez-Reyes has spent many hours answering my very basic questions and demonstrating techniques of incredibly complex virus creation. The Urocortin 3 overexpression virus was his brilliant idea and creation and its use would not be possible without him. Dr. Patrice Guyenet not only provides excellent edits, he generously lent his lab equipment and kind postdoc, Dr. Stephen Abbott, for a number of Urocortin 3 experiments. Dr. Craig Nunemaker has counseled me on careers and provided a much-needed perspective on jobs from a successful academia position.

Thank you to Nadia Badr Cempre and Tracy Mourton for patiently guiding through every step of the neuroscience graduate program and answering the most basic and obvious questions without once giving up on me.

On a more personal note, I would like to thank my wonderful family for their love and support. Our chaotic gatherings are always a lovely respite from the intellectual coolness of academia. Christoph Koch has also provided immense emotional and personal support and his gently baffled smile during my seminar on anatomical inputs to the paraventricular nucleus will always warm the cockles of my heart. Thank you to my wonderful friends, among them Dr. Chazz Domingo, Mary Butcher, Kayla Quinnies, and Emily Andre, for providing stress relief and extremely high brow, intellectual discourse. And I would not be moderately sane if it were not for my garden and tendency to run around in 10 mile circles in the snow.

To all of you, thank you for your invaluable help and support. The following work would not exist if not for you, and I am immeasurably grateful to everyone and forever appreciative.

Table of Contents

List of figures

1. Introduction: Central regulation of energy balance

Obesity: a disorder of dysregulated energy balance

Body weight is the product of a delicate balance between caloric intake and energy expenditure, and the current obesity crisis results from an energy imbalance favoring calorie consumption. More than a third (35%) of American adults are considered obese today, a staggering increase from 23% in 1988 (Flegal et al., 2012). Obesity is correlated with myriad health risks, including cardiovascular and reproductive disorders, diabetes, and cancer (Padula et al., 2014), and children today could have shorter life spans than their parents if the obesity epidemic continues unchecked (Olshansky et al., 2005). The most effective treatment, diet and exercise, is frustrating, prone to relapse, and nearly impossible for many obese patients. Currently only limited drugs are available for treating obesity, and many of them have serious side effects (Bray, 2014). Thus, it is essential to understand the underlying mechanism behind energy regulation to work towards a more effective treatment.

Hypothalamic control of energy balance

The brain plays a critical role in regulating energy balance, controlling everything from the reward and emotional value of food to the motor output of eating. Signals from the periphery containing information about recent meals and activity are relayed to the brain, balanced with reward cues and environment, and a decision is formed about eating (Schwartz et al., 2000). Integration of reward valuation, environmental cues, and emotion

is essential to determining behavior (Schwartz et al., 2000). Calorie intake from meal to meal or day to day is variable, but overall energy balance is remarkably stable in the long term, which is what enables people to stay generally the same weight over time (Schwartz et al., 2000).

The hypothalamus is a key brain area in energy regulation, detecting chemical signals passed through the blood and then integrating neuronal signals about levels of energy in the body to regulate feeding and energy expenditure. Both clinical and animal studies have demonstrated that dysregulated neuronal function in the hypothalamus can cause over-eating, decreased energy expenditure, and, consequently, obesity (Bray, 2014; Zigman, 2003).

Basic hypothalamic anatomy was characterized in the early part of the 20th century (Griffiths, 1939). The hypothalamus is a small structure on the ventral portion of the brain below the thalamus and above the pituitary, which it connects to and controls. The hypothalamus is remarkably richly vascularized, positioned atop and around the third ventricle, and privy to a leaky blood-brain barrier (Griffiths, 1939). There are many small specialized nuclei clustered around the third ventricle that make up the hypothalamus (Griffiths, 1939). The combination of blood-brain barrier leakiness, extensive vascularization, and proximity to the third ventricle position the hypothalamus to sense peripheral signals including hormones and nutrients that convey information about the visceral environment (Griffiths, 1939).

The different hypothalamic nuclei are often broadly characterized as centers for hunger or satiety. When individually stimulated, two satiety centers, the paraventricular

nucleus of the hypothalamus (PVH) and ventromedial hypothalamus (VMH), sharply suppress feeding while lesions result in extreme hyperphagia (Scallet and Olney, 1986). Conversely, the lateral hypothalamus (LH) results in insatiable feeding when stimulated, and starvation due to lack of interest in food when ablated (Zigman, 2003). Extensive studies have shown that the arcuate nucleus of the hypothalamus (ARH), residing ventral of the VMH near the median eminence, is another critical area in integrating peripheral signals to modulate feeding and energy homeostasis (Sobrino Crespo et al., 2014). Each of these hypothalamic nuclei expresses a number of neurosubstrates including neuropeptides; these peptides play a crucial role as molecular mediators in regulating energy homeostasis.

Hypothalamic brain areas and neural substrates in the regulation of energy balance

Arcuate nucleus

The arcuate nucleus of the hypothalamus (ARH) is an established regulator of energy homeostasis. Privy to a particularly leaky blood brain barrier, the ARH serves as a converging point for peripheral and central signals concerning peripheral energy status (Magoul et al., 1994; Sasaki and Kitamura, 2010). After integrating various peripheral inputs (discussed in the "Peripheral signals" section below) the ARH signals multiple downstream targets including the PVH, LH, and VMH to modulate energy homeostasis (Bagnol et al., 1999; Balthasar et al., 2005; Chen et al., 2011).

There are two primary populations of neurons in the ARH that are critical in regulating energy homeostasis: those that are agouti-related peptide

(AgRP)/Neuropeptide Y (NPY)-expressing and those that are proopiomelanocortin (POMC)/cocaine-and amphetamine-regulated transcript (CART)-expressing (Sobrino Crespo et al., 2014). They have oppositional effects on feeding and are often regulated in a differential manner by peripheral signals. In general, the NPY/AgRP neurons are orexigenic, are downregulated by signals that decrease feeding (e.g. leptin and insulin), and are upregulated by food deprivation and signals such as ghrelin that increase feeding (Cupples, 2003; Flores et al., 2006; Zigman, 2003). Conversely, the POMC/CART neurons are anorexigenic, upregulated by anorexigenic signals, and downregulated by orexigenic signals (Flores et al., 2006; Sobrino Crespo et al., 2014; Zigman, 2003).

NPY acts on five G protein-coupled receptors, Y1, Y2, Y4, Y5, and Y6; Y5 is expressed in the LH and known to mediate the feeding effects of NPY (Sobrino Crespo et al., 2014). AgRP is a powerful feeding activator, stimulating hyperphagia for up to seven days after intracerebroventricular (ICV) infusion (Cupples, 2003; Sobrino Crespo et al., 2014). AgRP has been shown to function rather unusually, as it is a natural antagonist on the melanocortin receptors MC3R and MC4R and prevents these receptors from becoming activated by melanocortins (Sobrino Crespo et al., 2014). In POMC/CART neurons, POMC is cleaved to produce the melanocortins, which activate the melanocortin receptors MC1R, MC2R, MC3R, MC4R, and MC5R (Millington, 2007). The effect of central melanocortin peptide on energy homeostasis is mainly mediated by MC3R and MC4R (Millington, 2007). The receptor for CART is not yet known (Lin et al., 2011b). Restraint stress and overfeeding increase while food deprivation decreases the expression of POMC (Cupples, 2003; Millington, 2007; Zigman, 2003). It has also been shown that NPY/AgRP neurons directly inhibit POMC/CART neurons through a local circuit,

mirroring the general dichotomy of these two neuron populations in their regulation of food intake (Zigman, 2003).

Paraventricular nucleus

The PVH modulates an array of physiological functions, including autonomic regulation, reproduction, growth, fluid balance, the stress response, and food intake (Ferguson et al., 2008; Herman et al., 2008). There are two broad divisions of the PVH: the magnocellular and parvicellular parts. The magnocellular division contains mainly oxytocin (OXT)- and vasopressin (AVP)-positive neurons that project to the posterior pituitary, while the parvicellular neurons synthesize and release a number of neuropeptides including corticotrophin releasing factor (CRF), thyrotropin-releasing hormone (TRH), and Urocortin 3 (Ucn 3) that project to several brain areas including the spinal cord and median eminence (ME). The PVH also contains GABAergic interneurons that inhibit CRF and AVP both tonically and during the stress response as a feedback mechanism to suppress the stress response (Ferguson et al., 2008; Kovacs et al., 2004). When stimulated, the PVH suppresses food intake, while animals with PVH lesions are hyperphagic and become extremely obese.

OXT and its receptor OXTR are most famous for their roles in milk ejection, social bonding, and maternal behaviors, but OXT neurons in the PVH have also been implicated in feeding suppression (Atasoy et al., 2012; Ferguson et al., 2008; Katsurada et al., 2014; Neumann and Landgraf, 2012; Sarnyai and Kovács, 2014). Atasoy and colleagues elegantly used specific optogenetic manipulation to show that ARH AgRP neurons project to OXT neurons and inhibit their activity (Atasoy et al., 2012). These OXT neurons are a specific population that project to the hindbrain and spinal cord and,

importantly, their inhibition is necessary for feeding induced by AgRP (Atasoy et al., 2012). OXT in the PVH has also been linked to food aversion (Cupples, 2003). Prader-Willi syndrome, a disease that causes loss of OXT in humans, results in obesity (Atasoy et al., 2012).

Like OXT, to which it is closely related, AVP is involved in social behavior, anxiety, and food intake regulation (Langhans et al., 1991; McGregor et al., 2008; Neumann and Landgraf, 2012). The receptors for AVP, AVPR1A, AVPR1B, and AVPR2, share 85% homology with OXT receptors, though AVP and OXT appear to have the opposite effect on many social and anxiety behaviors (McGregor et al., 2008). However, like OXT, AVP also inhibits food intake and is linked to food aversion (Cupples, 2003; Langhans et al., 1991). The anorexigenic peptide CART, found primarily in the ARH, is co-expressed with AVP neurons in the PVH (Sobrino Crespo et al., 2014).

There are two neuron populations of TRH in the PVH, those in the PVH proper that project to the median eminence and those in the PVHap and adjacent perifornical area that project to forebrain areas (Wittmann et al., 2009a; Wittmann et al., 2009b). Both populations in the PVH receive innervations from ARH NPY/AgRP and POMC/CART neurons (Xi et al., 2012). ICV-injected TRH, stimulating the TRH receptors TRH-R1 and TRH-R2, decreases food intake and induces hyperglycemia (Wittmann et al., 2009b). The median eminence-projecting population of TRH regulates the hypothalamic-pituitary-thyroid axis and controls thyroid hormone secretion (Wittmann et al., 2009a). The precise physiological function of the PVHap population is not known, although it has been implicated in thermogenesis and some TRH-containing cells in the PVHap have been shown to co-express Ucn 3 (Wittmann et al., 2009a; Xi et al., 2012).

CRF is best known for its role in the stress response. It governs the hypothalamic-pituitary-adrenal axis activity, resulting in release of glucocorticoids from the adrenal glands and inducing hypophagia in response to stress (Pelleymounter et al., 2000). CRF in the PVH has also been implicated in learning and memory, suggesting that CRF has broad central actions (Lucas et al., 2013). CRF and its neuropeptide family are discussed in more detail in the "Stress and energy balance" section below.

Ventromedial hypothalamus

The VMH, located immediately above the ARH near the third ventricle, is another nucleus involved in regulation of food intake, as well as aggression, blood glucose levels, and sexual behavior (Chen et al., 2010; Flanagan-Cato, 2011; Lin et al., 2011a). The VMH consists of two major parts, the ventrolateral and dorsomedial portions. Lesions targeting the VMH increase meal frequency and size and result in spectacular levels of obesity (King, 2006; Scallet and Olney, 1986). For a few days after VMH lesions in rats, daily food intake can double and body weight increase by 10 grams per day, eventually leveling out to up to triple the original body weight (King, 2006). This new body weight is resistant to change, raising the possibility that the VMH controls the body weight set-point (King, 2006). Interestingly, though the animals are hyperphagic, they are not willing to work very hard for food, suggesting that motivation for food is probably not controlled by the VMH (King, 2006).

In contrast to the other hypothalamic nuclei, specific peptides that influence food intake in the VMH are not very well defined. POMC and AgRP neurons project from the ARH to the VMH, which expresses low levels of MC3R and MC4R receptors; AgRP inhibits VMH neuron activity in overweight but not normal rats (King, 2006; Kishi et al.,

2003). Steroidogenic factor-1 (SF-1)-expressing neurons in the dorsomedial VMH may be responsible for much of the VMH-controlled energy regulation. Deletion of SF-1 in the VMH causes massive obesity through hyperphagia and reduced energy expenditure (Klockener et al., 2011; Lindberg et al., 2013). These SF-1 neurons express a number of receptors for peripheral signals including leptin and insulin (Klockener et al., 2011; Lindberg et al., 2013). Knockdown of insulin receptors on SF-1 neurons protects mice from high fat diet-induced leptin resistance, weight gain, adiposity, and impaired glucose tolerance (Klockener et al., 2011). Conversely, knockout of the leptin receptor in VMH SF-1 cells increases adiposity and metabolic syndrome symptoms, indicating that leptin works in the VMH to suppress food intake (Bingham et al., 2008; Dhillon et al., 2006). SF-1 neurons project to many established feeding centers including the ARH and PVH, as well as to autonomic centers in the brainstem (Lindberg et al., 2013).

Lateral hypothalamus

The LH has long been regarded as a hunger center in the brain. When electrically stimulated, the LH causes voracious eating while ablation of the area results in emaciation and aphagia (Jennings et al., 2015). Interestingly, the LH appears to be evolutionarily conserved in species ranging from lizards to humans (Jennings et al., 2015). The LH is downstream of the ARH, receiving inputs from leptin-sensitive POMC/CART and NPY/AgRP neurons (Zigman, 2003). In the LH, there are three primary neuron populations: those that express orexin, melanin-concentrating hormone (MCH), or GABA (Jennings et al., 2015; Sobrino Crespo et al., 2014; Zigman, 2003).

Orexin regulates a wide range of functions including metabolic rate, blood glucose concentration, food intake, and wakefulness through its receptors OXR1 and

OXR2 (Shiuchi et al., 2009). OXR1 is expressed on NPY neurons in the ARH and on neurons in the VMH, while OXR2 is found in the PVH (Shiuchi et al., 2009; Sobrino Crespo et al., 2014). Fasting decreases levels of orexin mRNA and, when administered ICV, orexin increases feeding (Zigman, 2003), aligning with the idea of the LH as a hunger center. MCH also appears to be an orexigenic peptide, as, similarly to orexin, ICV MCH stimulates feeding and mRNA levels are increased during fasting (Sobrino Crespo et al., 2014; Zigman, 2003). There are two receptors for MCH, MCH1R and MCH2R (Saito and Maruyama, 2006). MCH1R is found in the nucleus accumbens, an area known for reward behavior, and may be involved in feeding motivation (Sobrino Crespo et al., 2014). Both MCH and MCH1R knockout mice eat less than wildtype controls and are lean (Saito and Maruyama, 2006). Interestingly, GABA neurons in the LH have recently been found to be important regulators of both food intake and motivation for food (Jennings et al., 2015). There appear to be two populations of GABA neurons in the LH, one that controls consummatory behavior and one that modulates appetitive behavior (Jennings et al., 2015).

Peripheral signals that regulate food intake

The various neuronal systems in the hypothalamus are tightly regulated by peripheral signals that fluctuate according to energy status. The peripheral signals can be hormones or nutrients and from a variety of sources including the digestive tract, pancreas, and adipose tissue. Interestingly, there is only one peripheral signal, ghrelin, known to increase hunger while the rest suppress appetite (Sobrino Crespo et al., 2014). The anorexigenic signals such as leptin and insulin are upregulated after a meal whereas

ghrelin levels increase when energy stores are low. Below is a discussion of a number of peripheral signals involved in energy balance.

Leptin

Leptin is a satiety hormone released by adipocytes that strongly inhibits food intake (Gardner et al., 1998; Sobrino Crespo et al., 2014). Its levels are directly correlated with adipose tissue mass, which releases leptin in a pulsatile manner into the blood stream and through the blood brain barrier (Gardner et al., 1998; Sobrino Crespo et al., 2014). The leptin receptor, LEPR (also known as OB-R) has six isoforms, LEPRa-f (Peelman et al., 2014). LEPRb has been shown to be the major functional receptor mediating the effects of leptin in neurons (Peelman et al., 2014). Stimulation of LEPRb by leptin activates the janus-kinase signal transducer and activator or transcription-3 (STAT-3) signaling pathway in target cells (Peelman et al., 2014). LEPRb is expressed in the ARH, VMH, dorsomedial hypothalamus, and LH, where leptin has diverse effects (Elmquist et al., 1998; Ghamari-Langroudi et al., 2011; Zigman, 2003). In the ARH, leptin inhibits the orexigenic NPY/AgRP neurons by decreasing mRNA levels and hyperpolarizing the neurons while it stimulates the anorexigenic POMC/CART neurons by increasing mRNA levels and depolarizing the neurons (Zigman, 2003). In the PVH, CRF neurons express leptin receptors and leptin increases CRF mRNA (Gardner et al., 1998; Nishiyama et al., 1999). Conversely, antagonizing CRF receptors decreases the inhibitory effect of leptin on feeding (Gardner et al., 1998; Nishiyama et al., 1999). In the VMH, there are leptin receptors on SF-1 neurons, deletion of which results in obesity (Ghamari-Langroudi et al., 2011; Huang et al., 2006; Klockener et al., 2011). Leptin

administration also increases the expression of the type 2 CRF receptor (CRF_2) in the VMH (Ghamari-Langroudi et al., 2011; Huang et al., 2006; Klockener et al., 2011).

As leptin strongly inhibits food intake, it is a seemingly obvious treatment for obesity. Unfortunately, obese animals and people with their high levels of circulating leptin released from generous adipocyte stores develop leptin resistance and it loses its ability to inhibit food intake (Cupples, 2003; Sobrino Crespo et al., 2014; Zigman, 2003). Perhaps even more unfortunate is what happens after hard earned weight loss: leptin is less effective at decreasing food intake, and the decrease of circulating leptin from reduced fat stores after caloric restriction sharply increases appetite and decreases energy expenditure—exactly what one tries to avoid during a diet and exercise regimen (Zigman, 2003). When food was less easily available, leptin resistance was beneficial. High fat diet-induced leptin resistance happens soon after diet change and before body composition change so the animal or human can bulk up fat stores to use during leaner times (Cupples, 2003; Zigman, 2003). However, in the current environment of plentiful calories, leptin resistance is quite harmful. Leptin sensitivity on a normal diet predicts obesity later; an animal that has a naturally lower sensitivity to leptin will become more obese on a high fat diet, perhaps explaining the variability of weights seen on the western diet (Cupples, 2003). While leptin resistance is a problem in today's worldwide food buffet, it's not all bad news: exercise increases sensitivity to leptin (Flores et al., 2006).

Ghrelin

Ghrelin is the opposite of leptin in many ways, primarily in that it increases food intake. It is released from the stomach and circulated through the blood (Sobrino Crespo et al., 2014). Ghrelin levels are directly correlated to satiety state, with a daily rhythm of

rising before a meal and decreasing afterwards (King, 2006; Sobrino Crespo et al., 2014; Zigman, 2003). When injected peripherally, ghrelin increases feeding, motivation to obtain a palatable reward, and gastric motility (Gong et al., 2013; Sobrino Crespo et al., 2014; Tabarin et al., 2007). The receptor for ghrelin is the growth hormone secretagogue receptor (GHS-R), stimulation of which increases adiposity and decreases utilization of fat as fuel (King, 2006). Ghrelin works primarily through the ARH, NTS, ventral tegmental area, and lateral septum (Gong et al., 2013; Sobrino Crespo et al., 2014). In contrast to leptin, ghrelin stimulates the orexigenic NPY/AgRP neurons and inhibits anorexigenic POMC neurons in the ARH (Sobrino Crespo et al., 2014; Zigman, 2003). In the ventral tegmental area, ghrelin works to increase preference for and motivation to obtain highly palatable food (King, 2006). The NTS mediates some of ghrelin's orexigenic effects, while the LS appears to be involved in ghrelin-stimulated gastric motility (Gong et al., 2013; King, 2006).

As with leptin, ghrelin levels vary in different body weights: low body weight humans have high ghrelin levels after fasting while high body weight humans have lower ghrelin levels after fasting (Zigman, 2003). Like leptin, ghrelin levels are altered after formerly obese people's weight loss as compared to people who were never overweight—plasma ghrelin levels are higher after weight loss, and might be a reason for the very common rebound in weight gain after dieting (Zigman, 2003). Fascinatingly, gastric bypass surgery decreases ghrelin levels even before weight loss occurs (Zigman, 2003), being perhaps another mechanism for surgery-induced weight loss in addition to the physically smaller stomach.

Insulin

The peripheral effects of insulin in regulating glucose levels are well known, but insulin also acts in the brain to decrease food intake. Insulin is released from the pancreas and transported through the blood brain barrier to act in the hypothalamus (Sobrino Crespo et al., 2014). It acts at largely the same brain areas as leptin to decrease feeding, decreasing NPY expression and inhibiting NPY/AgRP neuron activity while increasing POMC expression and stimulating POMC/CART neurons in the ARH (Flores et al., 2006). The receptors for insulin are IRS-1 and IRS-2, which are found on the POMC/CART and NPY/AgRP neurons in the ARH and on SF-1 neurons in the VMH, many of which are also sensitive to glucose (Flores et al., 2006; Klockener et al., 2011). Central insulin acts in a synergy with CRF, as it increases the feeding inhibition effect of CRF when co-injected (Cupples, 2003). As with leptin, exercise increases insulin's ability to decrease food intake (Flores et al., 2006).

Glucose

Glucose is a circulating nutrient used as energy by muscles and the brain that is also able to regulate energy homeostasis as an indicator of peripheral energy status. ICV injections of glucose cause satiety, in part by increasing levels of anorexigenic POMC and CART peptides and decreasing levels of orexigenic NPY and AgRP peptides in the ARH (Cha et al., 2008). Glucose diffuses through the blood brain barrier and is taken up by neurons expressing the Glut2 glucose transporter (King, 2006; Verberne et al., 2014). These glucose-sensing neurons, located in the LH, ARH, and VMH, are either depolarized (glucose-excited) or hyperpolarized (glucose-inhibited) by glucose (Verberne et al., 2014). An estimated 25-45% of neurons in the VMH alone are glucose-sensitive,

hinting at a very involved role in energy regulation (King, 2006). Interestingly, fructose, though similar to glucose, has the opposite effect on feeding by increasing hunger and lowering POMC mRNA (Cha et al., 2008). The western diet is saturated with high-fructose corn syrup which may wreak havoc on the hypothalamic regulation of feeding.

GLP-1

GLP-1 is an anorexigenic peptide that is released from the gut into circulation in response to nutrients (Sobrino Crespo et al., 2014). GLP-1 is also synthesized by a small population of neurons in the central nucleus of the solitary tract in the brainstem, which express the leptin receptor and project to the PVH (Maniscalco et al., 2013). GLP-1 reduces food intake in humans and rodents, slows gastric emptying, and stimulates insulin secretion under hyperglycemic conditions (Sobrino Crespo et al., 2014). The receptor for GLP-1, GLP-1R, is expressed in the PVH, on CRF-positive neurons, in the ARH, and in the VMH (King, 2006; Maniscalco et al., 2013; Sobrino Crespo et al., 2014).

Stress and energy balance

Stress was first defined in 1936 by Hans Selye as a general adaptation syndrome when he noticed that a variety of noxious stimuli elicited a similar physical response across many individuals (Selye, 1936; Selye, 1950). He observed that patients with diverse diseases had a similar air of “being sick”, and that rats exposed to different demanding situations (restraint, cold immersion, etc) had similar physical symptoms (Selye, 1936). The response was termed the “stress response”, the stimuli as “stressors”,

and the interaction between a stimuli and response as “stress” (Selye, 1950). Restraint, open field tests, conditioned fear, loud sounds, cold exposure, water avoidance, inescapable tail or foot shocks, and social defeat are all stressors used in stress research (Taché and Brunnhuber, 2008).

Stress as a defined biological concept did not exist before these seminal papers, and since then, a picture of the neurosubstrates and physical characteristics involved in the stress response has emerged. Selye defined three stress stages: the alarm reaction, the stage of resistance, and the stage of exhaustion (Selye, 1936; Selye, 1950; Selye, 1976). Up to 48 hours after stressor exposure is the alarm stage, in which the thymus, spleen, lymph glands, liver, and fat tissue shrink, body temperature and blood glucose rises, and digestive tract erosions appear (Selye, 1936; Selye, 1950). If the stress continues for weeks, apparent normality returns in the resistance stage with organs regaining normal appearance and function (Selye, 1936). However, exhaustion sets in after the resistance stage, with similar symptoms as the alarm stage (Selye, 1936). Currently, the alarm stage is referred to as acute stress, while the exhaustion stage is chronic stress. Both acute and chronic stress affect energy balance. Consistent with the idea of readying the organism for a stressor-induced immediate reaction, acute stress suppresses feeding, elevates blood glucose, and increases body temperature (Taché and Brunnhuber, 2008). Chronic stress prevents normal weight gain in rodents even after feeding returns to nearly normal levels (Jeong et al., 2013).

Though colloquial use of “stress” has a negative connotation, the stress response is essential to survival by enabling an organism to respond to demanding circumstances (“fright, flight, or fight”) (de Kloet, 2013). Some stress is healthy, called “eustress” vs.

the unhealthy, bad “distress”. The deleterious effects of stress are seen when the stress response is prolonged or inappropriate for the circumstances (Selye, 1976). Indeed, in humans, short term stress can be an immune system booster while chronic stress results in depressed immune function, poor sleep, and bad mood (Auvinen et al., 2011; NIMH, 2015). Even believing in the detrimental effects of stress paired with high self-reported stress levels leads to higher mortality (Keller et al., 2012).

In response to stress, hypothalamic-pituitary-adrenal (HPA) axis activity is greatly elevated. In the hypothalamus, CRF is co-released with AVP from the PVH into the portal blood system through the median eminence (de Kloet, 2013). CRF acts on the type 1 CRF receptor (CRF_1) in anterior pituitary corticotrophs to stimulate the release of adrenocorticotropic hormone (ACTH) (de Kloet, 2013). While ACTH secretion is increased during the stress response, secretion of other pituitary hormones is suppressed, including that of follicle-stimulating hormone, luteinizing hormone, prolactin, and thyrotropin (Selye, 1950). Released, circulating ACTH reaches the adrenal gland and acts on melanocortin receptor type 2 in the adrenal cortex to release the glucocorticoids (cortisol and corticosterone), which act on the glucocorticoid receptor to modulate an array of physiological functions including elevation of blood glucose levels, suppression of the immune response, and mobilization of energy from the liver and fat stores (de Kloet, 2013; Szabo et al., 2012). ACTH and stimulation of the sympathetic nervous system also result in catecholamine secretion from the adrenal medulla, which mediates a number of physiological regulations including stress-induced behavioral alertness and arousal (Selye, 1950). Glucocorticoids then act at the level of both the pituitary and brain to decrease the expression and release of CRF and ACTH as a negative feedback

mechanism (de Kloet, 2013). It has been shown that chronic stress can override this negative feedback loop to produce a constant state of arousal that results in metabolic syndrome and physical exhaustion (de Kloet, 2013).

CRF

In a satisfyingly linear manner, Selye identified the stress response, then his student Roger Guillemin proved the existence of a corticotrophin releasing factor, and then Guillemin's student Wylie Vale identified the chemical structure, other family members, and receptors of CRF (Taché and Brunnhuber, 2008). Using only 495,000 sheep hypothalami, Guillemin and Vale isolated and characterized CRF (Vale et al., 1981). The type 1 and type 2 CRF receptors (CRF_1 and CRF_2) were subsequently identified (Chen et al., 1993; Lovenberg et al., 1995). Importantly, it was found that CRF has only modest affinity for CRF_2, suggesting the existence of additional, not yet identified ligands for CRF_2 (Bale and Vale, 2004; de Kloet, 2013; Hsu and Hsueh, 2001; Lewis et al., 2001). This notion led to the identification of the Urocortin (Ucn) peptides 1, 2, and 3 (de Kloet, 2013; Hsu and Hsueh, 2001; Lewis et al., 2001; Reyes et al., 2001; Vaughan et al., 1995). Ucn 1 has equal affinities for CRF_1 and CRF_2, while Ucn 2 and 3 are more selective for CRF_2 (Chalmers et al., 1995; Hsu and Hsueh, 2001; Lewis et al., 2001; Van Pett et al., 2000). Ucn 2 binds and stimulates CRF_1 at high concentrations, but Ucn 3 is very selective to CRF_2 while displaying minimal affinity to CRF_1 (Hsu and Hsueh, 2001; Lewis et al., 2001). Orthologs and homologs of CRF and Ucns are found throughout the animal kingdom including invertebrate species, indicating that these peptides are highly conserved and important for survival (Stengel and Taché, 2014). The central actions of Ucn peptides may account for some stress-related effects originally

attributed to CRF (Bale and Vale, 2004; Hashimoto et al., 2004; Jamieson et al., 2006; Kuperman et al., 2010; Venihaki et al., 2004). For example, Ucn 1 appears to be involved in the later stage of the stress response and adaptation to stress, while Ucns 2 and 3 have been hypothesized to play a role in attenuating the stress response (Ryabinin et al., 2012).

CRF_1 and CRF_2 are G-protein coupled receptors, and amino acid sequence analysis has shown that the two receptors share approximately 70% homology (Bale and Vale, 2004). They signal predominantly through increased intracellular cAMP production, but additional signaling pathways including Ca2+, mitogen activated kinase, phospholipase C, protein kinase B, and ion channels have also been described (Brar et al., 2002; Grammatopoulos, 2000; Kiang, 1997). CRF_1 and CRF_2 have distinct roles and different distributions in the brain. CRF_1 is responsible for the stimulation of release of ACTH and is found in the pituitary, cortex, medial septum, amygdala, and cerebellum (Chalmers et al., 1995; Van Pett et al., 2000). CRF_2 has three variants that differ in their N-terminal domains, $CRF_{2\alpha}$, $CRF_{2\beta}$, and $CRF_{2\gamma}$. Mainly found in the brain, $CRF_{2\alpha}$ is present in the hypothalamus, lateral septum, and choroid plexus (Chalmers et al., 1995; Van Pett et al., 2000). $CRF_{2\beta}$ is found primarily in the periphery, including skeletal muscle, the gastrointestinal tract, and the heart (Kanno, 1999). $CRF_{2\gamma}$ is found only in the human brain (Kostich et al., 1998).

A circulating protein has been identified that binds CRF. It has been suggested that the purpose of this CRF binding protein (CRFBP) is mainly to sequester CRF and reduce its HPA-axis stimulation (Goland, 1986). Levels of CRFBP are elevated in pregnancy to dampen the negative effect of stress responses on the developing fetus (Goland, 1986). In addition to CRFBP, a splice variant of CRF_2 has been identified that

contains only the extracellular domain of the receptor and shown to circulate, bind, and sequester CRF as well (Chen et al., 2005). This splice variant also binds Ucn 1 but has very low affinity for Ucn 2 and 3 (Chen et al., 2005).

Central CRF peptides are involved in regulating energy homeostasis. CRF and the Ucns all decrease food intake, delay gastric emptying, and increase blood glucose levels when centrally injected (Spina et al., 1996; Stengel and Taché, 2014). CRF-induced food intake suppression is immediate and short lasting, while Ucn stimulation shows a delayed onset of food intake suppression (Stengel and Taché, 2014). CRF_2 appears to be responsible for mediating this effect on feeding and energy expenditure. Antagonists of CRF_2, but not CRF_1, eliminate CRF-induced anorexia, and CRF_2 deficient mice are resistant to Ucn peptide-induced anorexia (Coste et al., 2000; Pelleymounter et al., 2000). Moreover, mice with reduced CRF_2 in the ventromedial hypothalamus (VMH) eat more and have increased adiposity in white adipose tissue than control mice (Chao et al., 2012). VMH expression of CRF_2 is downregulated in animals that are obese, diabetic, or food-deprived, and is upregulated in the presence of the satiety signal leptin (Makino et al., 1998; Nishiyama et al., 1999). These observations suggest that the CRF_2 in the VMH potentially plays a critical role in mediating the effect of the CRF family of peptides in energy homeostasis.

Ucn 1

Ucn 1 is a 40 amino acid peptide that shares 45% homology with rat/human CRF, located in highest concentration in or near the Edinger-Westphal nucleus in the brainstem (Pan and Kastin, 2008; Stengel and Taché, 2014). It is also expressed, albeit in low levels, in other brainstem areas (lateral superior olive, facial, hypoglossal, and ambiguual

motor nuclei), the supraoptic nucleus, and caudal lateral hypothalamus (Florio et al., 2004; Pan and Kastin, 2008; Stengel and Taché, 2014). In the periphery, Ucn 1 is found mainly in the heart and reproductive system (Florio et al., 2004; Yang et al., 2010). Though basal levels in the hypothalamus are low, Ucn 1 mRNA is increased by restraint stress (Pan and Kastin, 2008). Behaviorally, Ucn 1 plays a critical role in anxiety-like and depressive behavior, and may be involved in the predisposition of alcohol consumption (Ryabinin et al., 2012; Vetter et al., 2002). Peripheral administration of Ucn 1 decreases cardiac output and heart rate, and may be protective against ischemia (Angeles-Castellanos et al., 2007; Hashimoto et al., 2004; Latchman, 2002). Finally, Ucn 1 and CRF receptors have been found in the auditory system (Graham et al., 2010) and the peptide appears to be involved in the development and maintenance of hearing (Vetter et al., 2002).

Ucn 2

Ucn 2 is a 39 amino acid peptide with 34% homology with rat/human CRF and 42% with rat/human Ucn 1 (Reyes et al., 2001; Stengel and Taché, 2014). It is expressed in POMC-expressing cells in the anterior and intermediate pituitary, a number of hypothalamic nuclei (the PVH, supraoptic nucleus, and ARH), and the locus coeruleus in the brainstem (Kuperman and Chen, 2008; Nemoto et al., 2010). Peripherally, Ucn 2 is found in the adrenal gland, lung, GI tract, and in high concentrations in the skeletal muscle and skin (Kuperman and Chen, 2008). Ucn 2 may modulate glucose utilization and insulin sensitivity in the skeletal muscle (Kuperman and Chen, 2008). Ucn 2 deficiency improves glucose and insulin homeostasis on a normal diet and Ucn 2 mutant mice are protected from high fat diet-induced glucose intolerance and insulin resistance

(Chen et al., 2006; Kuperman and Chen, 2008). Ucn 2 also has psychological effects. Ucn 2 appears to be linked to depression but not anxiety (Ryabinin et al., 2012), and influences social behavior, including aggression (Breu et al., 2012), as mice without Ucn 2 are less aggressive and prefer passive social interaction.

Ucn 3

Ucn 3 is the latest addition of the CRF family of peptides, identified in the brains of humans and rodents (Hsu and Hsueh, 2001; Lewis et al., 2001). Ucn 3 is a 38 amino acid peptide with 26% homology with rat/human CRF and 21% homology with rat/human Ucn 1 (Lewis et al., 2001). Ucn 3 is found both in the periphery and in the brain. In the periphery, it is expressed in the digestive tract, muscle, thyroid and adrenal glands, pancreas, heart, spleen, and skin (Hsu and Hsueh, 2001; Lewis et al., 2001). In the brain, neurons expressing Ucn 3 are concentrated in the medial amygdala (MEA) and hypothalamus (Lewis et al., 2001; Li et al., 2002). In the hypothalamus, the major Ucn 3 cell population is near the rostral perifornical hypothalamic area (Li et al., 2002). Specifically, Ucn 3-positive cells are gathered around the fornix in the rostral perifornical hypothalamus (rPFH) lateral to the paraventricular nucleus of the hypothalamus (PVH). This group extends rostrally and stays close to the fornix into the posterior part of the bed nucleus of the stria terminalis (BSTp) and medially into the anterior parvicellular part of the PVH (PVHap). This hypothalamic Ucn 3 cell population is complex: its rostral part (PVHap/BSTp) projects to the VMH, whereas its caudal part (rPFH) innervates the lateral septum (Chen et al., 2011). A group of Ucn 3-positive cells is also located in the median preoptic nucleus (Li et al., 2002). In the forebrain, Ucn 3 nerve fibers and

terminals are in the VMH, the lateral septum, MEA and BST (Li et al., 2002), and these areas express high levels of CRF_2 (Chalmers et al., 1995; Van Pett et al., 2000).

Ucn 3 levels are influenced by various factors. Leptin increases Ucn 3 mRNA (Yamagata et al., 2013), and acute restraint stress increases Ucn 3 mRNA levels in the MEA and the perifornical hypothalamic area, while hemorrhages and food deprivation decrease MEA mRNA levels (Jamieson et al., 2006). As mentioned above, the Ucn 3 cell population in the rostral perifornical area can be subdivided into two groups (the PVHap/BSTp and the rPFH) based on their anatomical projections. It remains to be determined whether stress differentially regulates Ucn 3 expression in these two different subpopulations.

When directly infused into the lateral ventricles, Ucn 3 decreases nocturnal food intake, when greatest spontaneous food intake naturally occurs, by decreasing meal frequency (Fekete et al., 2006). The effect was eliminated with concomitant CRF_2 antagonist treatment (Fekete et al., 2006). The anorectic effect of Ucn 3 is not due to distaste for food, as no concurrent taste aversion develops (Fekete et al., 2006). Consistent with pharmacological evidence, genetic Ucn 3 deficiency appears to lead to overeating. Though Ucn 3 knockout (KO) mice have similar body weights to WT animals, KO mice eat more and have increased cumulative food intake (Chao et al., 2012). Similar to CRF_2 null mice, Ucn 3 KO mice exhibit elevated nocturnal feeding (Chao et al., 2012). The mechanism of Ucn 3-induced anorexia has not been directly studied, but central administration of CRF_2 agonists, including Ucn 3, have been shown to inhibit gastric emptying (Ohata and Shibasaki, 2011; Stengel and Tache, 2009), and elevate blood glucose levels (Chen et al., 2010; Jamieson et al., 2006). Both decreased

gut motility and hyperglycemia have been shown to induce satiety and reduce feeding (Cha et al., 2008; Koob and Heinrichs, 1999; Scopinho et al., 2008; Wang and Kotz, 2002). Therefore, multiple mechanisms are potentially involved in mediating the anorectic effect of Ucn 3 in the brain.

The specific brain areas responsible for Ucn 3 feeding modulation have been investigated with site specific injection studies. Ucn 3 injection directly into the VMH results in suppression of feeding and elevation of blood glucose, but not stimulation of the HPA axis (Chen et al., 2010; Fekete et al., 2006). When injected into the amygdala or other areas of the hypothalamus, Ucn 3 has no effect on feeding or blood glucose levels (Chen et al., 2010; Fekete et al., 2006). Mice with CRF_2 knockdowns in the VMH gain more weight, mostly white fat, than control mice. They eat more after overnight fasting, similar to Ucn 3 null mice (Chao et al., 2012). As Ucn 3 is the primary CRF_2 ligand sending input to the VMH, these data suggest that the VMH is a critical area mediating the effect of Ucn 3 on feeding and energy modulation. Ucn 3 afferent inputs to the VMH originate primarily from the PVHap, with some from the MEA (Chen et al., 2011). This Ucn 3 PVHap-VMH pathway is potentially positioned to control stress-induced energy modulation. As discussed above, Ucn 3 cells in the rPFH area mainly project to the lateral septum (Chen et al., 2011). Importantly, an earlier report shows that overexpression of Ucn 3 in the rPFH does not modulate food intake (Kuperman et al., 2010), as mice with Ucn 3 overexpression in the rPFH consume a similar amount of food as control mice (Kuperman et al., 2010). The rPFH-specific Ucn 3-overexpressing mice show a trend towards being heavier, but retain the same fat-lean mass percentages as control mice (Kuperman et al., 2010).

Specific aims

Current evidence suggests that central Ucn 3 plays an important role in regulating energy homeostasis by modulating feeding and blood glucose levels, and the VMH has been identified as a downstream target area in mediating the effect of Ucn 3 in the brain. Moreover, Ucn 3, similarly to other CRF family peptides, is stimulated by stress. Thus, it is conceivable that Ucn 3 plays a critical role in mediating stress-induced energy adaptation including suppression of appetite, elevation of blood glucose, and mobilization of energy stores. Ucn 3 neurons in the PVHap provide major Ucn 3 input into the VMH. Currently, it is not known if Ucn 3 cells in the PVHap can be stimulated by stress. Secondly, little is known about PVHap Ucn 3 cells, other than that they project to the VMH (Chen et al., 2011). A better understanding of the anatomical characteristics of these neurons will provide significant insight into the neurocircuit of Ucn 3 in regulating energy homeostasis. Finally, it is critical to determine if enhanced Ucn 3 expression in the PVHap recapitulates energy adaptation induced by stress. In my thesis studies, I propose three specific aims to address these important questions in order to better understand the Ucn 3 neurons in the paraventricular nucleus:

Aim 1. To determine the effect of acute restraint stress on Ucn 3 expression in the rat brain and to examine stress-activated neural input into the PVHap.

Aim 2. To characterize the anatomical architecture and to determine the efferent output of Ucn 3 neurons in the PVH.

Aim 3. To validate a method for studying the functional consequence of heightened Ucn 3 output from the PVHap.

2. Aim 1: Stress-activated afferent inputs into the anterior parvicellular part of the paraventricular nucleus of the hypothalamus: Insights into Urocortin 3 neuron activation

Abstract

Urocortin 3 (Ucn 3) is a member of the corticotropin-releasing factor family, which plays a major role in coordinating stress responses. Ucn 3 neurons in the anterior parvicellular part of the paraventricular nucleus of the hypothalamus (PVHap) provide prominent input into the ventromedial nucleus of the hypothalamus (VMH), a well known satiety center, where Ucn 3 acts to suppress feeding and modulate blood glucose levels. In the present study, we first determined that Ucn 3 expression in the PVHap was stimulated by acute restraint stress. We then performed retrograde tracing with fluorogold (FG) combined with immunohistochemistry for *Fos* as a marker for neuronal activation after restraint stress to determine the stress-activated afferent inputs into the PVHap. Substantial numbers of FG/*Fos* double labeled cells were found in the bed nucleus of the stria terminalis, lateral septal nucleus, the medial amygdala, and a number of nuclei in the hypothalamus including the VMH, the arcuate nucleus, the posterior nucleus, and the ventral premammillary nucleus. In the brainstem, FG/*Fos* positive cells were found in the periaqueductal gray, the nucleus of the solitary tract, and the ventrolateral medulla. In conclusion, the present study showed that acute stress rapidly stimulates Ucn 3 expression in the PVHap and identified specific stress-sensitive brain areas that project to

the PVHap. These areas are potentially important in mediating the stress-induced activation of Ucn 3 neurons in the PVHap.

Introduction

Urocortin 3 (Ucn 3) is a peptide of the corticotropin-releasing factor (CRF) family initially identified in the brains of humans and rodents (Hsu and Hsueh, 2001; Lewis et al., 2001). It has high affinity for the type 2 CRF receptor (CRF_2) and low affinity for the type 1 CRF receptor (Hsu and Hsueh, 2001; Lewis et al., 2001). Ucn 3-expressing neurons are concentrated in the medial amygdala (MEA) and the hypothalamus (Lewis et al., 2001; Li et al., 2002). In the murine hypothalamus, the major Ucn 3 cell population is found near the rostral perifornical area (Li et al., 2002), with Ucn-3 positive somata clustered around the fornix. This cell group then extends rostrally into the anterior parvicellular part of the paraventricular nucleus of the hypothalamus (PVHap) and laterally into the posterior part of the bed nucleus of the stria terminalis (BSTp). In addition to the rostral perifornical area, a small population of Ucn 3-positive cells is located in the median preoptic nucleus (Li et al., 2002). Ucn 3-positive nerve fibers and terminals are found predominantly in the forebrain, including the VMH, the lateral septal nucleus (LS), the MEA, and the bed nucleus of the stria terminalis (BST) (Li et al., 2002). These areas also express high levels of CRF_2 (Chalmers et al., 1995; Van Pett et al., 2000), supporting the notion that Ucn 3 is a CRF_2-selective ligand.

Ucn 3 in the brain is involved in regulating energy homeostasis; central administration of Ucn 3 suppresses feeding, elevates blood glucose levels, and induces hyperthermia (Jamieson et al., 2006; Ohata and Shibasaki, 2004; Telegdy et al., 2006).

Site-specific injection studies revealed that Ucn 3 injection into the VMH results in suppression of feeding and elevation of blood glucose (Chen et al., 2010; Fekete et al., 2006), suggesting that the VMH is a critical brain area for mediating the effect of central Ucn 3 on feeding and energy modulation. Our previous anatomical study showed that the main source of Ucn 3 input into the VMH originates in the PVHap and the adjacent BSTp. The MEA provides moderate Ucn 3 afferent projections (Chen et al., 2011). Ucn 3 cells in the median preoptic nucleus supply negligible input into the nucleus (Chen et al., 2011). Interestingly, Ucn 3 neurons in the rostral perifornical hypothalamus just caudal and lateral to the PVHap area do not project to the VMH; these cells instead send projections to the LS (Chen et al., 2011). This Ucn 3 population in the rostral perifornical area thus appears to be anatomically heterogeneous.

The expression of Ucn 3 in the brain is sensitive to stress and metabolic challenges. In the MEA, acute restraint stress increases Ucn 3 mRNA levels, while hemorrhages and food deprivation decrease Ucn 3 expression (Jamieson et al., 2006). Restraint stress increases Ucn 3 expression in a time dependent manner in the rostral perifornical area as well (Jamieson et al., 2006; Venihaki et al., 2004). As mentioned above, the Ucn 3 cell population in the rostral perifornical area can be sub-divided into two groups (PVHap/BSTp and rostral perifornical hypothalamus) based on their anatomical projections; it remains to be determined whether stress differentially regulates Ucn 3 expression in these two different sub-populations.

In the present study, we first confirmed the earlier report (Jamieson et al., 2006) that restraint stress stimulates Ucn 3 expression in the MEA and further demonstrated that acute restraint stress greatly increases Ucn 3 mRNA levels in the PVHap/BSTp area,

but not in the rostral perifornical hypothalamus. This finding, combined with the PVHap providing prominent Ucn 3 input into the VMH, raised an important question of what brain areas provide stress-activated input into the PVHap. Thus, using retrograde tracing combined with *Fos*, an immediate early gene product as a marker for neuronal activation, we then examined stress-sensitive afferent inputs into the PVHap. Our results show that the PVHap is innervated by a broad range of areas that are activated by stress, revealing an intricate circuitry of input into the PVHap that potentially conveys stress signals to activate Ucn 3 neurons.

Materials and methods

Animals

Adult male Sprague-Dawley rats (Charles River, Wilmington, MA) weighing between 250-300 g were housed in a temperature-controlled room with lights on between 0600-1800 hr. All experimental protocols and procedures were approved by The University of Virginia Animal Use and Care Committee, University of Virginia protocol number 3537.

Stress paradigm

To determine the effect of stress on Ucn 3 gene expression, male rats (6-7 animals per group) were subjected to restraint stress for 30 minutes or 4 hours with a rat restrainer before euthanization. Control animals remained in their home cages. Brains were quickly removed after stress, deep frozen in powdered dry ice, and stored at -80°C until use.

Tracer injection

A separate cohort of rats was anesthetized with isoflurane and placed in a stereotaxic apparatus (David Kopf Instruments). A glass micropipette with a tip diameter of 25-30 μm was filled with a retrograde tracer, FG (2% w/v in physiological saline), and inserted into the PVHap. FG was then injected by iontophoresis with 5 μA current pulsed at 7 second intervals for 10 minutes. The stereotaxic coordinates for the PVHap were: 1.1 mm caudal and 0.2 mm lateral to the bregma, and 7.6 mm ventral to the dura. Ten days after tracer injection, animals were subjected to 30 minutes of restraint stress and were perfused with 4% formaldehyde (pH 9.5) in borate buffer 90 minutes after the onset of the stress paradigm. The brains were removed and sectioned coronally at 25 μm thickness and stored in cryoprotectant at -20°C until use.

In situ hybridization

Frozen rat brains were sectioned (20μm thickness) coronally with a cryostat. *In situ* hybridization for detecting Ucn 3 mRNA was performed as previously reported (Li et al., 2002). Briefly, a Ucn 3 complementary RNA (cRNA) probe was transcribed from a linearized vector containing a full-length rat Ucn 3 sequence and flanking the 30bp untranslated region (total 528 bp) in the presence of the 33 P-labeled UTP (Perkin-Elmer, Oak Brook, IL). Brain sections were treated with a fresh solution containing 0.25% acetic anhydride in 0.1 M triethanolamine (pH 8.0) followed by a rinse in 2X SSC. The sections were then exposed to the cRNA probe overnight at 55°C. After hybridization, the brain sections were washed in increasingly stringent SSC, in RNase, and in 0.1X SSC at 60°C, dehydrated through a graded series of alcohol, and dried. Slides were dipped in NTB emulsion (Kodak, New Haven, CT), exposed for 7 days at 4°C, and developed. Following development, the slides were counterstained with cresyl violet to identify anatomical landmarks. Results were examined on a Nikon light microscope, and images were acquired with a Qimaging digital camera (Biovision) controlled by iVision imaging software.

Immunohistochemistry

For *Fos* immunohistochemistry, brain sections were washed with potassium phosphate-buffered saline (KPBS) and then were incubated in rabbit anti-*Fos* antibody (Santa Cruz, 1:20,000) in KPBS with 0.4% Triton-X 100 for 48 hrs at 4°C. After incubation, the sections were washed and incubated in biotinylated donkey anti-rabbit IgG (Jackson ImmunoResearch, 1:600) for 1 hr at room temperature. They were then incubated for 1 hr at room temperature in an avidin-biotin complex solution (Vectastain

ABC Elite Kit, Vector Laboratories). Nickel enhanced 3,3diaminobenzdine (DAB) reaction was used as a chromogen to visualize *Fos* immunoreactivity. After the color development, brain sections were washed with KPBS and were incubated in rabbit anti-FG antibody (Millipore, 1:15,000) in KPBS with 0.4% Triton-X 100 for 48 hrs at 4°C. The sections were then incubated in biotinylated donkey anti-rabbit IgG for 1 hr at room temperature, followed by a 1 hr incubation in an avidin-biotin complex solution. The FG antibody-peroxidase complex was revealed with a DAB reaction. Brain sections were then mounted onto gelatin-coated slides, dehydrated, and cover slipped with Permount.

Antibody characterization

FG antiserum (Millipore, AB153): The FG antiserum recognized fluorogold (hydroxystilbamidine) and aminostilbamidine with immunohistochemical analyses and has been extensively used to label the retrograde tracer (manufacturer's datasheet). The antiserum labeled cells and processes in FG-injected, but not in non-injected, animals (Chen et al., 2011; Li et al., 1999b).

Fos antibody (Santa Cruz, sc-52): The antibody recognized *Fos* in cell lysates of HEK293T cells transfected with mouse *Fos* cDNA with western blot analysis and in phorbol ester-induced HeLa cells and Hep G2 cells with immunofluorescence (manufacturer's datasheet). The antibody is affinity purified rabbit polyclonal IgG raised against the N-terminus residues 3-16 of the human *Fos* (FSGFNADYEASSSR) (manufacturer's datasheet). The antibody labeled nuclei in neurons in rat brains after stimulation (Hou et al., 2008; Li et al., 1999b).

Data analysis

For *in situ* hybridization, one-in-four series of the coronal brain sections that were processed for the experiments were first anatomically matched across animals using the rat brain atlas of Swanson (1998) to match brain areas. Three parallel coronal sections that evenly contained the rostrocaudal levels of the PVHap were used for quantifying hybridization signal by ImageJ. For the rostral perifornical hypothalamus and MEA, five and seven sections were used, respectively, for quantification. The hybridization signals were quantified as previously described (Li et al., 1999a) using ImageJ image analysis system. Briefly, the system identified silver grains as the brightness of the image under darkfield illumination in a marked area that covered the area of interest in each tissue section. Hybridization signal for each area of interest was obtained by subtracting a background reading taken from nearby brain regions (the striatum for the PVHap and rPFH, and the cortex for the MEA) where no discernible Ucn 3 hybridizing signal was found (Li et al., 2002). Results for each brain area are presented as mean ± SEM. The combined effects of stress and time on Ucn 3 mRNA levels were analyzed using a two-way ANOVA followed by post hoc analysis for between group comparisons, with a significance level set at 0.05.

Results from the FG/*Fos* double label tracing study were examined and captured by a Nikon 80i microscope coupled with a QImaging CCD camera (BioVision, Exton, PA) controlled by iVision software. The images were adjusted to balance brightness and contrast in Photoshop before importing into Canvas (version 8.0) for assembly into plates. An FG immunoreactive neuron was considered to be double labeled if the nucleus of the FG cell had a black nickel-DAB reaction product indicative of *Fos* immunoreactivity. Brain atlas plates by Swanson (1998) were used as templates to plot

the distribution of *Fos*, FG, and double labeled cells in the rat brains. The number of *Fos*, FG, and double labeled cells in the areas of interest in each animal were counted, and the mean number of cells per section for each of the areas was then determined for each animal. Data are presented as mean ± SEM in Table 1.

Results

Effect of restraint stress on Ucn 3 mRNA levels in the PVHap, rostral perifornical hypothalamus, and MEA

Male rats were restraint stressed for 30 minutes or 4 hours to determine the effect of stress on Ucn 3 expression in the perifornical hypothalamic area. As shown in Fig. 2-1, the Ucn 3 mRNA hybridization signal was significantly elevated in the PVHap area and in the adjacent BSTp after 30 minutes of restraint stress compared to non-stressed controls ($p<0.05$); a two-way ANOVA showed significant effects of stress [$F_{(1, 24)}=33.6$, $p<0.001$] and interaction between stress and time [$F_{(1, 24)}=62.4$, $p<0.001$] on Ucn 3 mRNA levels in the PVHap. Conversely, Ucn 3 mRNA signals near the fornix showed no significant differences [$F_{(1, 24)}=0.33$, $p<0.57$] in acute stressed animals compared to that of non-stressed controls (Fig. 2-1). Consistent with an earlier report (Jamieson et al., 2006), a significant effect of stress [$F_{(1, 24)}=4.2$, $p<0.05$] and interaction between stress and time [$F_{(1, 24)}=10.9$, $p<0.05$] were found on Ucn 3 mRNA levels in the MEA. Ucn 3 mRNA hybridization signal was significantly elevated in the MEA of rats subject to 30 min restraint stress ($p<0.05$) (Fig. 2-1). Levels of Ucn 3 mRNA in rats stressed for 4 hrs showed no significant differences as compared to non-stressed animals in the areas examined (Fig. 2-1).

Identification of stress-activated afferent inputs into PVHap

Injection of a retrograde tracer, fluorogold, to identify neurons that project to PVHap

To determine neuronal projections to the PVHap that are activated by acute stress, rats were first injected with a retrograde tracer, fluorogold (FG), into the PVHap, where

Ucn 3 cells are concentrated (Chen et al., 2011; Lewis et al., 2001) (Fig. 2), before being subjected to acute restraint stress. Out of twenty tracer-injected animals, five cases with injection sites centered in the PVHap were included for analysis. Due to the proximity of the target area to other parts of the paraventricular nucleus of the hypothalamus (PVH), there was minor spillover in some of the cases into the periventricular nucleus and the medial parts of the PVH (Fig. 2-2).

PVHap input as identified through FG-positive cells

Neurons that project to the PVHap were identified by brown precipitate in the cell body, marking them as FG-positive. Rostrally, FG-positive cells were found in parts of the prefrontal cortex including the prelimbic and infralimbic cortex, particularly in the deep layers close to corpus callosum (Figs. 2-3 and 2-4, Table 1). Moderate numbers of tracer-labeled neurons were found in the BST (Figs. 2-3 and 2-4, Table 1), particularly the medial part. Compared to other brain areas (Table 1), the LS had a high concentration of FG-labeled cells; abundant FG-positive cells were found in the ventral part of the nucleus, with reduced density toward the rostral division (Figs. 2-4 and 2-5). Scattered FG cells were also found in the caudal parts of the LS (Fig. 2-4). The hypothalamus had a large number of FG-labeled cells (Table 1), including in the VMH (Figs. 2-3 and 2-4), the posterior hypothalamic nucleus (PH, Fig. 2-4), and the ventral premammillary nucleus (Fig. 2-4). Areas of the hypothalamus with moderate numbers of FG-labeled cells included the anterior hypothalamic area (Fig. 2-4), the arcuate nucleus (ARH, Fig. 2-4), and dorsomedial hypothalamus (Fig. 2-4). In the amygdala, FG-positive cells were found

in the MEA (Table 1), particularly concentrated in the anterodorsal and posterior parts (Figs. 2-3 and 2-4).

In the brainstem, discrete clusters of FG-positive cells were observed throughout the rostral-caudal axis, with decreasing concentrations toward the caudal levels (Table 1). Rostrally, abundant FG-labeled cells were found throughout the periaqueductal gray (PAG, Figs. 2-4 and 2-6). Lateral to the PAG, the peripeduncular nucleus had a moderate number of FG cells (Fig. 2-4). At the caudal levels of the PAG, FG-labeled neurons were concentrated in the laterodorsal tegmental nucleus (Fig. 2-4), while a few FG-positive cells were noted in the pedunculopontine area (Fig. 2-4). On the ventral surface of the brainstem, there were moderate levels of tracer labeled cells in the ventral tegmental area (Figs. 2-3 and 2-4) and interpeduncular nucleus (Figs. 2-3 and 2-4). There were a few FG-labeled cells found in the nucleus brachium inferior colliculus (Fig. 2-3). At the caudal levels of the brainstem, there were scattered FG-positive cells in the pontine central gray (Figs. 2-3 and 2-4), the nucleus of the solitary tract (NTS, Figs. 2-4 and 2-6), and the lateral reticular nucleus in the rostral ventrolateral medulla (RVLM, Figs. 2-4 and 2-6).

Stress-activated neurons as identified by Fos after restraint stress

To determine stress-activated afferent inputs into the PVHap, tracer-injected rats were subjected to acute restraint stress and *Fos* was used to identify cells activated by stress. In general, restraint stress precipitated a stereotyped pattern of neuronal *Fos* expression, similar to those characterized previously (Cullinan et al., 1995). An

additional group of non-stressed rats were processed in parallel as a control. The non-stressed rats showed minimal *Fos* activation throughout the brain (data not shown).

Fos-positive cells were seen throughout the brain of stressed rats (Table 1). The brain areas with the densest numbers of *Fos* cells were the pontine gray on the ventral surface of the pons, and the piriform cortex in the ventrolateral region of the brain (Table 1). There were also extensive *Fos*-positive cells in hypothalamic areas such as the PVH, the ARH, dorsomedial nucleus, the PH, and the premammillary nuclei. Prominent *Fos* expression was also observed in the prefrontal cortex, dorsal and ventral parts of the LS, the nucleus accumbens, and in the posterodorsal part of the MEA. Moderate numbers of *Fos* positive cells were found in a variety of areas including the anteromedial part of BST, the VMH, thalamic areas (paraventricular thalamic nucleus), the dentate gyrus, and the lateral habenular nucleus (Fig. 2-4). In the brainstem, there were a moderate number of *Fos*-positive cells in the PAG, peripeduncular nucleus, interpeduncular nucleus, laterodorsal tegmental nucleus, superior colliculus, and the trapezoid and olive bodies. There was a light smattering of *Fos* cells in the ventral tegmental area, pedunculopontine area, pontine central gray, NTS, and RVLM (Fig. 2-4).

Stress-activated input to PVHap as identified by FG and Fos labeling

Stress-induced *Fos* staining combined with FG retrograde labeling was used to determine stress-activated afferent inputs in the PVHap. FG/*Fos* double-labeled cells were observed in a wide range of structures throughout the rostral to caudal axis of the brain (Table 1). In the forebrain, double labeled cells were concentrated in the ventral part of the LS near the lateral ventricle, extending with a lighter density of double labeled

cells into the rostral parts of the nucleus (Figs. 2-4 and 2-5). A few scattered double labeled cells were also noted in the caudal part of the LS close to the lateral ventricle (Fig. 2-4). In the BST, double labeled cells were observed in the posterior division of the principal nucleus (Figs. 2-4 and 2-5). FG/*Fos*-positive cells were observed throughout the hypothalamus with prominent double labeled cells found in the VMH, (Fig. 2-4), the PH (Fig. 2-4), and the ventral premammillary nucleus (Fig. 2-4), with a moderate number in the ARH (Fig. 2-4). In the VMH, FG/*Fos* positive cells were observed mainly in the ventrolateral part of the nucleus (Figs. 2-4 and 2-5). In the amygdala, abundant FG/*Fos* double labeled cells were found in the anterodorsal part of the MEA, with scattered double labeled cells observed in the posterodorsal and posteroventral parts of the MEA (Figs. 2-4 and 2-5). There were a few double labeled cells found in the anterior hypothalamus and dorsomedial nucleus of the hypothalamus (Table 1).

In the brainstem (Table 1), FG/*Fos* double labeled cells were found throughout the rostral-caudal axis of the PAG (Figs. 2-4 and 2-6). At the levels of the caudal PAG, there was a cluster of neurons double labeled with *Fos* and FG in the laterodorsal tegmental nucleus (Fig. 2-4). A moderate number of double labeled cells were observed in the peripeduncular nucleus (Fig. 2-4) and the pedunculopontine nucleus (Fig. 2-4). In the NTS there was a small cluster of FG and *Fos* double labeled neurons close to the central canal (Figs. 2-4 and 2-6). The far caudal region of the RVLM had a small tangle of FG-labeled neurons in the lateral reticular nucleus near the A1 noradrenergic cell group with a high degree of colocalization with *Fos* (Figs. 2-4 and 2-6). Though the absolute number of double labeled cells in the NTS and RVLM was not high (Table 1),

the percentage of FG-positive cells that were also *Fos*-positive was remarkable (approximately 50%).

Table and figures

Table 2-1.

	Area	FG	SEM	*Fos*	SEM	FG/*Fos*	SEM
Prefrontal cortex	Prelimbic	92	9.4	102	30.8	2	0.5
	Infralimbic	98	16.5	86	16.3	1	0.6
	Piriform cortex	0	0.0	159	12.8	0	0.0
	Nucleus accumbens	1	0.3	69	8.6	0	0.0
	Lateral septum	114	26.4	144	16.4	18	1.8
	Bed nucleus of the stria terminalis	56	5.8	43	10.8	13	0.8
	Medial preoptic nucleus	27	2.4	12	3.4	1	0.2
Thalamus	Paraventricular thalamic nucleus	9	1.8	60	9.7	1	0.2
Hypothalamus	Anterior hypothalamic area	65	10.1	25	2.2	3	0.4
	Paraventricular nucleus of the hypothalamus	*note		141	13.3	*note	
	Periventricular hypothalamic nucleus	20	6.4	34	4.1	0	0.0
	Arcuate nucleus	32	4.0	37	5.7	7	0.6
	Ventromedial hypothalamus	128	27.2	53	5.3	19	2.5
	Dorsomedial nucleus	48	8.4	79	10.7	4	1.2
	Posterior hypothalamic nucleus	99	11.8	63	4.5	16	3.1
	Ventral premammillary nucleus	64	5.7	69	12.3	16	3.4
Amygdala	Medial amygdala	78	9.3	105	9.3	14	1.0
Brainstem	Periaqueductal gray	105	12.1	137	12.9	14	1.8
	Peripeduncular nucleus	63	11.4	100	25.8	10	2.9
	Superior colliulus	17	10.0	81	17.1	1	0.8
	Pontine gray	2	0.3	440	65.7	0	0.0
	Laterodorsal tegmental nucleus	39	7.2	53	12.5	10	2.7
	Pedunculopontine area	18	2.1	27	3.7	7	0.6
	Trapezoid/olivary bodies	6	2.7	73	5.0	1	0.6
	Ventral tegmental area	27	7.4	29	10.1	2	0.7
	Interpeduncular nucleus	18	1.1	44	5.3	1	0.4
	Nucleus brachium inferior colliculus	16	1.4	57	7.0	2	0.4
	Pontine central gray	19	4.2	37	8.7	1	0.5
	Nucleus of the solitary tract	10	1.7	23	3.1	5	0.4
	Rostral ventrolateral medulla	13	2.3	14	3.1	5	0.6

*note: FG cells were not determined due to excessive accumulation of FG near the injection site.

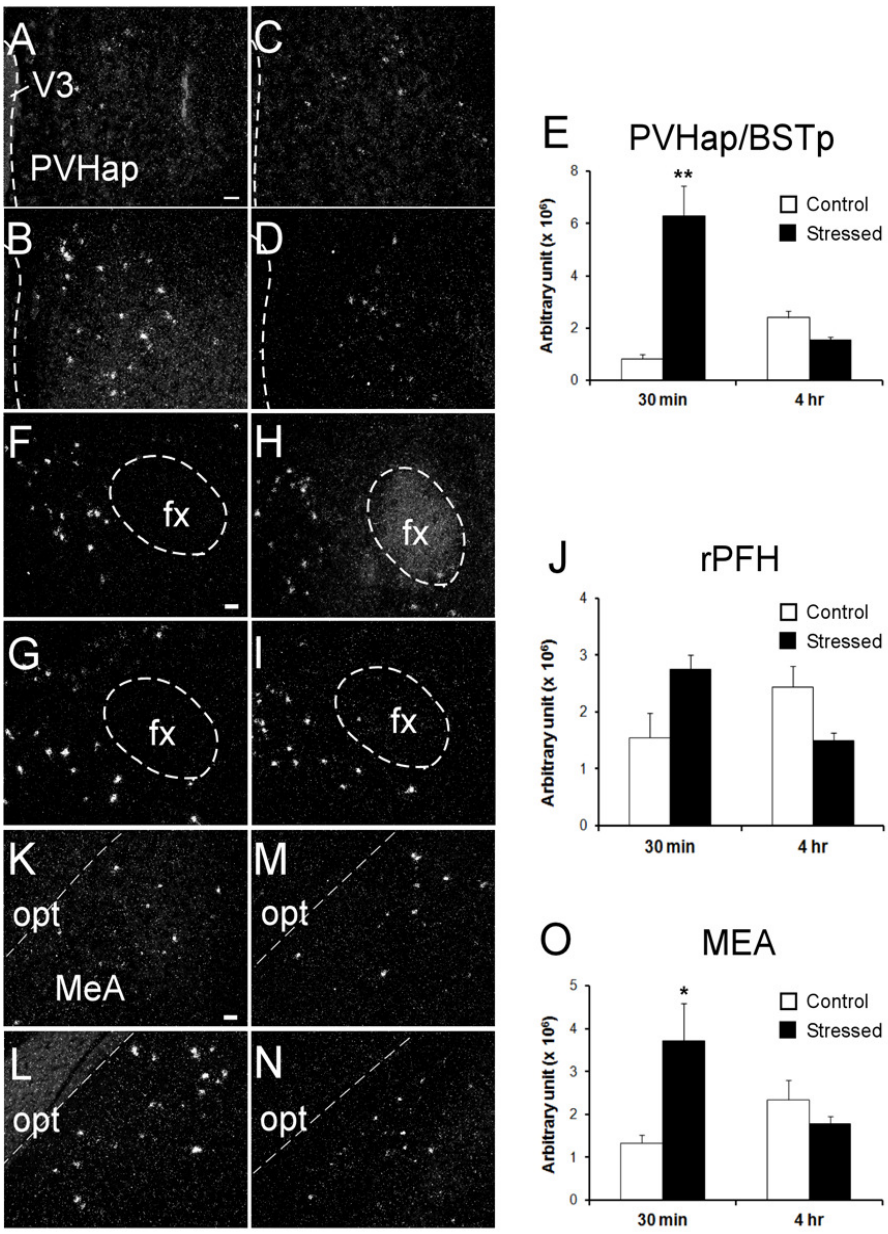

Figure 2-1. Ucn 3 mRNA expression after restraint stress. Representative darkfield photomicrographs showing silver grains by in situ hybridization for Ucn 3 mRNA in the paraventricular nucleus of the hypothalamus, anterior parvicellular part (PVHap) and posterior part of the bed nucleus of the stria terminalis (BSTp) (A-D), rostral perifornical hypothalamus (F-I) and medial amygdala (MEA) (K-N) with 30 min (B,G,L) or 4 hrs (D,I,N) restraint stress. Non-stress control for 30 min (A,F,K) and 4 hrs (C,H,M) in each area were also shown. E,J,O: Summary of Ucn 3 mRNA levels in the PVHap (E), rostral perifornical hypothalamus (J) and MEA (O). **P<0.01, *P<0.05 vs. non stressed control. Scale bars = 50 µm

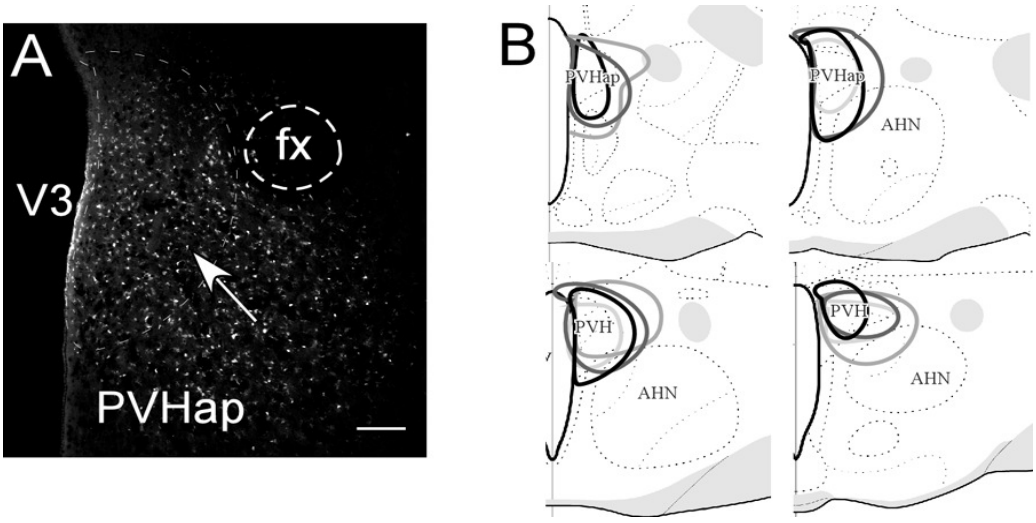

Figure 2-2. Representative darkfield photomicrograph showing injection site (A) and schematic drawing showing a reconstruction of injection sites (B) in the PVHap. Circles indicate extent of dye placement for each case.

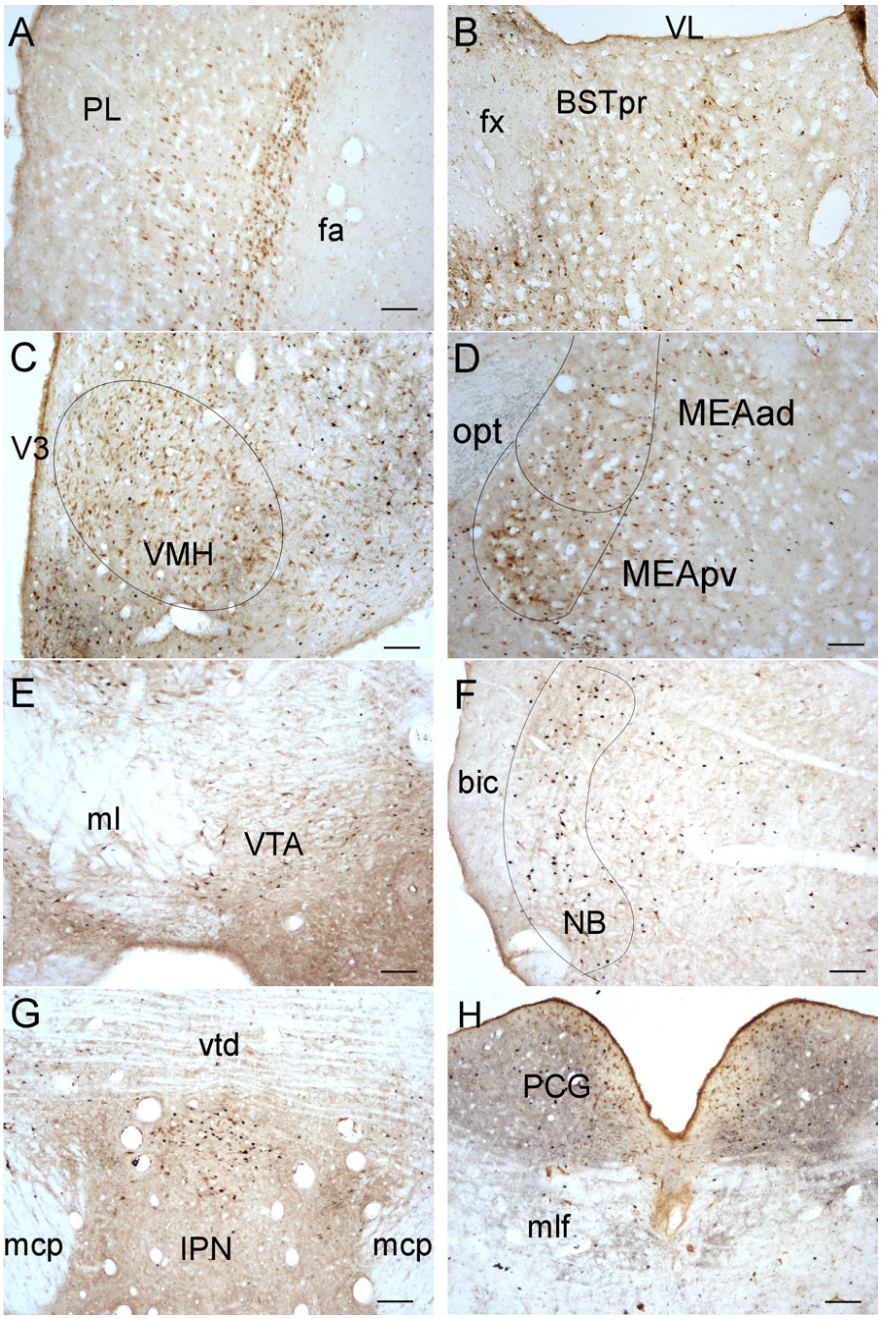

Figure 2-3. Representative brightfield photomicrographs showing fluorogold (FG, light brown precipitate in cytosol) staining in the prefrontal cortex (A), bed nucleus of the stria terminalis (BST) (B), the ventromedial hypothalamus (VMH) (C), the MEA (D), the ventral tegmental area (E), the nucleus brachium inferior colliculus (F), the interpeduncular nucleus (G), and the pontine central gray (H) of animals injected in the PVHap. Scale bars = 100 µm.

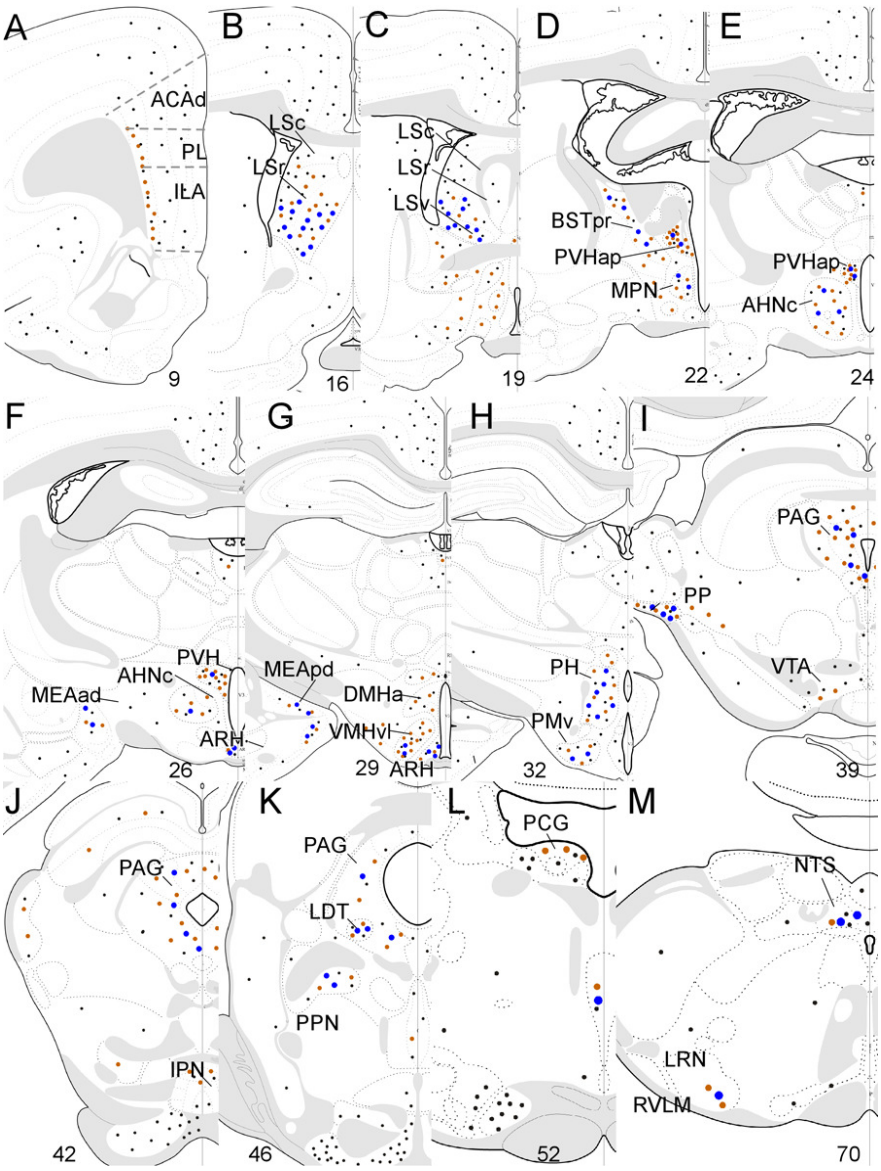

Figure 2-4. Representative illustrations showing neurons stained with *Fos* (black), FG (light brown), and double labeled (blue) in the prefrontal cortex (A), lateral septal nucleus (LS) (B-C), principal nucleus of the posterior division of the BST, PVHap, and medial preoptic nucleus (D), PVHap, anterior hypothalamic nucleus (E), paraventricular nucleus of the hypothalamus, anterior hypothalamic nucleus, arcuate nucleus of the hypothalamus (ARH), and MEA (F), posterodorsal part of the MEA, anterior part of the dorsomedial nucleus of the hypothalamus, ARH, and ventrolateral part of the VMH (G), PH and ventral premammillary nucleus (H), periaqueductal gray (PAG), peripeduncular nucleus, and ventral tegmental area (I), PAG and interpeduncular nucleus (J), PAG, laterodorsal tegmental nucleus, and pedunculopontine nucleus (K), pontine central gray (L), and nucleus of the solitary tract (NTS), lateral reticular nucleus in the rostral ventrolateral medulla (RVLM) (M) of animals injected in the PVHap.

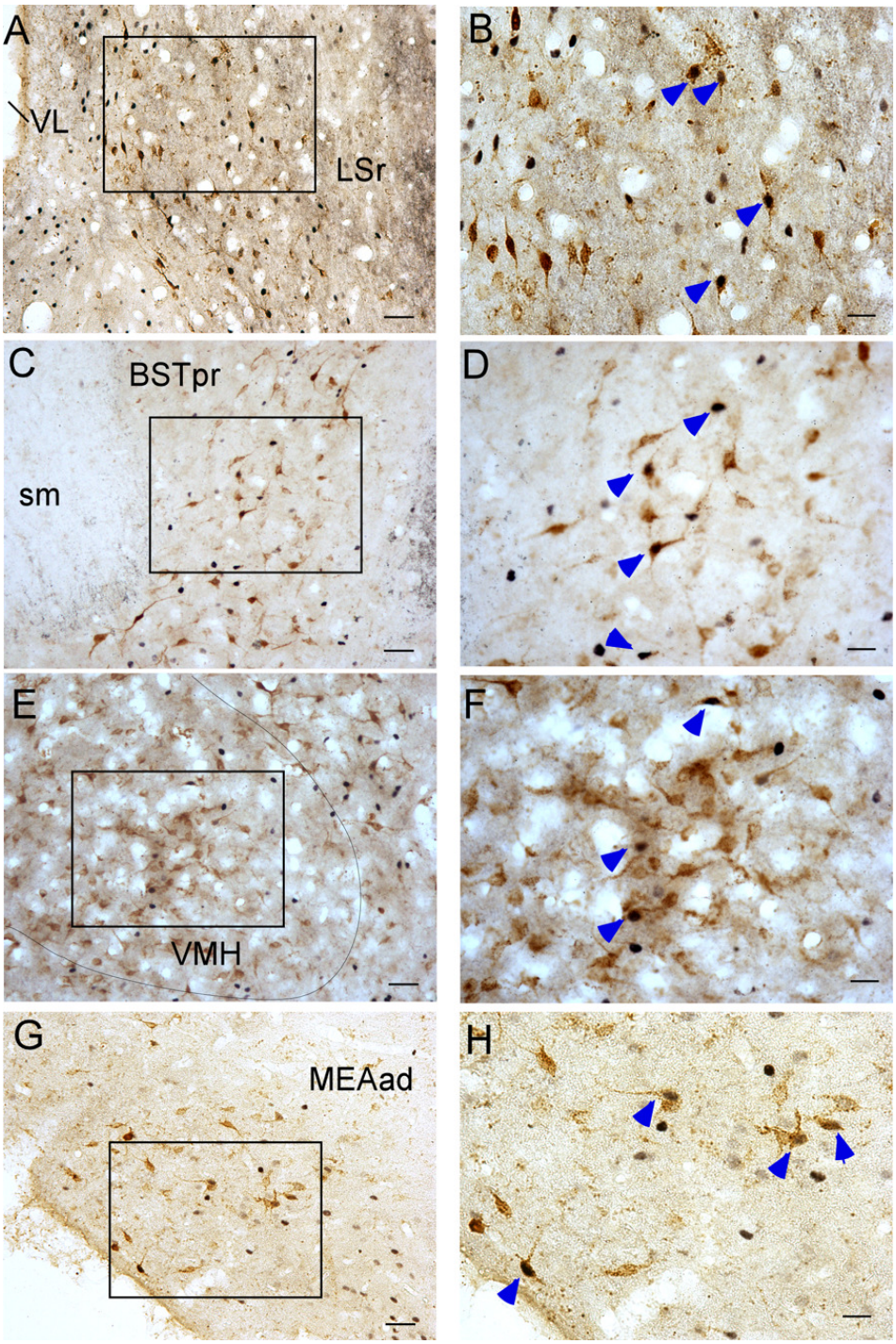

Figure 2-5. Representative brightfield photomicrographs showing immunoreactive FG (light brown precipitate in cytosol) and *Fos* (dark nuclear precipitate) staining in the forebrain areas of the LS (A), BST (C), the VMH (E), and the MEA (G) of animals injected in the PVHap. B, D, F, H: High power magnification of boxed area in A (B), C (D), E (F) and G (H). Representative FG/*Fos* double labeled cells were indicated by blue arrowheads. Scale bars = 50 µm (A, C, D, E, G), and 20 µm (B, D, F, H).

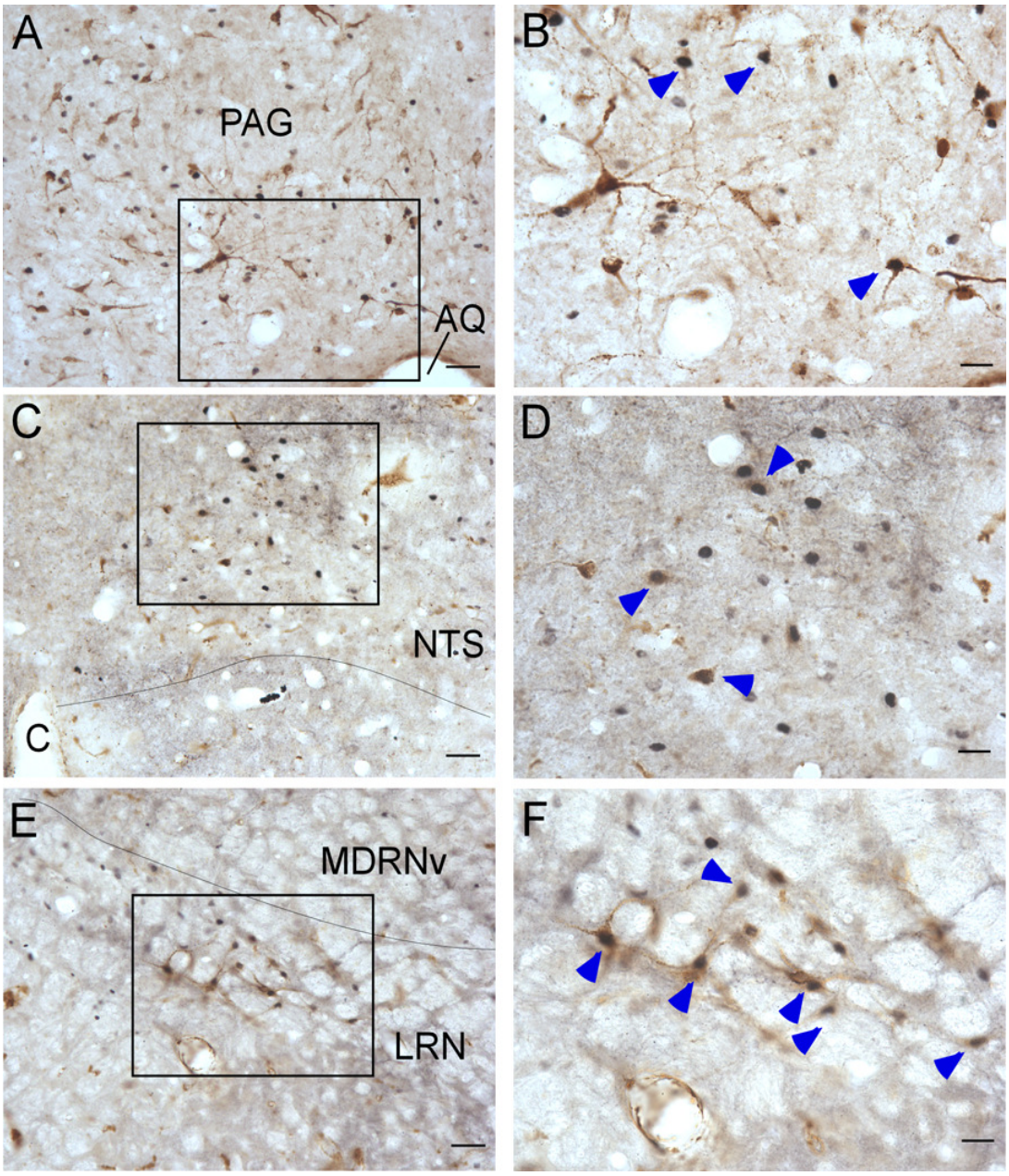

Figure 2-6. Representative brightfield photomicrographs showing immunoreactive FG (light brown precipitate in cytosol) and *Fos* (dark nuclear precipitate) staining in the brainstem areas of the PAG (A), the NTS (C), and the lateral reticular nucleus of the RVLM (E) of animals injected in the PVHap. B, D, F, H: High power magnification of boxed area in A (B), C (D), and E (F). Representative FG/*Fos* double labeled cells were indicated by blue arrowheads. Scale bars = 50 µm (A, C, D, E, G), and 20 µm (B, D, F, H).

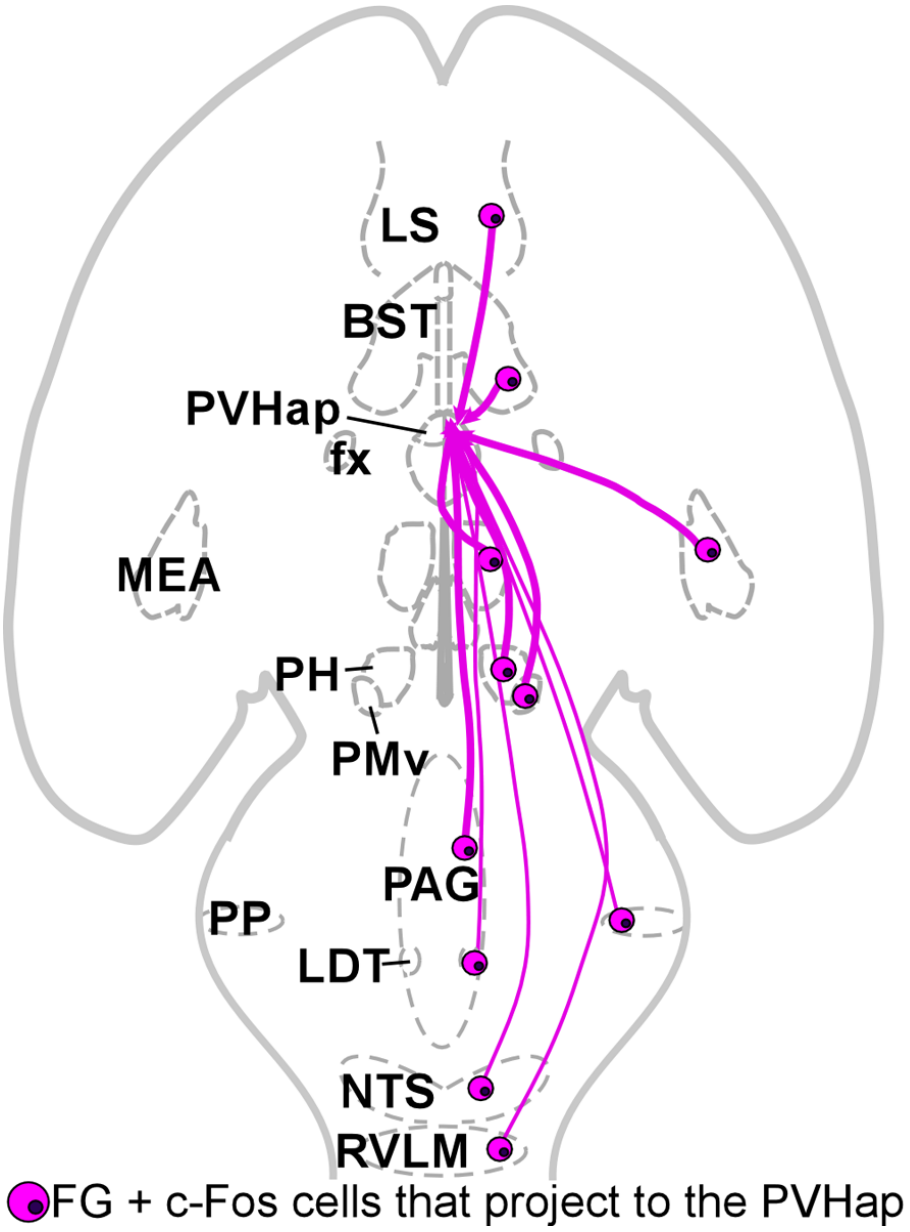

Figure 2-7. Summary of the stress-activated input to the PVHap. Circles represent areas with FG and *Fos* double labeling. Pink arrows represent PVHap neural circuit inputs and the thickness of the lines signifies degree of innervation.

Abbreviations used in figures and text:
Ucn 3, Urocortin 3
CRF, corticotropin-releasing factor
CRF_2, type 2 CRF receptor
ACAd, Dorsal part of the anterior cingulate area
AHN, Anterior hypothalamic nucleus
AHNc, Central part of the anterior hypothalamic nucleus
AHNp, Posterior part of the anterior hypothalamic nucleus
AQ, Cerebral aqueduct
ARH, Arcuate nucleus of the hypothalamus
BA, Bed nucleus of the accessory olfactory tract
bic, Brachiam of the inferior colliculus
BN, Basal nucleus of the dorsal horn
BST, bed nucleus of the stria terminalis
BSTp, Posterior division of the BST
BSTad, Anterodorsal area of the anterior division of the BST
BSTpr, Posterior part of the principal nucleus of the BST
COAa, Anterior part of the cortical nucleus of the amygdala
COApl, Lateral zone of the posterior part of the cortical nucleus of the amygdala
DMHa, Anterior part of the dorsomedial nucleus of the hypothalamus
fa, Anterior forceps of the corpus callosum
fx, Columns of the fornix
ILA, Infralimbic area
IPN, Interpeduncular nucleus
LDT, Laterodorsal tegmental nucleus
LHA, Lateral hypothalamic area
LRN, Lateral reticular nucleus
LS, lateral septal nucleus
LSc, Caudal part of the LS
LSr, Rostral part of the LS
LSv, Ventral part of the LS
mcp, Middle cerebellar peduncle
MDRNv, Ventral part of the medullary reticular nucleus
MEA, Medial amygdala
MEAad, Anterodorsal part of the MEA
MEApd, Posterodorsal part of the MEA
MEApv, Posteroventral part of the MEA
ml, Medial lemniscus
mlf, Medial longitudinal fascicle
MPN, Medial preoptic nucleus
NB, Nucleus brachium inferior colliculus
NTS, Nucleus of the solitary tract
opt, Optic tract
PAG, Periaqueductal grey
PCG, Pontine central grey
PH, Posterior hypothalamic nucleus

PL, Prelimbic area
PMv, Ventral premammillary nucleus
PP, Peripeduncular nucleus
PPN, Pedunculopontine nucleus
PVH, Paraventricular nucleus of the hypothalamus
PVHap, Anterior parvicellular part of the PVH
rPFH, Rostral perifornical hypothalamus
RVLM, Rostral ventrolateral medulla
SC, Superior colliculus
sm, Stria medullaris
V3, Third ventricle
VL, Lateral ventricle
VMH, Ventromedial nucleus of the hypothalamus
VMHvl, Ventrolateral part of the VMH
VTA, Ventral tegmental area
vtd, Ventral tegmental decussation

Discussion

Ucn 3 plays a critical role in the brain in regulating energy homeostasis (Chen et al., 2010; Fekete et al., 2006; Jamieson et al., 2006; Ohata and Shibasaki, 2004; Pelleymounter et al., 2004; Telegdy et al., 2006) and, like other members of the CRF family, Ucn 3 expression in the brain is regulated by stress (Jamieson et al., 2006; Venihaki et al., 2004). Our previous work determined that the PVHap/BSTp is the main source of Ucn 3 afferent input to the VMH, a brain area well known to modulate energy balance and sympathetic outflow (Chen et al., 2011; Chen et al., 2012a; King, 2006). Consistent with an earlier report (Jamieson et al., 2006), the present study confirmed that acute restraint stress stimulated Ucn 3 expression in the MEA. Notably, we found that restraint stress rapidly enhances Ucn 3 expression in the PVHap/BSTp, but not in neurons in the rostral perifornical hypothalamus lateral to the PVHap, suggesting that stress selectively stimulates Ucn 3 neurons in the PVHap/BSTp area. Interestingly, Ucn 3 expression in animals after 4 hours restraint stress showed a non-significant trend toward decreased levels compared to controls. It is possible that additional signals may be recruited under extended stress conditions as a feedback mechanism to negatively regulate Ucn 3 expression in the PVHap. This slightly lowered Ucn 3 expression in 4hr stressed animals may be due to an overshoot by the feedback mechanism in reducing Ucn 3 expression. Consistent with this notion, it has been shown that CRF expression in the PVH is slightly reduced in rats with repeated cold stress compared to naïve rats (Hatalski et al., 1998).

To investigate the possible neural mechanisms by which acute stress stimulates Ucn 3 expression in the PVHap, the current study combined retrograde tracing and stress-

induced *Fos* staining to determine stress-sensitive afferent input into the PVHap. In general, stress-activated afferent input into the PVHap originates from a wide range of brain areas including the rostral and ventral parts of the LS, various parts of the hypothalamus (ARH, VMH, PH, and ventral premammillary nucleus), and the MEA, with a lesser input from the BSTp and brainstem areas (PAG, the laterodorsal tegmental nucleus, the peripeduncular nucleus, the NTS, and the RVLM) (Fig. 2-7).

Forebrain stress-activated afferent input into the PVHap

Hypothalamic input

Arcuate nucleus of the hypothalamus

Consistent with earlier reports of ARH projections (Atasoy et al., 2012; Li et al., 2000; Magoul et al., 1994), FG-positive cells were observed in the ARH of rats injected with FG in the PVHap. A significant number of these FG-positive cells were double labeled with *Fos*, indicating that the arcuate-PVHap pathway is stress sensitive. The ARH is an established regulator of energy homeostasis, serving as a converging point for peripheral and central signals concerning peripheral energy status (Sasaki and Kitamura, 2010). After integrating various inputs, the ARH then signals multiple downstream targets including the PVH, lateral hypothalamus, and amygdala to modulate energy homeostasis (Bagnol et al., 1999; Balthasar et al., 2005). For example, orexigenic neurons from the ARH inhibit oxytocin neuron activity in the PVH to stimulate feeding (Atasoy et al., 2012). Thus, it is conceivable that stress activates anorexigenic neurons in the ARH, which in turn target and stimulate Ucn 3 cells in the PVHap to inhibit feeding

in response to stress. It will be of great interest to identify the phenotypes of neurons in the ARH and their projections into the PVHap to further substantiate this possibility.

Ventromedial hypothalamus

Our previous study showed that the PVHap projects to the VMH (Chen et al., 2011) and the present study demonstrated that there are afferent projections from the VMH to PVHap, indicating reciprocal connections between the two areas. VMH projections to the PVHap have been previously confirmed through anterograde tracing (Canteras et al., 1995). While there were FG labeled cells throughout the VMH, the stress-activated neurons appeared to be concentrated in the ventrolateral portion of the nucleus, which has been implicated in regulating behaviors including aggression (Lin et al., 2011a) and female sexual behavior (King, 2006). The connection from the ventrolateral VMH to the PVHap could be involved in modulating stress-associated behaviors.

Currently, the role of the ventrolateral VMH in energy balance is less clear. Interestingly, a number of recent studies have implicated the estrogen receptor in the VMH in energy balance. Stimulation of the estrogen receptor in the VMH promotes thermogenesis in brown adipose tissue (Martinez de Morentin et al., 2014) and mice with estrogen receptor knockout in the VMH exhibit altered energy balance and are obese (Correa et al., 2013). Most of the estrogen receptors in the VMH are found in the ventrolateral part of the nucleus (Cao and Patisaul, 2011; Gonzales et al., 2012; Simerly et al., 1990), suggesting a potential role of the ventrolateral VMH in regulating energy balance. This raises the possibility that the ventrolateral VMH-PVHap pathway may be involved in regulating energy balance in response to stress.

Posterior hypothalamic nucleus and ventral premammillary nucleus

The PH and ventral premammillary nucleus contained a moderate number of cells double labeled with FG and *Fos* in animals injected with FG into the PVHap. The projection of both areas to the PVHap has been confirmed by previous studies (Canteras et al., 1992; Silverman et al., 1981). The PH has been associated with the regulation of cardiovascular function through sympathetic nervous system activity and locomotion; stimulation of the nucleus results in hypertension and increased movement (Eferakeya and Buñag, 1974; Martin et al., 1988; Young et al., 2011). The current result suggests that the PH may regulate sympathetic activity and locomotion by communicating with the PVHap in response to stress. The ventral premammillary nucleus has been shown to play a crucial role in regulating various aspects of reproduction including maternal aggression, pheromone sensing in male rats, and reproductive hormone secretions in response to nutrition (Cavalcante et al., 2006; Donato and Elias, 2011; Motta et al., 2013). More studies are needed to determine the precise role of the ventral premammillary nucleus projections to the PVHap in acute stress.

Extra-hypothalamic input

Lateral septal nucleus

Previous studies found that the LS provides modest projections to the PVHap, with most of the PVHap-projecting cells located in the ventral part of the LS (Risold and Swanson, 1997). Consistent with this earlier report, the present study found prominent FG-positive cells in the ventral LS with scattered double labeled cells in the caudal part of the LS. Many of the FG-positive cells were activated by acute stress. The LS has been implicated in feeding (Angeles-Castellanos et al., 2007; Koppell and Sodetz, 1972; Mitra

et al., 2011), with both suppression and stimulation of feeding reported. Infusing noradrenaline into the LS increases feeding, whereas infusion of Ucn 1 decreases feeding (Scopinho et al., 2008; Wang and Kotz, 2002), suggesting the functional role of the nucleus in feeding is signal dependent. The present study suggests that the lateral septal neurons may mediate stress-associated energy adaptation by recruiting PVHap cells, including Ucn 3 neurons, which subsequently modulate feeding and sympathetic outflow.

Bed nucleus of the stria terminalis

Both anterograde and retrograde studies (Dong and Swanson, 2004; Gaykema et al., 2007) have demonstrated that neurons in the BST provide projections to the PVHap, and the current study identified many of the PVHap-projecting cells as *Fos* positive. The BST receives inputs carrying information about olfaction (Dong et al., 2001) and gustation (Li and Cho, 2006)**,** and has been functionally linked to integration of behavioral and autonomic responses to stress (Cecchi et al., 2002; Davis et al., 1997; Khoshbouei et al., 2002). Moreover, a number of studies have indicated that the BST negatively regulates food intake (Ciccocioppo et al., 2003; Kocho-Schellenberg et al., 2014; Roman et al., 2012). Taken together, it is conceivable that the BST is involved in conveying the olfactory and gustatory aspects of acute stress to the PVHap to modulate physiological functions including feeding.

Medial amygdala

Consistent with earlier reports (Canteras et al., 1995; Coolen and Wood, 1998), the present study found neurons in the MEA that project to the PVHap, and further defined the pathway by showing that it is activated by acute stress. Functional and genetic studies show that the MEA can act as a satiety center (Rollins and King, 2000; Xi

et al., 2012), suggesting that the MEA-PVHap pathway may contribute to hypophagia induced by acute stress. In addition to feeding and stress regulation, the MEA is a major regulator of defense behaviors and emotional responses to olfactory stimuli (Dielenberg et al., 2001; Keshavarzi et al., 2014; Lehman et al., 1980). Lesions of the MEA eliminate defensive responses to predator odor (Martinez et al., 2011) and sexual response to odors of potential mates in mice (Lehman et al., 1980). The MEA-PVHap pathway may potentially be involved in regulating these behaviors in response to stress.

Brainstem stress-activated afferent input into the PVHap

Periaqueductal gray

The PAG contained FG labeled cells throughout its rostral to caudal axis, many double labeled with *Fos*, confirming the previously described projection (Pelosi et al., 2009). The PAG is well known for its role in modulating pain (Lau and Vaughan, 2014), but is also involved in a wide range of activities from hunting to fear learning. It has been shown that the PAG is activated by negative and life threatening experiences (Kincheski et al., 2012), and stimulation of the PAG in humans induces panic attacks and intense feelings of terror, panic, and anxiety (Schenberg et al., 2014). As restraint stress is a negative psychological experience, it is possible that the projection to the PVHap is involved in processing the negative nature of acute restraint stress.

Rostral ventrolateral medulla

Previous anterograde tracing studies have shown that the RVLM sends moderate projections to the PVHap (Cunningham and Sawchenko, 1988; Rinaman et al., 1995). A small number of FG-positive cells were observed in this area with a high percentage of

Fos double labeling, indicating that this pathway is important in conveying stress signals. The medulla-PVH pathway has been implicated in inhibition of food intake by cholecytokinin, a gut secreting peptide (Rinaman et al., 1995). Thus, it is possible that this medullary projection to the PVHap may be involved in stress-induced hypophagia.

The RVLM is also extensively involved in sympathetic nervous system regulation and vascular tone (Allen et al., 2009; Allen, 2011; Pilowsky et al., 2008). A range of physical challenges activate C1 neurons in the RVLM, which then maintains cardiac, respiratory, and glucose homeostasis (Guyenet et al., 2013; Verberne et al., 2014). There is also a group of A1 noradrenergic neurons near the area where the FG/*Fos* neurons were observed but it is unlikely that A1 neurons sent stress-activated projections to the PVHap as they appear to send efferent output only to the caudal magnocellular part of the PVH and not the parvicellular divisions (Woulfe et al., 1990). Though we did not identify input to Ucn 3 cells specifically, it is conceivable that the RVLM projection targets Ucn 3 neurons in the PVHap, which project to the VMH. As Ucn 3 acts in the VMH to increase blood glucose levels (Chen et al., 2010), the RVLM may recruit the PVHap-VMH pathway to increase blood glucose levels during acute stress.

Nucleus of the solitary tract

In the present study, a small number of FG cells were found in the NTS, which is consistent with previous anterograde studies that observed moderate projections from the NTS to the PVHap (Cunningham and Sawchenko, 1988; Rinaman et al., 1995). Importantly, a high percentage of these cells were double labeled with *Fos*. The NTS has an established role as a center that receives, integrates, and relays visceral gastrointestinal, gustatory, cardiovascular, and respiratory information to higher centers

(Bradley and Grabauskas, 1998; Rinaman, 2010; Zhang and Mifflin, 2010; Zoccal et al., 2014). The NTS is also stress-responsive; during hypoxic stress, the NTS integrates neural signals from chemoreceptors and then initiates responses to increase blood oxygen (Zoccal et al., 2014). Thus, it is conceivable that the NTS is relaying visceral information to the PVHap during acute restraint stress.

Conclusion

The present study shows that, during acute restraint stress, the PVHap receives information from a diverse range of areas such as those concerning learning and behavior (LS, BST, amygdala) and autonomic regulation (hypothalamus, brainstem) (Fig. 2-7). Areas associated with behavioral regulation (peripeduncular nucleus, laterodorsal tegmental nucleus) also contained double labeled FG/*Fos* neurons, though the precise role of these stress-activated projections to the PVHap remains to be determined. Although these stress-activated inputs do not necessarily or specifically activate Ucn 3 neurons or enhance Ucn 3 mRNA production in the PVHap, it is likely that at least some of these inputs target Ucn 3 neurons, as the FG injections covered the entire PVHap area in which Ucn 3 cells reside. As such, the data provide a basic framework to further determine the neural inputs that activate Ucn 3 cells in the PVHap during stress.

3. Aim 2: Phenotypic characterization and efferent projections of Urocortin 3 neurons in the paraventricular nucleus of the hypothalamus

Abstract

Urocortin 3 (Ucn 3) is a member of the corticotropin-releasing factor family, which plays a major role in coordinating the stress response. Ucn 3 neurons in the anterior parvicellular part of the paraventricular nucleus of the hypothalamus (PVHap) provide prominent input into the ventromedial nucleus of the hypothalamus (VMH), a well known satiety center, where Ucn 3 acts to suppress feeding and modulate blood glucose levels. Currently, little is known about the anatomical characteristics of the Ucn 3 neurons in the PVHap. In the present study, a transgenic mouse model in which Ucn 3-positive cells express the fluorescent protein mCherry as a reporter was used to anatomically characterize Ucn 3 neurons in the PVHap. We determined that Ucn 3 in the PVHap does not colocalize with a number of major neuropeptides including corticotropin-releasing factor, oxytocin, or vasopressin, indicating that Ucn 3 cells are an anatomically distinct population in the PVH. We also determined that melanocyte-stimulating hormone and Neuropeptide Y fibers and terminals are present in close proximity to Ucn 3 neurons in the PVHap. Finally, we mapped the efferent projections of Ucn 3 neurons from the PVHap and found that these neurons prominently project to the VMH and the external zone of the median eminence. In conclusion, Ucn 3 cells are located in a unique niche within the PVH and their efferent outputs suggest that these neurons are in a position to modulate energy homeostasis and neuroendocrine function.

Introduction

Corticotropin-releasing factor (CRF) is vitally important for coordinating physiological and behavioral responses to stress by activation of the hypothalamic-pituitary-adrenal axis to regulate glucocorticoid secretion from the adrenal gland. Once thought to be in a class of its own, CRF is actually a member of a family of peptides that includes the series of Urocortins (Ucn), Ucn 1, 2, and 3. The function of CRF and the Ucns are mediated through type 1 and 2 CRF receptors (CRF_1 and CRF_2). CRF preferentially binds CRF_1, Ucn 1 binds both receptors with equal affinity, and Ucn 2 and 3 bind selectively to CRF_2 (Hsu and Hsueh, 2001; Lewis et al., 2001). These CRF-like peptides may mediate some stress-related functions previously attributed to CRF. Ucn 3 is the most recent addition to the CRF family (Hsu and Hsueh, 2001; Lewis et al., 2001), with Ucn 3-expressing neurons located in the medial amygdala and the hypothalamus. In the hypothalamus, the Ucn 3 cell populations reside in the median preoptic nucleus, the posterior part of the bed nucleus of the stria terminalis, the anterior parvicellular part of the paraventricular nucleus of the hypothalamus (PVHap), and clustered around the fornix in the rostral perifornical hypothalamus (rPFH) laterally and slightly caudally to the PVHap (Li et al., 2002). Ucn 3 nerve fibers and terminals are present in the lateral septal nucleus, bed nucleus of the stria terminalis, ventromedial hypothalamus (VMH), and medial amygdala (Li et al., 2002). These areas in which Ucn 3 terminals are located express high levels of CRF_2 (Chalmers et al., 1995; Van Pett et al., 2000), reinforcing the idea that Ucn 3 is an endogenous ligand for CRF_2.

The precise function of Ucn 3 in the brain is not yet clear, but when injected intracerebroventricularly, Ucn 3 increases body temperature, suppresses feeding, elevates

blood glucose levels, and stimulates the hypothalamic-pituitary-adrenal axis (Fekete et al., 2006; Jamieson et al., 2006; Ohata and Shibasaki, 2004; Pelleymounter et al., 2004; Telegdy et al., 2006; Telegdy and Adamik, 2008), indicating that Ucn 3 in the brain may play an important role in regulating energy homeostasis. Site specific injection studies have been performed to determine the specific brain areas that may mediate these effects. Ucn 3 injection into the VMH results in suppression of feeding and elevation of blood glucose, but not stimulation of the hypothalamic-pituitary-adrenal axis (Chen et al., 2010; Fekete et al., 2006). When injected into the amygdala or other areas of the hypothalamus, Ucn 3 has no effect on feeding or blood glucose levels (Chen et al., 2010; Fekete et al., 2006). Mice with CRF_2 knockdowns in the VMH gain more weight, mostly white fat, than control mice, and they eat more after overnight fasting, similar to Ucn 3 null mice (Chao et al., 2012). These data suggest that the VMH is a critical area mediating the effect of Ucn 3 on feeding and energy modulation.

Ucn 3 afferent inputs to the VMH originate primarily from the PVHap, with moderate inputs from the medial amygdala (Chen et al., 2011). Though they are anatomically close, the PVHap population of Ucn 3 neurons appears to be a separate group from those in the median preoptic nucleus and the rPFH. Ucn 3-expressing neurons in the PVHap project to the VMH and not the lateral septal nucleus while Ucn 3 neurons in the rPFH project to the lateral septal nucleus with only a few fibers projecting to the VMH (Chen et al., 2011). The PVHap population is activated by stress, unlike the rPFH (van-Hover and Li), and, furthermore, the rPFH Ucn 3 neurons co-express thyrotropin-releasing hormone (TRH) while the PVHap cells do not (Wittmann et al., 2009a).

The PVH regulates food intake, the stress response, and pituitary hormone secretion (Ferguson et al., 2008; Herman et al., 2008) by releasing CRF, oxytocin (OXT), and vasopressin (AVP). To better define the physiological role of Ucn 3 cells in the PVH, we used a novel mouse model to determine anatomical characteristics of Ucn 3 neurons and found that Ucn 3 appears to occupy a unique niche within the PVHap, as there was little colocalization of Ucn 3 with OXT, AVP, or CRF neuropeptides. We also determined that melanocyte-stimulating hormone (MSH) and Neuropeptide Y (NPY) fibers and terminals are present in close proximity to Ucn 3 neurons in the PVHap. Finally, we examined projections of Ucn 3 neurons in the PVHap and found that they target selectively the dorsomedial part of the VMH and the external zone of the median eminence (MEex), suggesting that in addition to regulating energy homeostasis, Ucn 3 may send neuroendocrine signals to regulate pituitary function.

Materials and methods

Generation of Ucn 3-mCherry reporter mice

Transgenic mice with Cre recombinase (cre) expressed in Ucn 3-positive cells (Ucn 3-cre mice, STOCK Tg(Ucn3-cre)KF31Gsat/Mmucd, Gensat MMRRC, New York, NY) were used to visualize the distribution of Ucn 3 in mouse brains. The specificity of cre expression was first tested by crossing these Ucn 3-cre mice with transgenic mice carrying a cre-regulated mCherry reporter gene driven by a ROSA promoter (strain: B6;129S-*Gt(ROSA)26Sor*$^{tm1.1Ksvo}$/J, Jackson laboratory, Bar Harbor, ME). This cross generated transgenic mice with mCherry expressed in Ucn 3-cre cells (Ucn3-cre-mCherry mice), allowing visualization of Ucn 3. All mice were housed in a temperature controlled room with lights on between 0600-1800 hr. All experimental protocols and procedures were approved by The University of Virginia Animal Use and Care Committee.

Combined immunohistochemistry and in situ hybridization

To visualize mCherry and Ucn 3 mRNA simultaneously to examine mCherry specificity for Ucn 3 neurons, combined immunohistochemistry for mCherry and *in situ* hybridization for Ucn 3 mRNA was performed on Ucn 3-cre-mCherry mouse brain sections. Ucn3-cre-mCherry mice were perfused transcardially with sodium borate buffered paraformaldehyde (pH 9.5) and brains were sectioned coronally at 25 μm thickness with a sliding microtome. All solutions for the immunohistochemical procedure were prepared with RNase-free H_2O. Perfused mouse brain sections were washed with potassium phosphate-buffered saline (KPBS), followed by incubation in rabbit anti-DsRed antibody (1:3,000, Clontech, Mountain View, CA) in KPBS with 0.4% Triton-X

100 for 48 hrs at 4°C. After primary antibody incubation, the sections were washed and incubated in biotinylated donkey anti-rabbit IgG (1:600, Jackson ImmunoResearch, West Grove, PA) for 1 hr at room temperature. They were then washed and incubated for 1 hr at room temperature in avidin-biotin complex solution (Vectastain ABC Elite Kit, Vector Laboratories, Burlingame, CA). The DsRed antibody-peroxidase complex was revealed with 3,3 diaminobenzdine (DAB) as a chromogen. After the color development, brain sections were washed with KPBS and prepared for *in situ* hybridization for detecting Ucn 3 mRNA, performed as previously reported (Li et al., 2002). Briefly, a Ucn 3 complementary RNA (cRNA) probe was transcribed from a linearized vector containing a full-length mouse Ucn 3 sequence and flanking the 30bp untranslated region (total 528 bp) in the presence of 33 P-labeled UTP (Perkin-Elmer, Oak Brook, IL). Brain sections were treated with a fresh solution containing 0.25% acetic anhydride in 0.1 M triethanolamine (pH 8.0) followed by a rinse in 2X SSC. The sections were then exposed to the cRNA probe overnight at 55°C. After hybridization, the brain sections were washed in increasingly stringent SSC, in RNase, and in 0.1X SSC at 60°C. Brain sections were then mounted onto gelatin coated glass slides, dehydrated through a graded series of alcohols, and dried. Slides were dipped in NTB emulsion (Kodak, New Haven, CT), exposed for seven days at 4°C, and developed.

Immunofluorescence staining

For immunofluorescence staining, brain sections from perfused Ucn 3-cre-mCherry mice were washed with KPBS and then incubated in primary antibodies in KPBS with 0.4% Triton-X 100 for 48 hrs at 4°C. After incubation, the sections were washed and incubated in fluorophore-conjugated secondary antibodies raised in donkey

in 0.4% Triton-X 100 (1:400) for 1 hr at room temperature. Brain sections were then washed with KPBS, mounted onto gelatin-coated slides, and coverslipped with buffered glycerol. Antibodies used in this study were rabbit anti-CRF antibody (1:1,500, provided by Dr. Wylie Vale, The Salk Institute, San Diego, CA), guinea pig anti-AVP antibody (1:1,000, Peninsula Laboratories LLC, Bachem. Torrance, CA), rabbit anti-OXT antibody (1:1,500, Millipore, Billerica, MA), sheep anti-NPY antibody (1:3,000, Millipore, Billerica, MA), and sheep anti-MSH antibody (1:1,100, Millipore, Billerica, MA).

Anterograde viral tracing

To trace Ucn 3 projections from the PVHap, a cohort of adult Ucn 3-cre mice were anesthetized with isoflurane and placed in a stereotaxic apparatus (David Kopf Instruments, Tujunga, CA). A Hamilton microsyringe was filled with an adeno-associated virus (AAV, serotype 2) expressing a cre-dependent ChannelRhodopsin-mCherry reporter gene and inserted into the PVHap. 200 nL of viral vector was injected via a perfusion pump. The stereotaxic coordinates for the PVHap were: 0.37 mm rostral and 0.18 mm lateral to bregma, and 5.5 mm ventral to the dura. Six weeks after injection, animals were transcardially perfused with 4% paraformaldehyde (pH 9.5). The brains were removed and sectioned coronally at 25 μm thickness and stored in cryoprotectant at -20°C until use.

To visualize virally labeled projections, brain sections were washed with KPBS and then incubated in rabbit anti-DsRed antibody (1:3000, Clontech, Mountain View, CA) in KPBS with 0.4% Triton-X 100 for 48 hrs at 4°C. After incubation, the sections

were washed and incubated in biotinylated donkey anti-rabbit IgG (1:600, Jackson ImmunoResearch, West Grove, PA) for 1 hr at room temperature. They were then washed and incubated for 1 hr at room temperature in avidin-biotin complex solution (Vectastain ABC Elite Kit, Vector Laboratories, Burlingame, CA). A nickel enhanced DAB reaction was used as a chromogen to visualize mCherry immunoreactivity. After the color development, brain sections were washed with KPBS, mounted onto gelatin-coated slides, dehydrated, and coverslipped with Permount.

To test the presence of cre in mCherry cells in non-Ucn 3-expressing brain areas, a cre-dependent farsenylated green fluorescent protein (GFPf) virus (Lindberg et al., 2013) was injected into the striatum of adult Ucn 3-cre-mCherry mice with a Hamilton microsyringe as described above. The stereotaxic coordinates for the striatum were: 0.35 mm rostral and 2.0 mm lateral to bregma, and 4.0 mm ventral to the dura. Four weeks after injection, animals were perfused with 4% paraformaldehyde (pH 9.5). The brains were removed and sectioned coronally at 25 μm thickness and stored in cryoprotectant at -20°C until use.

For GFP immunofluorescence staining, brain sections were washed with KPBS and then incubated in rabbit anti-GFP antibody (1:15,000, Invitrogen, Walthan, MA) in KPBS with 0.4% Triton-X 100 for 48 hrs at 4°C. After incubation, the sections were washed and incubated in donkey anti-rabbit cy-2 (1:400, Jackson ImmunoResearch, West Grove, PA) in KBPS with 0.4% Triton-X 100 for 1 hr at room temperature. Brain sections were then washed with KPBS, mounted onto gelatin-coated slides, and coverslipped with buffered glycerol.

Data analysis

Results from the immunofluorescence study were examined on a Nikon 80i microscope a 40x magnification and images were acquired with a confocal microscopy system (Nikon C1-plus). Results from the mCherry/Ucn 3 double-labeling and the anterograde tracing study were examined at 40x magnification and acquired by a QImaging CCD camera (BioVision, Exton, PA) controlled by iVision software (BioVision, Exton, PA). A cell was considered to be mCherry-positive if it had brown cytoplasmic staining, and to be double labeled if it had a cluster of black grains representing Ucn 3 mRNA overlaying the brown staining. For the anterograde tracing study, black fibers with branching and nodules were considered mCherry-positive terminals, while smooth, featureless black fibers were identified as fibers of passage. The brightness and contrast of all images were adjusted in Adobe Photoshop (San Jose, CA) to provide optimal picture quality, and photo resolution was adjusted to 300 dpi before import into Canvas (version 8.0, ACD Systems, Seattle, WA) for assembly into plates. The mouse brain atlas by Paxinos and Franklin (2001) was used for schematic illustration of CRF, AVP, OXT, and Ucn 3 cells in the PVH as well as mCherry fibers and terminals in the mouse brain.

Results

Ucn 3-cre-mCherry reporter mice

To visualize Ucn 3 in the brain, Ucn 3-cre mice were crossed with a cre-dependent reporter mouse line, generating Ucn 3-cre-mCherry mice with mCherry expressed in Ucn 3-cre cells. As expected, a high degree of colocalization of Ucn 3 mRNA and mCherry labeling was observed in known Ucn 3 enriched areas including the PVHap (Fig. 3-1A-C), rPFH (Fig. 3-1D), and medial amygdala (Fig. 3-1E-F). Cells positive for mCherry but not Ucn 3 mRNA were also observed in a number of brain areas including the striatum that are not known to express Ucn 3 in adult mice (Fig. 3-1G). The ectopic mCherry expression in the Ucn 3-cre-mCherry mice is probably due to transient expression of cre during development, resulting in permanent expression of mCherry in these brain areas in adult mice. To test this hypothesis, a cre-dependent GFPf virus (Lindberg et al., 2013) was injected into the striatum of adult Ucn 3-cre-mCherry mice to determine if cre is expressed in this area in the adult mouse. We observed no GFP-positive cells or fibers in the striatum after viral injection (Fig. 3-1H), indicating that functional cre is not expressed in the striatum of adult Ucn 3-cre-mCherry mice.

Ucn 3 neurons are distinct from CRF, OXT, and AVP cells in the PVH

The PVH houses a number of well defined peptidergic cell populations including CRF, OXT, and AVP, and we assessed whether Ucn 3 neurons co-express any of these neuropeptides. To achieve this, we immunolabeled brain sections from Ucn 3-cre-mCherry mice for CRF and AVP or OXT and AVP. Ucn 3 cells in the PVH were located near the periventricular zone of the anterior parvicellular division (Figs. 3-2A, 3-3A, and

3-4A), and were separate from CRF, AVP, and OXT-positive neurons. As expected, CRF neurons appeared concentrated mainly in the parvocellular parts of the PVH (Figs. 3-2B-C and 3-4B-C). AVP (Figs. 3-2B, 3-3B, and 3-4B-C) and OXT (Figs. 3-3B-C and 3-4B-C) neurons had large cell bodies located in the magnocellular parts of the PVH. Additional OXT-positive neurons were seen in the parvicellular division of the PVH close to the third ventricle and along the borders of the PVH (Fig. 3-3A). A few AVP neurons were also found in the parvicellular part near the ventricular wall (Figs. 3-2B and 3-3B). Ucn 3 neurons and AVP neurons were clearly separate populations (Figs. 3-2B and 3-3B), as were CRF cells and Ucn 3 cells (Fig. 3-2B). A few OXT neurons and Ucn 3 neurons were nestled closely together in the PVHap and OXT-positive fibers intermingled with Ucn 3 neurons (Fig. 3-3A), but OXT and Ucn 3 immunoreactivity was not observed in the same cells. A separate group of Ucn 3 cells were observed just lateral to the PVH near the fornix in the rPFH (Fig. 3-3D). Fibers from OXT and AVP cells were seen extending from the PVH to the perifornical group of Ucn 3 cells (Fig. 3-3D).

Ucn 3, CRF, OXT, and AVP-positive fibers were also observed in the ME. While none of the fibers appeared to show double or triple labeling, they were in close proximity and appeared as large fiber tracts crossing through the area (Figs. 3-2D and 3-3E). Ucn 3 and CRF fibers coursed through the external zone of the ME (Fig. 3-2D) while AVP and OXT fibers were mostly confined to the internal zone (Fig. 3-3E).

Anatomical relationship of NPY or MSH fibers and Ucn 3 neurons in the PVHap

Both MSH and NPY fibers innervated the PVHap with distinct fiber distributions. MSH fibers heavily innervated PVHap areas where Ucn 3 neurons were concentrated

(Fig. 3-5A) and appeared to make contact with Ucn 3 cells (Fig. 3-5B). NPY fibers concentrated in the periventricular area of the PVH, with fewer fibers observed in Ucn 3 neuron-rich area (Fig. 3-5C). However, a number of NPY fibers and terminals were found in close proximity of Ucn 3 cell bodies (Fig. 3-5D).

Anterograde tracing of Ucn 3 neurons in the PVHap

To further define possible physiological functions of Ucn 3 cells in the PVHap, we determined their efferent projections. An anterograde adeno-associated virus (AAV) expressing a cre-dependent ChannelRhodopsin-mCherry reporter gene was injected into the PVHap area of Ucn 3-cre mice as previously described (Bochorishvili et al., 2014). Four animals with injection sites centered in the PVHap were included for analysis (Fig. 3-6). One of the four animals had minor spillover near the rPFH (Fig. 3-6H).

mCherry-positive fibers and terminals in PVHap-injected animals were found mostly in the hypothalamus, with fibers that coursed through the PVH, the perifornical area, the anterior hypothalamic nucleus (Figs. 3-7A and 3-8A-B), the lateral hypothalamic area (Figs. 3-7B and 3-8A-B), and the VMH (Figs. 3-7C-D and 3-8C-D). Fibers found in these areas, with the exception of the VMH, were mostly smooth fibers without extensive branching suggestive of fibers of passage. In the VMH, mCherry-positive fibers and terminals with branching and bouton-like structures were observed mostly in the dorsomedial part of the nucleus (Fig. 3-7C-D). Interestingly, the only other brain area where mCherry fibers and terminals were observed was in the MEex (Figs. 3-7E-F and 3-8C-D). The case in which the injection spilled into the rPFH area showed fibers in the lateral septal nucleus, confirming previous studies (Chen et al., 2011;

Wittmann et al., 2009a), while the cases with injections confined to the PVHap did not have any lateral septal nucleus fibers. A number of animals with the AAV vector injected into the median preoptic nucleus were also examined as a control (Fig. 3-9). We found that mCherry-positive fibers in these animals concentrated mostly in preoptic areas (the medial preoptic area, anteroventral preoptic nucleus, and vascular organ of the lamina terminalis), not extending into other areas of the brain (Fig. 3-9A-B).

Figures

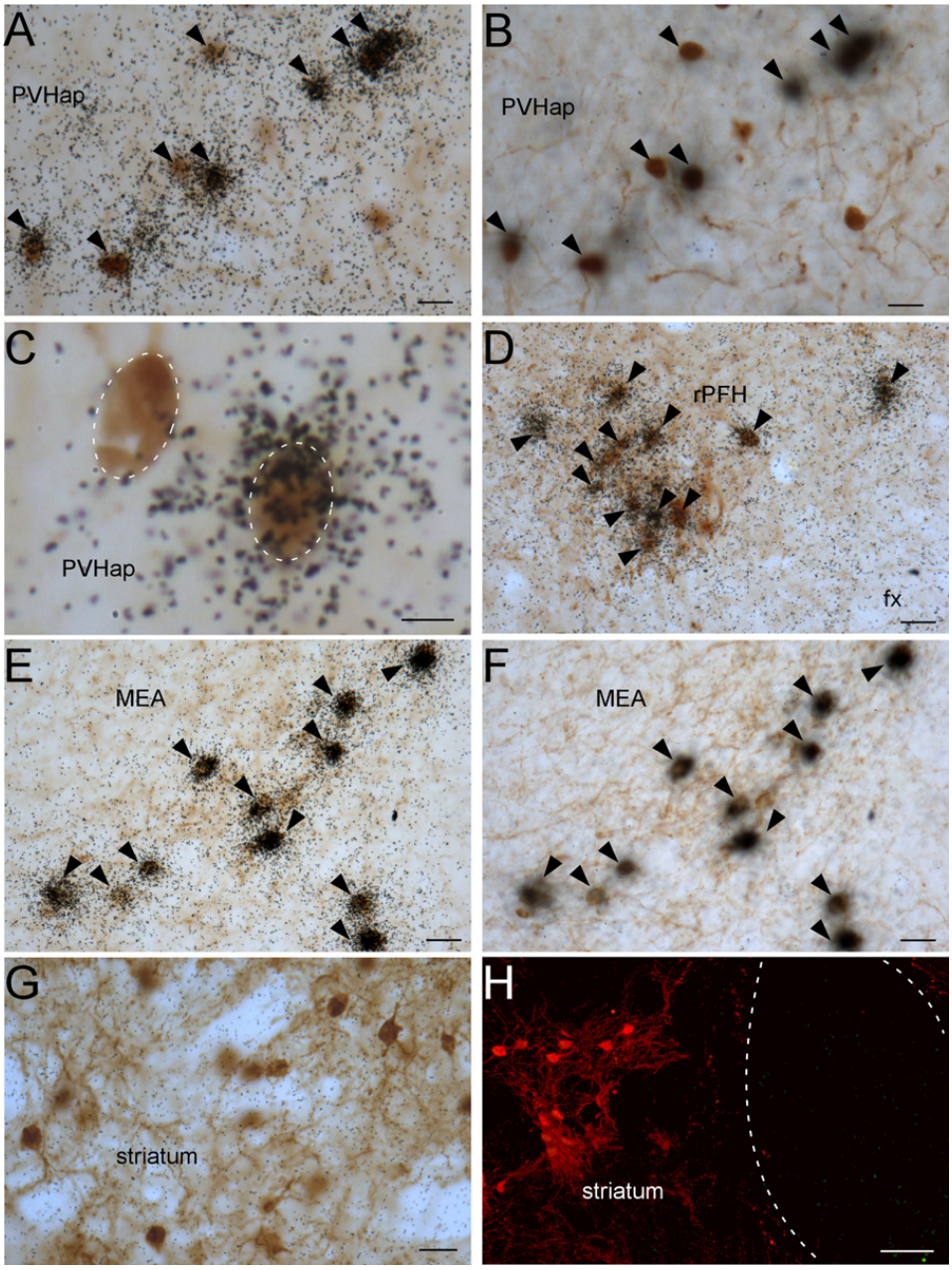

Figure 3-1. Validation of Ucn 3-cre-mCherry mice. The PVHap shows overlap of Ucn 3 mRNA (black grains, A) and mCherry cells (brown precipitate, B) in the PVHap. mCherry cells in the PVHap are either Ucn 3 mRNA-positive or ectopic expression (C). The rPFH (D) and MEA (Ucn 3 mRNA, E and mCherry, F) also show overlap of Ucn 3 mRNA and mCherry, while the striatum (G) does not. The mCherry-positive cells in the striatum do not have functional cre (H), as a cre-dependent fGFP AAV (injection site outlined) does not express GFP in the striatum. Scale bars = 20 µm (A, B, D-H) and 5 µm (C).

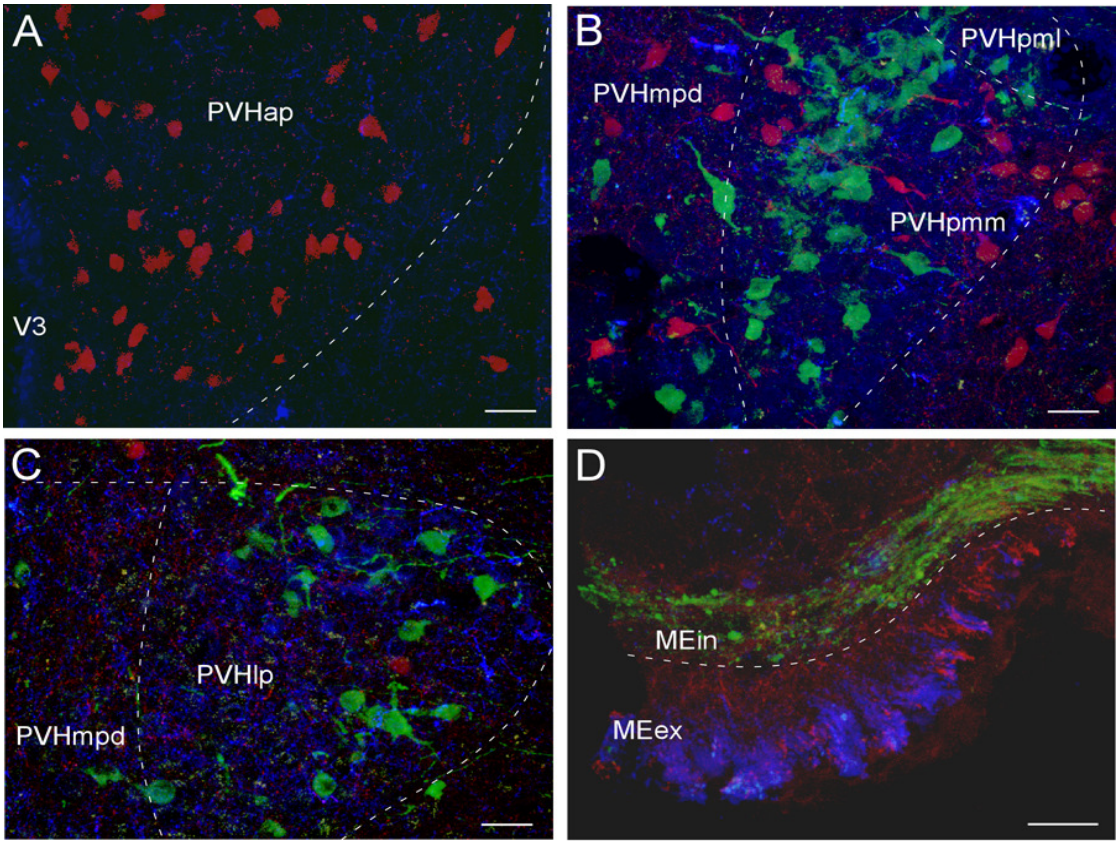

Figure 3-2. Representative confocal micrographs showing Ucn 3 (red), corticotropin-releasing factor (blue), and vasopressin (green) labeling neurons in the PVH (A-C) and ME (D). Abundant Ucn 3 neurons were observed in the PVHap (A) where scant corticotropin-releasing factor and vasopressin cells were found. Few Ucn 3 cells were found in the medial (B) and caudal (C) parts of the PVH, where there are abundant corticotropin-releasing factor and vasopressin neurons. In the ME (D), Ucn 3 and corticotropin-releasing factor fibers were observed in the external zone (MEex), whereas vasopressin fibers were found coursing through the internal zone of the ME (MEin). Scale bars = 10 µm.

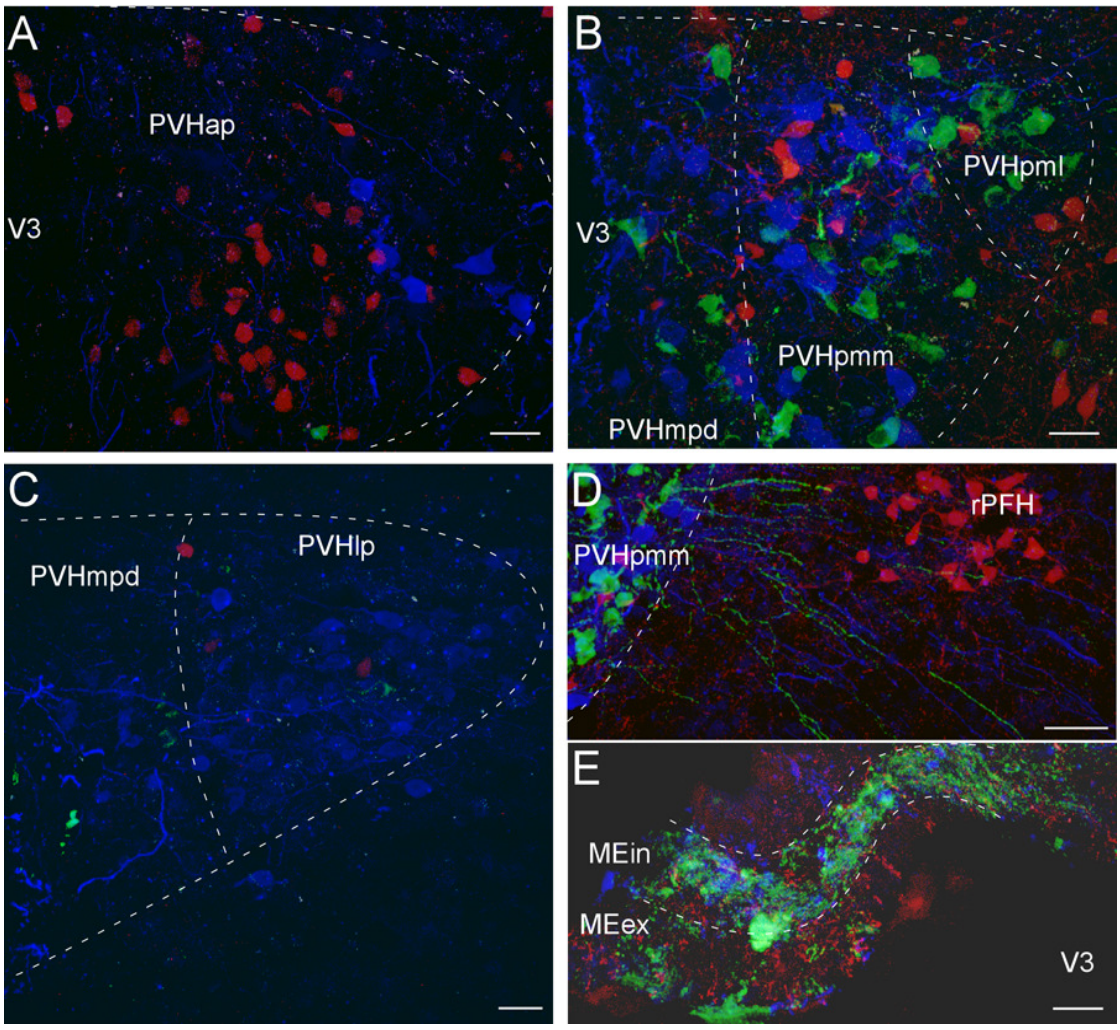

Figure 3-3. Representative confocal micrographs showing Ucn 3 (red), oxytocin (blue), and vasopressin (green) labeled neurons in the PVH (A-D) and ME (E). Abundant Ucn 3 and several oxytocin neurons were observed in the PVHap (A), with scant vasopressin cells. Few Ucn 3 cells were found in the medial (B) and caudal (C) parts of the PVH, where oxytocin and vasopressin neurons were abundant. Vasopressin and oxytocin fibers coursed through and around the rPFH group of Ucn 3 cells (D). In the ME (E), Ucn 3 fibers were observed in the external zone of the ME (MEex), whereas vasopressin and oxytocin were found primarily in the internal zone (MEin). Scale bars = 10 µm.

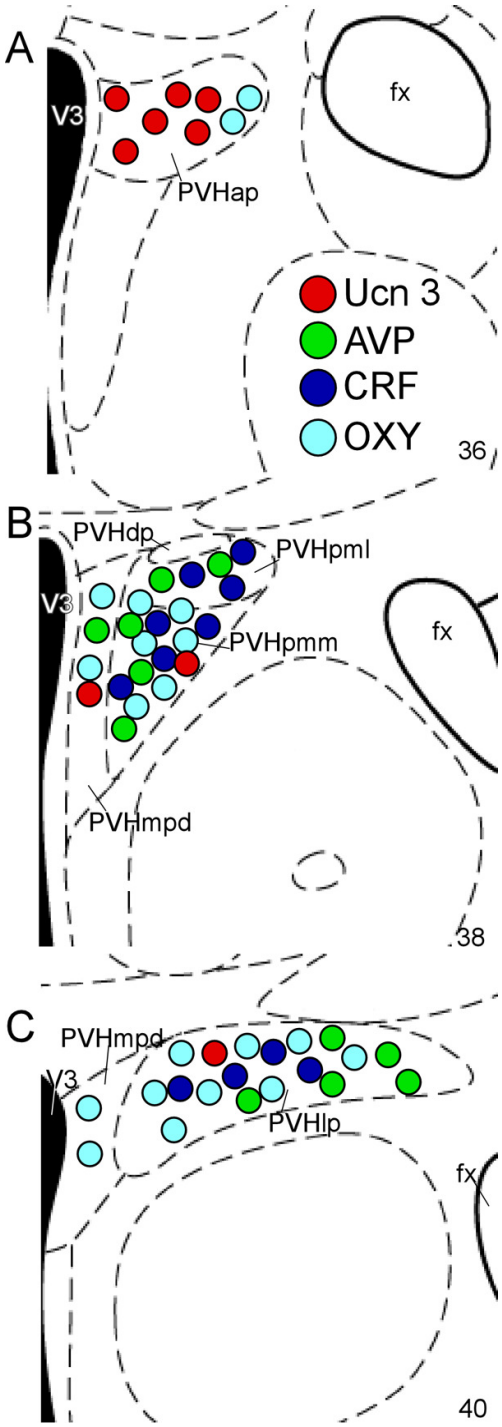

Figure 3-4. Summary of Ucn 3 (red), corticotropin-releasing factor (dark blue), oxytocin (light blue), and vasopressin (green) cell body locations in the PVH. The distribution is plotted onto a series of standard drawings of the mouse brain PVH that are arranged from rostral (A) to caudal (C).

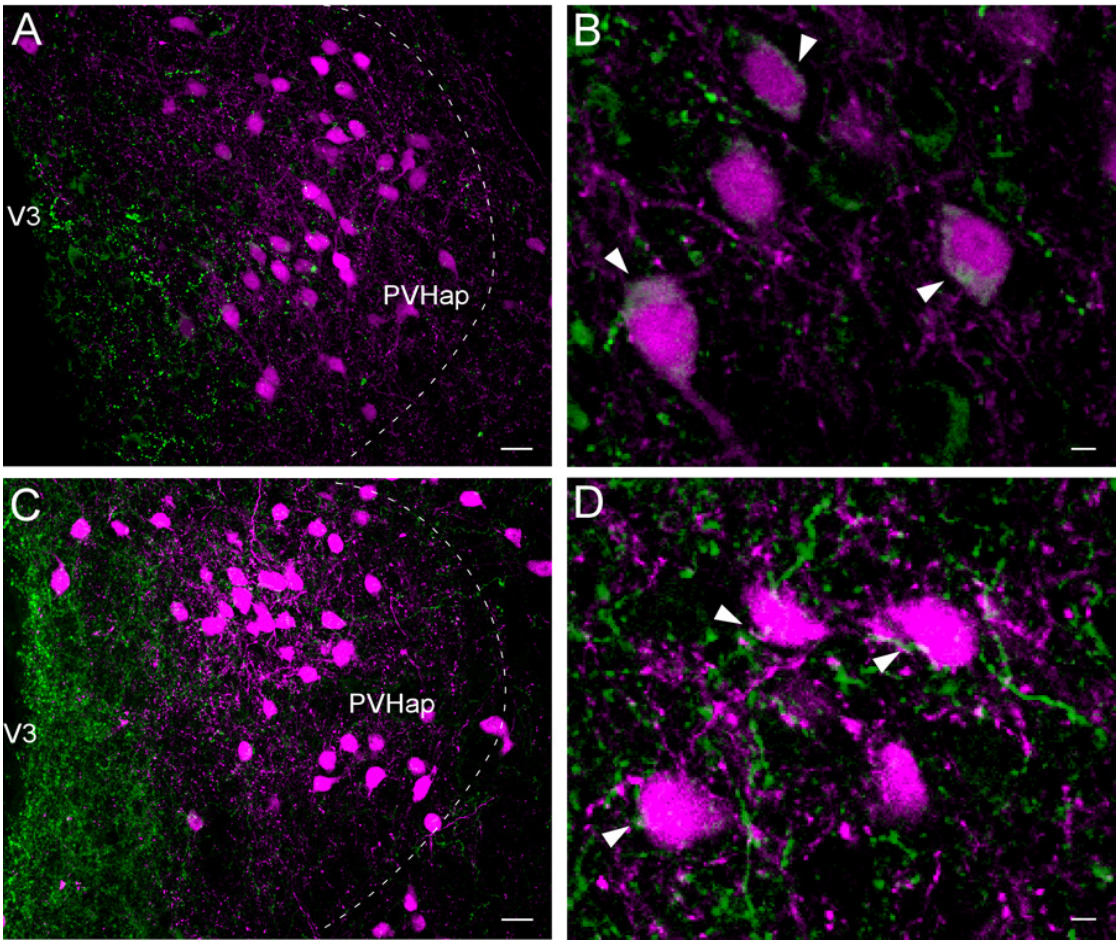

Figure 3-5. Ucn 3 (magenta) and melanocyte-stimulating hormone and Neuropeptide Y labeled fibers (green) in the PVHap. A confocal photomicrograph shows close apposition of Ucn 3 neurons and melanocyte-stimulating hormone fibers in the PVHap (A). A high magnification single optical section photomicrograph reveals intermingled Ucn 3 and melanocyte-stimulating hormone fibers (B, highlighted with white arrows). Ucn 3 neurons and Neuropeptide Y fibers are relatively separate in the PVHap (C). A high magnification single optical section photomicrograph shows a few intermingled Ucn 3 and Neuropeptide Y fibers (highlighted with white arrows, D). Scale bars = 10 µm (A, C) and 2 µm (B, D).

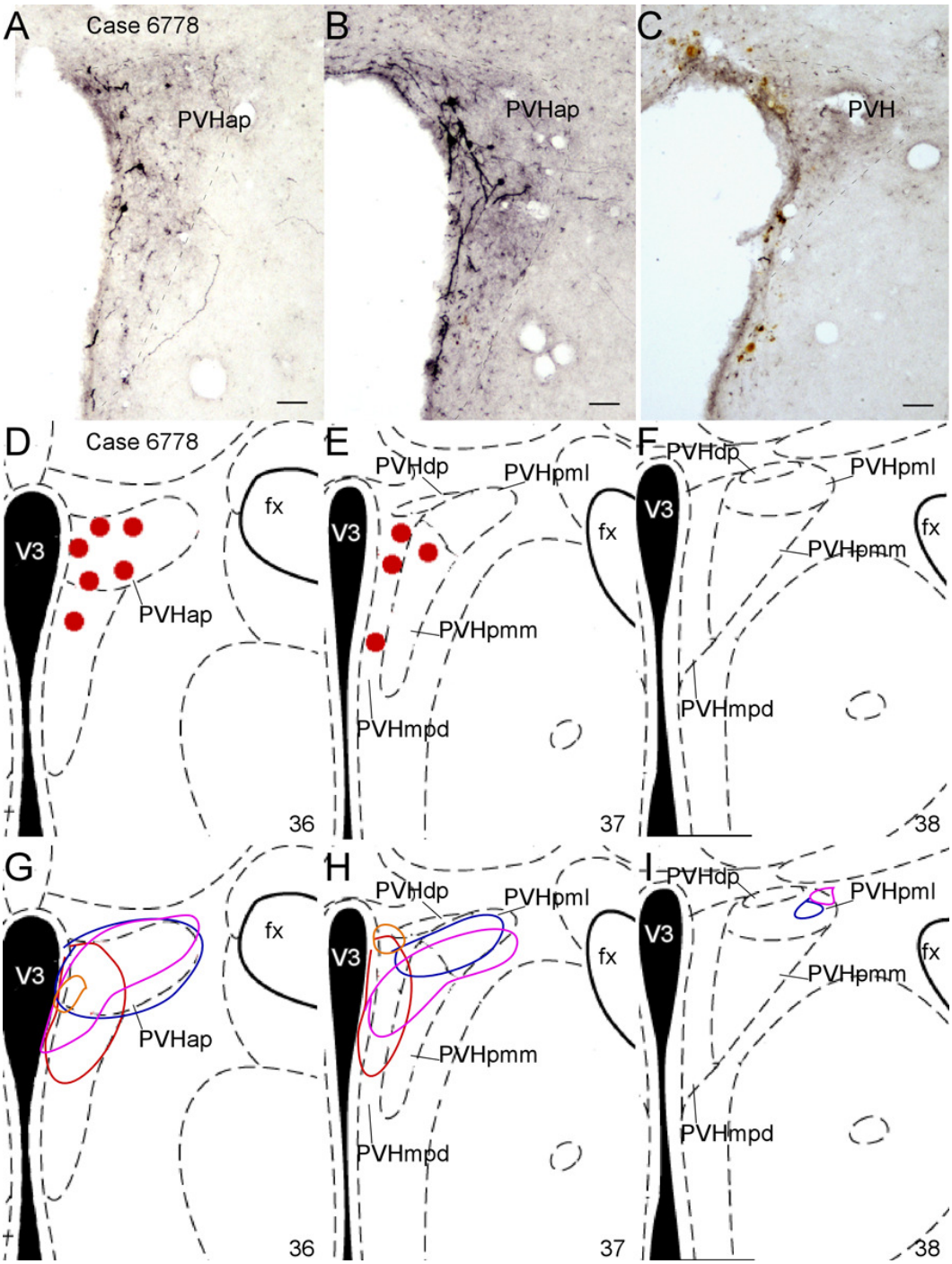

Figure 3-6. Anterograde tracer injection into the PVHap. Brightfield photomicrographs illustrating mCherry-labeled neurons (purple-black staining) in case 6778 after injection of an adeno-associated virus encoding cre-regulated mCherry into the PVHap of Ucn 3-cre mice (A-C). Schematic drawings of labeled neurons at injection site in case 6778 (D-F). Schematic drawings of the extent of labeled neurons at injection site of all animals included in the tracing study (G-I). The drawings or micrographs for each experiment are arranged from rostral to caudal (left to right), and the injection sites are represented in their entirety. Scale bars = 50 µm.

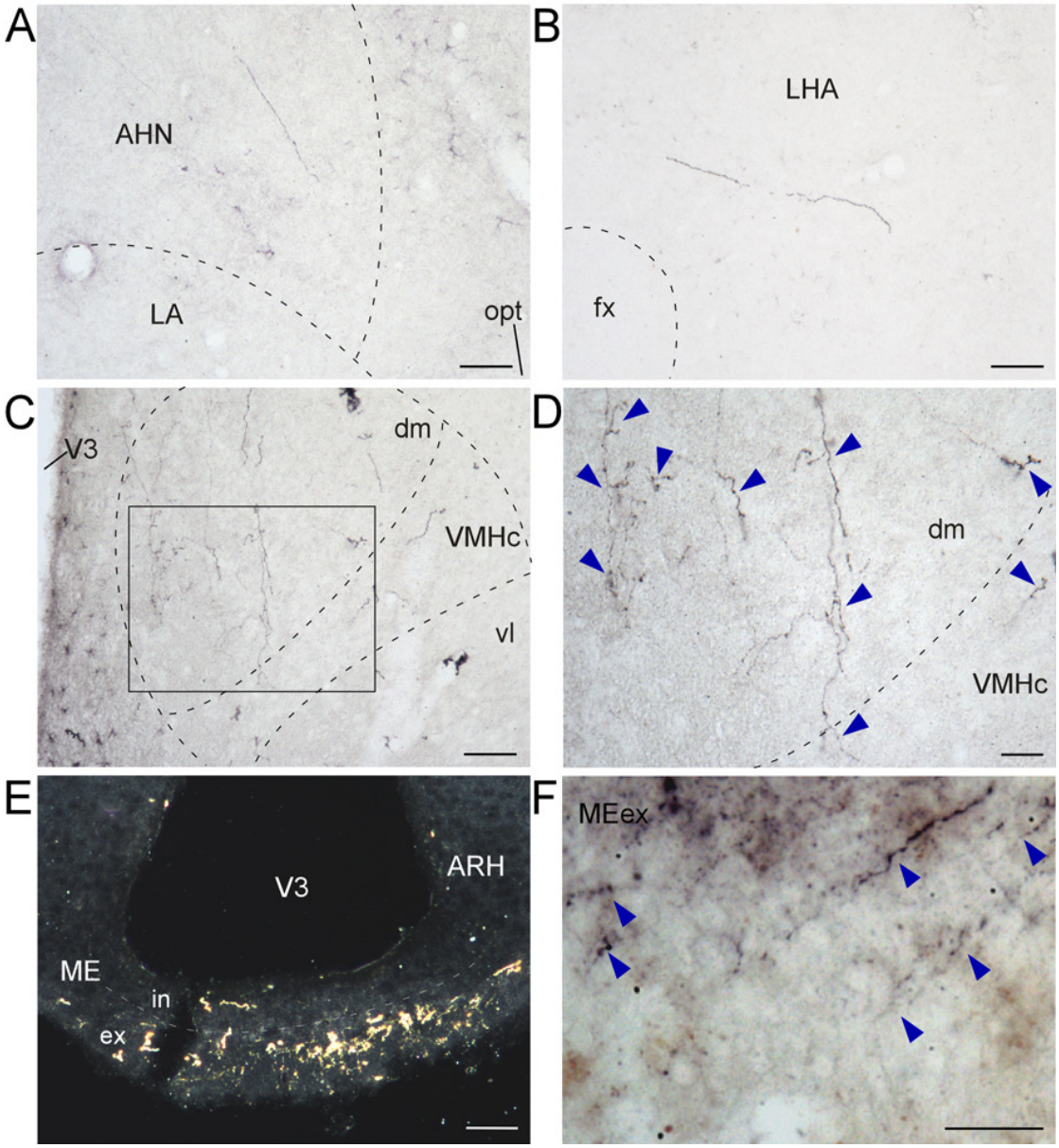

Figure 3-7. Ucn 3-positive fibers projecting from the PVHap to the VMH and ME. Brightfield photomicrographs show smooth mCherry-labeled fibers (purple-black color) of passage coursing through the anterior hypothalamus (A) and the lateral hypothalamic area (B). mCherry fibers were also in the ventromedial hypothalamic nucleus concentrated in the dorsomedial part (C). Many of the fibers had bouton-like structures and branching indicative of terminals (blue arrows, D). A darkfield photomicrograph shows Ucn 3 fibers (golden brown precipitates) within the median eminence concentrated in the external lamina (E). A high magnification brightfield photomicrograph shows terminal-like structures (blue arrows, F). Scale bars = 50 µm (A, C, E, F) and 20 µm (B, D).

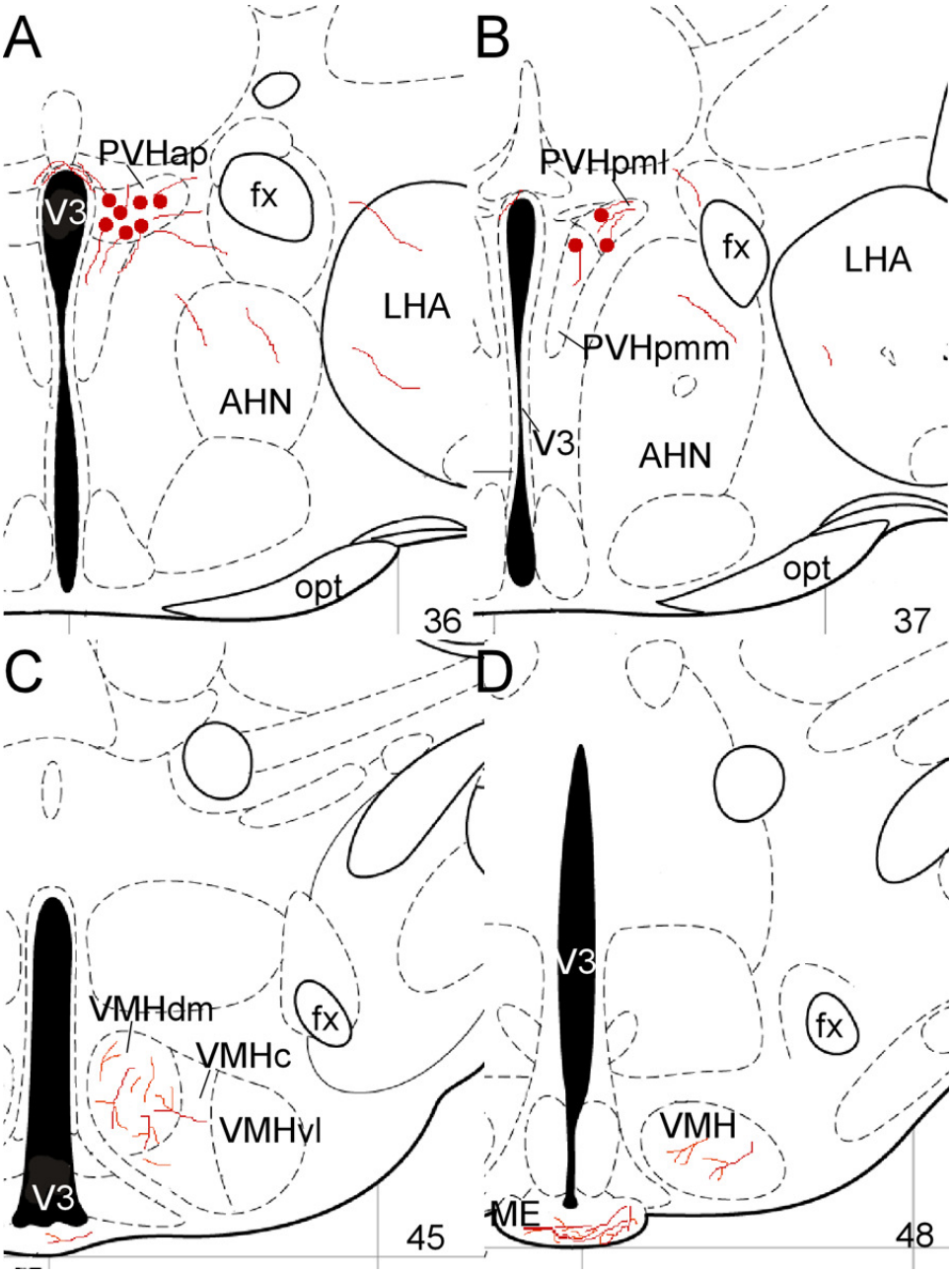

Figure 3-8. Summary of Ucn 3 projections from the PVHap. The distribution of mCherry-labeled fibers is plotted onto a series of standard drawings of the mouse brain that are arranged from rostral (A) to caudal (D). Notable areas are the ventromedial hypothalamus (C-D) and the external zone of the median eminence (C-D).

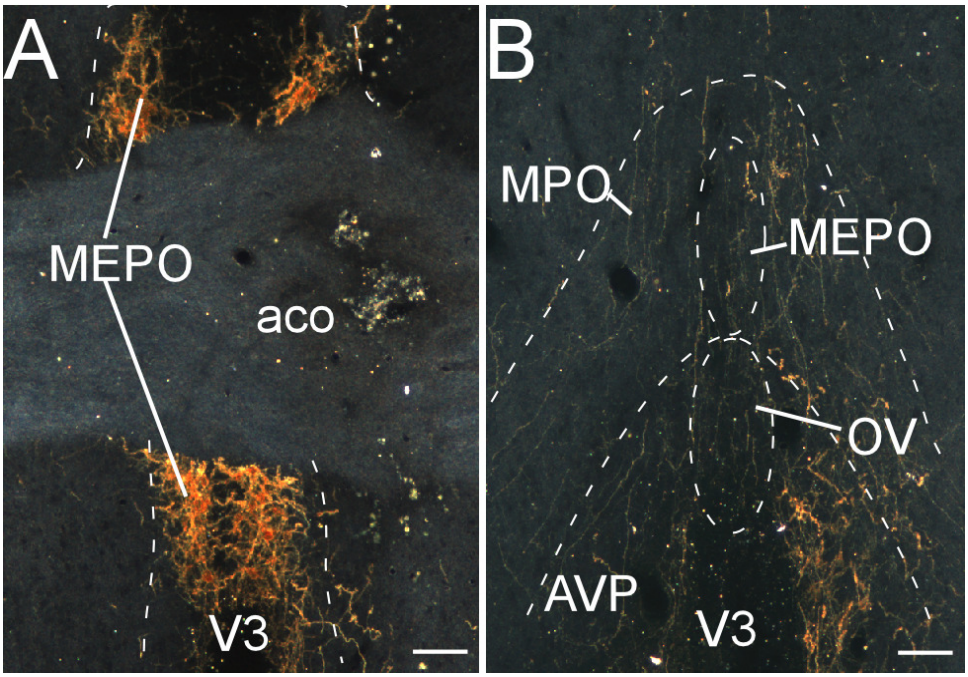

Figure 3-9. Ucn 3-positive fibers projecting from the median preoptic nucleus has a different projection profile than fibers from the PVHap. A darkfield micrograph photomicrograph illustrating mCherry-labeled neurons (golden staining) in case 6797 after injection of an adeno-associated virus encoding cre-regulated mCherry into the median preoptic nucleus of Ucn 3-cre mice (A). Darkfield micrograph showing that Ucn 3 fibers are restricted to the preoptic area (B). Scale bars = 50 µm.

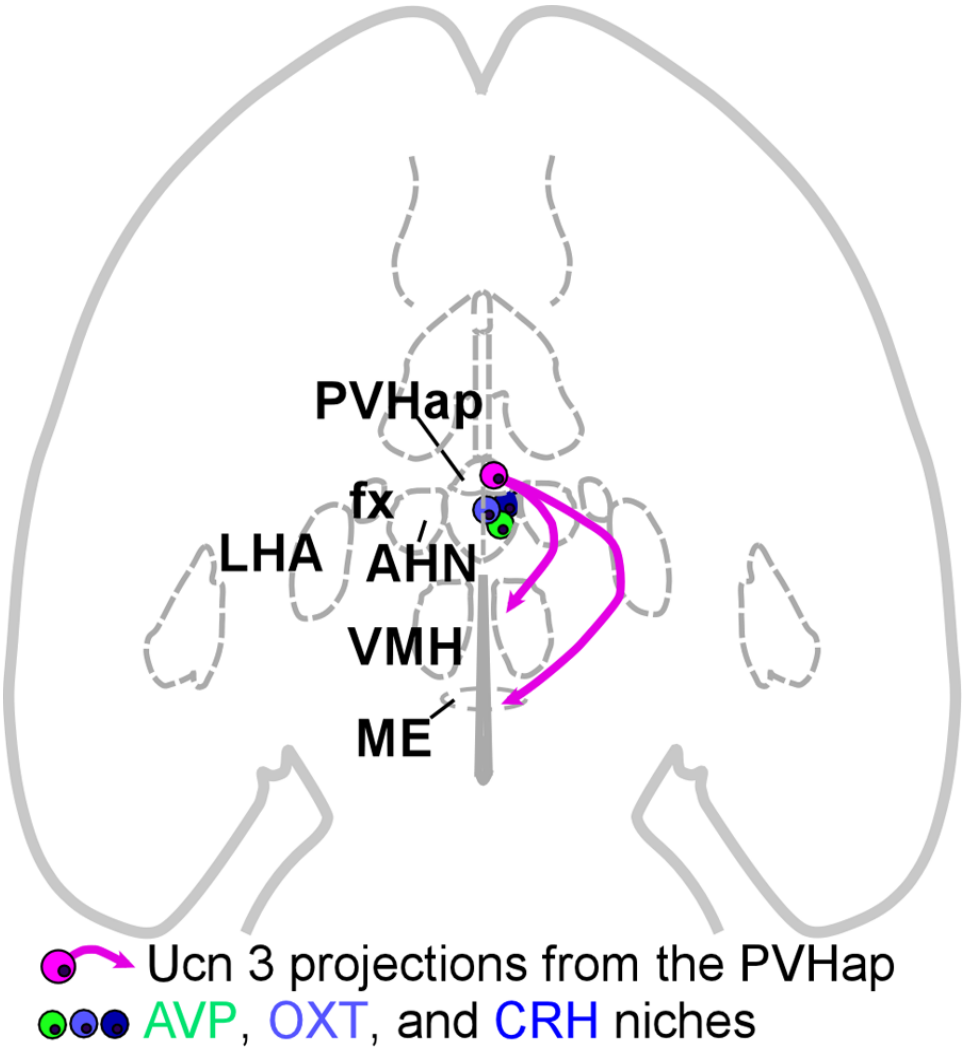

Figure 3-10. Summary of projections and Ucn 3 niche in the PVHap. Pink arrows show projection of Ucn 3 neurons in the PVHap traveling to the ventromedial hypothalamus and median eminence, and dots show relative locations of the Ucn 3, corticotropin-releasing factor, oxytocin, and vasopressin neurons in the PVH.

List of abbreviations used in figures:
aco, anterior commissure, olfactory limb
AHN, anterior hypothalamic nucleus
ARH, arcuate nucleus of the hypothalamus
AVP (anatomical), anteroventral preoptic nucleus
AVP (endocrine), vasopressin
CRF, corticotropin-releasing factor
fx, fornix
LA, lateroanterior hypothalamic nucleus
LHA, lateral hypothalamic area
MEA, medial amygdala
ME, median eminence
MEex, external zone of the ME
MEin, internal zone of the ME
MEPO, median preoptic nucleus
MPO, medial preoptic area
opt, optic tract
OV, vascular organ of the lamina terminalis
OXT, oxytocin
PVH, paraventricular nucleus of the hypothalamus
PVHap, anterior parvicellular part of the PVH
PVHdp, dorsal parvicellular part of the PVH
PVHlp, lateral parvicellular part of the PVH
PVHmpd, dorsal zone of the medial parvicellular part of the PVH
PVHpml, lateral zone of the posterior magnocellular part of the PVH
PVHpmm, medial zone of the posterior magnocellular part of the PVH
rPFH, rostral perifornical hypothalamus
V3, third ventricle
VMH, ventromedial hypothalamus
VMHc, central part of the VMH
VMHdm, dorsomedial part of the VMH
VMHvl, ventrolateral part of the VMH

Discussion

Ucn 3 has been shown to play a critical role in the brain in regulating energy homeostasis (Chen et al., 2010; Fekete et al., 2006; Jamieson et al., 2006; Ohata and Shibasaki, 2004; Pelleymounter et al., 2004; Telegdy et al., 2006) and, like other members of the CRF family, Ucn 3 expression in the brain is regulated by stress (Jamieson et al., 2006; van-Hover and Li, 2015; Venihaki et al., 2004). Our previous work determined that the PVHap is the main source of Ucn 3 afferent input to the VMH, a brain area well known to modulate energy balance and sympathetic outflow (Chen et al., 2011; Chen et al., 2012a; King, 2006), but other targets of these Ucn 3 neurons and their anatomical position among neuropeptides in the PVH were not known. The current study first characterized a novel mouse model for studying Ucn 3 anatomy by confirming a high degree of colocalization of Ucn 3 and mCherry in Ucn 3-cre-mCherry mice. This model then revealed that Ucn 3 neurons in the PVHap were not coexpressed with OXT, CRF, or AVP, indicating that Ucn 3 cells constitute a sub-population of the PVH (Fig. 3-10). In addition, MSH- and NPY-positive fibers, neuropeptides that innervate the PVH, were found to make close contact on Ucn 3 cells. Finally, the efferent projections of the Ucn 3 PVHap population were found to be very selective, terminating in the dorsomedial part of the VMH and the MEex (Fig. 3-10). The VMH projections confirmed an earlier study (Chen et al., 2011) but the ME projections were a novel discovery.

The soma of Ucn 3-positive neurons can be difficult to visualize with immunohistochemistry without using colchicines, which concentrates Ucn 3 in neuron cell bodies (Li et al., 2002; Wittmann et al., 2009a). The Ucn 3-cre-mCherry mice allow the visualization of Ucn 3 without using *in situ* hybridization or colchicines. Although the

present study showed that all Ucn 3 mRNA-labeled cells were also mCherry positive, there are limitations to this mouse model. There were a number of mCherry-positive cells that were not Ucn 3 mRNA-labeled, which may be due to a number of possibilities. First, the levels of Ucn 3 mRNA may be too low to be visualized by *in situ* hybridization, but high enough to allow expression of cre and thus mCherry. Secondly, the expression of mCherry may be due to transient expression of cre during development, resulting in permanent expression of mCherry in these cells. For example, prominent mCherry-positive cells were found in the striatum, an area that does not have detectable levels of Ucn 3 mRNA in adult animals (Li et al., 2002). Our study showed that these striatum neurons do not express functional cre in adult mice, indicating that the mCherry in the striatum of Ucn 3-cre-mCherry mice is likely due to a transient expression of Ucn 3 in this area during development. Nonetheless, we did not observe any colocalization of Ucn 3 and CRF, OXT, or AVP in the PVH even with the overrepresentation of Ucn 3 cells, thus reinforcing the notion that Ucn 3 neurons are a phenotypically distinct population in the PVH.

The PVH plays a critical role in an array of physiological regulations including autonomic nervous system activity, reproduction, growth, fluid regulation, adaptation to stress, and energy homeostasis (Ferguson et al., 2008; Herman et al., 2008). When activated, the PVH suppresses food intake; animals with PVH lesions are hyperphagic and become extremely obese (Atasoy et al., 2012). There are two broad divisions of the PVH: the magnocellular and parvicellular parts. The magnocellular division contains OXT and AVP-expressing neurons that project to the posterior pituitary, while the parvicellular neurons synthesize and release a number of neuropeptides including CRF

and TRH and project to several brain areas including the spinal cord and ME. CRF neurons in the parvicellular division of the PVH are critical in mediating the stress response, including the stimulation of the hypothalamic-pituitary-adrenal axis to release glucocorticoids (Pelleymounter et al., 2000; Perrin and Vale, 1999).

There was no colocalization of Ucn 3 cells and CRF in the PVH. CRF and Ucn 3 act on different receptors, with CRF favoring CRF_1 and Ucn 3 selective for CRF_2. Moreover, Ucn 3 and CRF fibers innervate distinct brain areas, implying different functional roles for the peptides (Bale and Vale, 2004; Li et al., 2002; Van Pett et al., 2000). CRF neurons in the PVH project to a number of brain areas including the MEex, the locus coeruleus, the ventral tegmental area, and the spinal cord (Ferguson et al., 2008; Lucas et al., 2013; Reyes et al., 2005; Rodaros et al., 2007; Swanson et al., 1983). Though the current study found that the Ucn 3 PVHap neurons also project to the MEex, there was no colocalization of CRF and Ucn 3 fibers in the MEex, confirming the divergent projection profiles of the two neuropeptides. Studies suggest that CRF_1 appears to be involved in the early phase of stress-induced anorexia while CRF_2 is important in late phase of hypophagia associated with stress (Bradbury et al., 2000). CRF in the PVH has been implicated in learning and memory in addition to stress responsiveness, suggesting that CRF has broad central actions (Lucas et al., 2013). The lack of colocalization in the PVHap between CRF and Ucn 3 solidifies the dual nature of the CRF family, working through separate receptors and in different parts of the brain. Both peptides are involved in stress-induced hypophagia but they appear to be acting on separate circuits at different phases of stress.

Though located on the same level of the PVH and often very close to one another, OXT and Ucn 3 cells were not colocalized, though OXT-positive fibers were found intermingling with Ucn 3 neurons. OXT-expressing neurons in the PVH have been implicated in a range of behaviors including satiation, learning and memory, and social behavior (Atasoy et al., 2012; Ferguson et al., 2001; Katsurada et al., 2014; Neumann and Landgraf, 2012; Sarnyai and Kovács, 2014). Atasoy and colleagues have shown that OXT neurons in the PVH are necessary for arcuate nucleus agouti-related peptide (AgRP) neuron-induced feeding (Atasoy et al., 2012). As Ucn 3 inhibits feeding (Ohata and Shibasaki, 2004), it is possible that Ucn 3 cells may be involved in modulating this circuitry. It is also possible, however, that Ucn 3 modulates stress-induced anorexia instead of the homeostatic feeding that the AgRP-OXT circuit regulates.

AVP and Ucn 3 did not appear to colocalize or show close apposition of fibers. AVP is involved in a range of functions, including social behavior, anxiety, and feeding (Langhans et al., 1991; Neumann and Landgraf, 2012), which probably do not involve Ucn 3. With the lack of colocalization of Ucn 3, OXT, CRF, and AVP, Ucn 3 occupies a unique niche within the PVHap.

NPY and MSH inputs into the PVH are closely linked to energy regulation (Cupples, 2003; Sobrino Crespo et al., 2014; Zigman, 2003). In the present study, NPY fibers generally avoided the PVHap area where Ucn 3 neurons are concentrated. MSH fibers, in contrast, were concentrated in the Ucn 3 neuron cluster, but both MSH and NPY fibers in the PVHap showed close apposition on Ucn 3 neurons. NPY fibers in the PVH originate from a number of cell populations including the arcuate nucleus and the dorsomedial nucleus of the hypothalamus (Sobrino Crespo et al., 2014; Zigman, 2003).

Conversely, MSH fibers in the PVH mostly arise from proopiomelanocortin (POMC)-positive neurons in the arcuate nucleus (Sobrino Crespo et al., 2014; Zigman, 2003). Functionally, NPY and MSH exert opposite actions on feeding (Schulz et al., 2010; Sobrino Crespo et al., 2014). NPY is released from AgRP/NPY expressing neurons and stimulates feeding, while MSH is released from POMC/cocaine-and amphetamine-regulated transcript (CART) expressing neurons and inhibits feeding (Schulz et al., 2010; Sobrino Crespo et al., 2014). This dichotomy is reflected at the cellular level, as MSH can stimulate a neuron that NPY inhibits (Ghamari-Langroudi et al., 2011). This may explain why neuropeptide fibers with such different actions were both seen on Ucn 3 cell bodies. Ucn 3 administered centrally inhibits food intake; MSH could be working in tandem with Ucn 3 to decrease food intake, while NPY could be inhibiting Ucn 3 to increase food intake (Fekete et al., 2006). More studies are needed to further determine the interaction of MSH, NPY, and Ucn 3.

Though we found that PVHap Ucn 3 neurons do not colocalize with major PVH neuropeptides, a previous study found that Ucn 3 and TRH, a peptide found in the PVH and perifornical area, have a complex pattern of colocalization (Wittmann et al., 2009a). The earlier report found that most Ucn 3 cells in the rPFH and some cells in the dorsal curve of the PVHap colocalize with TRH, though cells in the medial and ventral PVHap do not (Wittmann et al., 2009a). Our previous work also indicated an anatomical heterogeneity of the rPFH-PVHap Ucn 3 cells, as the rPFH neurons project primarily to the lateral septum while the PVHap Ucn 3 cells project to the VMH (Chen et al., 2011). Wittmann and colleagues showed that TRH-Ucn 3 double-labeled fibers were found in the lateral septal nucleus, posterior part of the bed nucleus of the stria terminalis, medial

amygdala, and VMH, suggesting that TRH/Ucn 3 neurons project to these areas (Wittmann et al., 2009a). In the current tracer study, we saw subtle but significant differences in projection targets with slight variation of injection sites. When restricted to the ventral and medial PVHap, the projections went only to the dorsomedial part of the VMH and the MEex. However, when the injection site included the dorsal PVHap and parts of the rPFH, there were more prolific projections that hit the dorsomedial part of the VMH, but also the lateral septal nucleus. Taken together, it appears that Ucn 3 neurons in the PVHap and rPFH may consist of a number of sub-populations, with some co-expressing TRH and projecting to an array of brain areas while some do not colocalize with TRH and project quite distinctly to the VMH and MEex.

There is a also population of Ucn 3 cells located in the median preoptic nucleus (Li et al., 2002), which is located rostral to the PVH. In the present study, a few animals with anterograde tracer injection sites in the median preoptic nucleus were included as controls. In general, these Ucn 3 neurons showed very local projections only to preoptic areas that express CRF_2. This reinforces the notion that the hypothalamic Ucn 3 population is anatomically heterogeneous, as all these different Ucn 3 sub-populations have distinct efferent projections. The functions of these different populations may be similarly diverse and need to be further investigated.

A novel finding in the present study was the identification of PVHap Ucn 3 projections to the MEex. Consistent with this observation, we also found mCherry-positive nerve fibers in the MEex of Ucn 3-cre-mCherry mice. These fibers were not positive for CRF or AVP, reinforcing the lack of colocalization of these neuropeptides in the PVH. The ME is a vitally important pathway connecting the brain to the portal blood

system and provides a means for neuropeptides released from hypothalamic neurons to reach the anterior pituitary (Rodriguez et al., 2010). The presence of Ucn 3 efferent fibers in the MEex suggests that Ucn 3 is released into the portal blood system and reaches the pituitary. CRF_2 has been shown to be expressed in the anterior pituitary in gonadotropes and may be involved in gonadotropin secretion (Kageyama et al., 2003). Successful reproductive cycles require tight control of the hypothalamic-pituitary-gonadal axis and precise release of hormones from the pituitary gonadotropes, and as such, are sensitive to disturbances like stress (Yin and Gore, 2010). CRF, working through CRF_1, can inhibit release of gonadotropin-releasing hormone and luteinizing hormone and is assumed to be the major mechanism for stress-induced reproductive suppression (Chand and Lovejoy, 2011). However, stimulation of CRF_2 both centrally and on gonatropes inhibits luteinizing hormone release (Li et al., 2005a; Nemoto et al., 2010), and, as CRF has low affinity for CRF_2, raises the possibility that Ucn 3 may modulate reproductive function at the level of the pituitary. Ucn 3 expression in the PVHap is stimulated by stress (van-Hover and Li, 2015) and we have now shown a pathway for Ucn 3 release into the portal blood system, where it may then bind CRF_2 on gonadotropes and suppress the secretion of reproductive hormones under stressful conditions. Clearly, more work needs to be done clarifying the possible role of Ucn 3 in reproduction.

Conclusions

The present study determined that Ucn 3 neurons in the PVH represent a neurochemically distinct population that is separate from CRF, OXT, and AVP cells. Projections from the PVHap Ucn 3 neurons are quite selective, targeting the dorsomedial

part of the VMH and the MEex, where Ucn 3 may contribute to stress-induced energy adaptation and modulation of reproduction.

4. Aim 3: Functional consequence of enhanced expression of Urocortin 3 in the anterior parvicellular part of the paraventricular nucleus of the hypothalamus

Abstract

Urocortin 3 (Ucn 3) is a neuropeptide expressed in neurons in the amygdala and hypothalamus. Central administration of Ucn 3 suppresses feeding, elevates blood glucose levels and body temperature, and activates the hypothalamic-pituitary-adrenal axis. Direct injection of Ucn 3 into the ventromedial hypothalamus (VMH) has been shown to potently suppress feeding and rapidly elevate blood glucose levels. Ucn 3 neurons in the anterior parvicellular part of the paraventricular nucleus of the hypothalamus (PVHap) provide the major Ucn 3 afferent input into the VMH. Together, these observations suggest that the Ucn 3 PVHap-VMH pathway contributes to energy homeostasis. In the current study, we tested this hypothesis in mice with enhanced Ucn 3 input into the VMH. We developed a viral vector to selectively overexpress Ucn 3 in the PVHap of male mice. A series of preliminary experiments were then conducted to validate Ucn 3 overexpression *in vitro* and *in vivo*. We found that chronically overexpressing Ucn 3 in the PVHap in mice modestly suppressed basal feeding but significantly elevated circulating glycerol levels, indicating enhanced levels of lipolysis. In conclusion, the Ucn 3 PVHap-VMH neuropathway appears to be involved in feeding and mobilizing fat stores. Moreover, the Ucn 3 overexpressing virus is a promising tool for studying the effect of enhanced Ucn 3 signaling in specific brain areas.

Introduction

Urocortin 3 (Ucn 3) is a member of the corticotropin-releasing factor (CRF) peptide family that plays a pivotal role in mediating the stress response. Central administration of Ucn 3 has been shown to increase body temperature, suppress feeding, elevate blood glucose levels, and stimulate hypothalamic-pituitary-adrenal (HPA) axis activity (Fekete et al., 2006; Jamieson et al., 2006; Ohata and Shibasaki, 2004; Pelleymounter et al., 2004; Telegdy et al., 2006; Telegdy and Adamik, 2008). Microinjection studies have identified the ventromedial hypothalamus (VMH) as an important brain area in mediating the effect of Ucn 3 on feeding and blood glucose levels (Chen et al., 2010; Fekete et al., 2006); reduced levels of the type 2 CRF receptor (CRF_2), the receptor for Ucn 3, in the VMH results in mild hyperphagia and increased adiposity (Chao et al., 2012). Considered together, these studies indicate that Ucn 3 signaling in the VMH contributes energy homeostasis. The Ucn 3-expressing neurons that provide input into the VMH originate primarily from a Ucn 3 cell group in the anterior parvicellular part of the paraventricular nucleus of the hypothalamus (PVHap), with moderate Ucn 3 input from the medial amygdala (Chen et al., 2011), implying that the effects of Ucn 3 actions in the VMH are moderated by either the PVHap or medial amygdala. As shown in Chapter 2, Ucn 3 expression in the PVHap is stimulated by stress (van-Hover and Li, 2015), raising the possibility that stress enhances Ucn 3 output from the PVHap, which then acts at the level of VMH to mediate stress-associated energy adaptation including suppression of feeding and stimulation of sympathetic outflow (de Kloet, 2013; Szabo et al., 2012).

To test this hypothesis, we have developed a viral approach to chronically overexpress Ucn 3 in the brain in a temporally- and spatially-specific manner. Our *in vitro* study showed that cells infected with the viral vector release high levels of functional Ucn 3. *In vivo* studies then showed that overexpression of Ucn 3 in the PVHap led to elevated Ucn 3 levels in terminals in the VMH, decreased basal feeding, and increased circulating glycerol levels, indicative of enhanced lipolysis activity. This preliminary study indicates that chronic elevation of Ucn 3 signaling in the VMH only modestly affects baseline food intake, but greatly promotes fat mobilization, presumably through stimulation of sympathetic outflow.

Materials and methods

Generation of a viral vector to temporally and spatially overexpress Ucn 3

A doxycycline (dox)-inducible, cre-dependent Ucn 3 expressing adeno-associated viral vector (AAV) to selectively overexpress Ucn 3 in distinct cell populations has been developed in collaboration with Dr. Perez-Reyes' lab at the University of Virginia. Briefly, a reverse tetracycline repressor (rtTR)-expressing cassette in reverse orientation with a cre-recognizing FLEX sequence (Schnutgen et al., 2003; Schnütgen and Ghyselinck, 2007) flanking both ends of the cassette was inserted into the upstream region of a dual Ucn 3- and GFP-expressing cassette in an AAV vector backbone (Fig. 4-1). A bi-directional mini-promoter consisting of seven copies of rtTR binding operator sequence (TetO) was inserted between the Ucn 3 and GFP coding sequence (Fig. 4-1). The expression of rtTR is normally silenced in cells due to reversed orientation of the expressing cassette. However, rtTR is expressed in cre-positive cells due to cre-mediated FLEX recombination that changes the orientation of the expressing cassette from the anti-sense to sense. The expressed rtTR binds and transactivates the bi-directional TetO operator between Ucn 3 and GFP coding sequences only in the presence of Dox (a *tet-on* system). This system thus allows us to induce over-expression of Ucn 3 and GFP in a time- and region-specific manner. The viral vector was then packaged into an adeno-associated virus (University of North Carolina viral core, Chapel Hill, NC).

In vitro validation of Ucn 3 o/e viral vector.

To test the efficacy of the AAV targeting plasmid in producing Ucn 3, three groups of HEK293 cells were transfected with the cre-regulated Ucn 3 o/e vector under

different cre/dox combinations: (1) cells expressing cre and treated with dox (+cre and +dox), (2) cells expressing cre not treated with dox (+cre and -dox), and (3) cells not expressing cre and not treated with dox (-cre and -dox). The media and lysate of each of these cell groups were collected 48 hours after the transfection for further analysis.

The levels of Ucn 3 in the media and lysate of these three groups were determined by a functional study. HEK cells stably expressing CRF_2 were maintained in growth media containing 10% fetal bovine serum with penicillin and streptomycin. On the day of the experiment, cells were incubated for 30 min with 0.1 mM 3-isobutyl-1-methyl-xanthine and then treated with the test solutions for 20 min. The test solutions were the media or lysate of the vector-infected cells, various concentrations of Ucn 3, or forskolin. After the incubation, cells were lysed with 0.1 N HCl in 95% ethanol for one hour at 4°C. Supernatants were then assayed for cAMP levels with a commercial EIA kit (Biomedical Technologies Inc., Stoughton, MA) by following the instructions provided by the manufacturer. Protein levels were determined by Bradford assay.

Viral injection

A cohort of Ucn 3-cre-mCherry mice were anesthetized with isoflurane and placed in a stereotaxic apparatus (David Kopf Instruments, Tujunga, CA). A Hamilton microsyringe was filled with the cre-regulated Ucn 3 o/e viral vector and bilaterally inserted into the PVHap. 150 nL of the vector was injected with perifusion pump. The stereotaxic coordinates for the PVHap were: 0.37 mm rostral and +/-0.18 mm lateral to bregma, and 5.5 mm ventral to the dura. Animals were allowed to recover for one week and then began the experimental paradigms. At the end of the experiments, animals were

perfused with 4% paraformaldehyde (pH 9.5). The brains were removed and sectioned coronally at 25 μm thickness with a sliding microtome and stored in cryoprotectant at -20°C until use.

In vivo validation of Ucn 3 o/e viral vector

Adult male Ucn 3-cre-mCherry mice injected with the Ucn 3 o/e viral vector into the PVHap were fed with control diet (AIN-93 base diet D12101801 from Research Diets, New Brunswick, NJ, kindly provided by Dr. Perez-Reyes) or dox chow (AIN-93 base diet D12101801 with 100 ppm doxycyline from Research Diets) for two weeks before perfusion. Brains were removed and sectioned, and sections were then processed for immmunofluorescence for GFP. mCherry fluorescence was used as a proxy for Ucn 3 neurons, and GFP was used as a marker for virally-infected cells that responded to dox treatment. For GFP immunofluorescence, brain sections were washed with potassium phosphate-buffered saline (KPBS) and then incubated in rabbit anti-GFP antibody (1:1,000, Invitrogen, Walthan, MA) in KPBS with 0.4% Triton-X 100 for 48 hrs at 4°C. After incubation, the sections were washed and incubated in cy-2 conjugated donkey anti-rabbit (1:400) for 1 hr at room temperature. Brain sections were then washed with KPBS, mounted onto gelatin-coated slides, and coverslipped with buffered glycerol.

Ucn 3 levels were determined immunohistochemically in Ucn 3 o/e virus-injected mice fed with dox chow or control chow. For Ucn 3 immunohistochemistry, brains were washed with KPBS and then incubated in rabbit anti-Ucn 3 antibody (code: #6570, 1:10,000; generously provided by the laboratory of Dr. Wylie Vale, The Salk Institute, La Jolla, CA) in KPBS with 0.4% Triton-X 100 for 48 hrs at 4°C. After incubation, the

sections were washed and incubated in biotinylated donkey anti-rabbit IgG (1:600, Jackson ImmunoResearch, West Grove, PA) for 1 hr at room temperature. They were then washed and incubated for 1 hr at room temperature in avidin-biotin complex solution (Vectastain ABC Elite Kit, Vector Laboratories, Burlingame, CA). A 3,3diaminobenzdine (DAB) reaction was used as a chromogen to visualize Ucn 3 immunoreactivity. After the color development, brain sections were washed with KPBS, mounted onto gelatin-coated slides, dehydrated, and cover slipped with Permount.

Food intake and energy mobilization under chronic Ucn 3 overexpression

A separate cohort of Ucn 3-cre-mCherry mice was injected with the cre-regulated Ucn 3 o/e virus and was fed with control chow for one week to establish baseline feeding. The mice were then switched to chow containing dox for one week. Food intake and body weight were monitored daily. Another cohort of mice with no viral injection or experimental manipulation was fed the control chow and dox chow to determine potential diet taste preference; food intake and body weight were monitored daily.

To determine plasma glycerol and triglyceride levels, blood samples were collected from mice with the Ucn 3 o/e virus fed either dox or control chow at the end of the above food intake experiment and before euthanization. The blood samples were centrifuged at 4°C for 10 min to remove blood cells. The plasma was collected and stored at -80°C for later analysis. The Free Glycerol Reagent kit (Sigma, St. Louis, MO) was used to measure glycerol and triglyceride levels. The assay was performed in duplicate following the manufacturers' protocols.

Statistical analysis

Data are expressed as mean +/-SEM in each graph. The effects of treatment on cAMP levels were analyzed using a one-way ANOVA with Dunnett's multiple post hoc comparisons comparing the treatments to the control. Statistical significance of plasma glycerol and triglyceride levels was evaluated using an unpaired Student's *t* test to compare the means of mice treated with control vs. dox chow. Statistical significance of food intake was evaluated using a paired Student's *t* test to compare the means of the control vs dox chow fed mice. Level of significance for both tests was set at $p<0.05$.

Results

In vitro validation of Ucn 3 o/e viral vector

Three groups of HEK cells were transfected with the cre-regulated Ucn 3 o/e vector (Fig. 4-1): (1) cells expressing cre and treated with dox (+cre and +dox), (2) cells expressing cre not treated with dox (+cre and -dox), and (3) cells not expressing cre and not treated with dox (-cre and -dox). The media and lysate of each of these cell groups were collected to treat HEK cells stably expressing CRF_2. The CRF_2-expressing cells were then lysed to determined cellular levels of cAMP as readout of CRF_2 activation. CRF_2-expressing cells treated with control media had negligible cAMP levels (Fig. 4-2). Ucn 3 stimulated an increase in intracellular cAMP levels in a dose dependent manner and forskolin (0.5 μM), which activates adenylyl cyclase, also stimulated cAMP production (Fig. 4-2). As expected, lysate and media from cells lacking either cre expression or dox treatment (-cre -dox and +cre -dox media/lysate) had minimal levels of cAMP production as compared to controls (Fig. 4-2). Importantly, CRF_2-expressing cells treated with the media and lysate from cre-positive, dox treated cells transfected with Ucn 3 o/e vector (+cre and +dox media/lysate) showed elevated levels of cAMP (Fig. 4-2) similar to that in cells treated with 1.0 nM Ucn 3.

In vivo validation of Ucn 3 o/e viral vector

To determine if the viral vector can induce Ucn 3 overexpression *in vivo*, the Ucn 3 o/e viral vector, which expresses Ucn 3 and GFP under the control of dox, was injected into the PVHap of the Ucn 3-cre-mCherry mice. The mice were then fed control chow or dox chow for two weeks after recovery from surgery. As shown in Fig. 4-3, there was a high degree of colocalization of GFP (Fig. 4-3A) and mCherry (Fig. 4-3B) in the PVHap

area of mice fed with dox chow (Fig. 4-3C), indicating that the GFP was expressed in Ucn 3-positive cells and was induced by dox. On the other hand, no GFP was observed in the brains of mice fed with a control diet (data not shown). It was estimated that about 55% of mCherry-positive cells were also GFP-positive, while nearly all GFP-positive cells were mCherry-positive (Fig. 4-3).

To validate overexpression of Ucn 3, immunohistochemistry for Ucn 3 was performed to examine the level of Ucn 3 in the brain in virus-injected, dox-treated mice. Compared to control diet treated animals (Fig. 4-4A), there were more Ucn 3-positive cells in dox treated animals (Fig. 4-4B) in the PVHap. Qualitatively, Ucn 3 immunoreactivity appeared to be more intense in dox-fed mice than in control diet mice (Fig. 4-4A-B). Importantly, there was more prominent Ucn 3 fiber staining in the VMH, the target of Ucn 3 PVHap neurons, of dox chow-treated mice (Fig. 4-4D) compared to that in control chow treated animals (Fig. 4-4C).

Effect of selective, chronic Ucn 3 overexpression on food intake

Virus injected mice were fed with control chow diet for seven days to establish baseline food intake, and then switched to dox food for an additional seven days. Food intake was monitored daily (Fig. 4-5A). Mice fed with dox chow showed a modest but significant decrease in average daily food intake compared to baseline control diet feeding (Fig. 4-5B-C; $p<0.05$). Interestingly, during days 10-13 of dox treatment, food intake of dox treated mice showed a wave-like pattern (Fig. 4-5A).

To examine potential distaste for the dox diet, mice with no virus injection were fed with control diet or dox chow and food intake was monitored daily. No differences

were observed in the average daily intake of mice fed control chow (3.7 +/- 0.2 g) and those fed with dox chow (3.8 +/- 0.1 g).

Effect of selective, chronic Ucn 3 overexpresssion on glycerol and triglyceride levels

To examine the effect of enhanced Ucn 3 on mobilization of energy stores, glycerol and triglyceride levels of animals with the Ucn 3 o/e virus fed either dox chow or control chow were determined. Plasma glycerol levels were significantly elevated in animals fed with dox chow (Fig. 4-6; $p<0.05$) while triglyceride levels showed a non-significant trend toward an increase in mice fed with dox chow compared to control chow (Fig. 4-6).

Figures

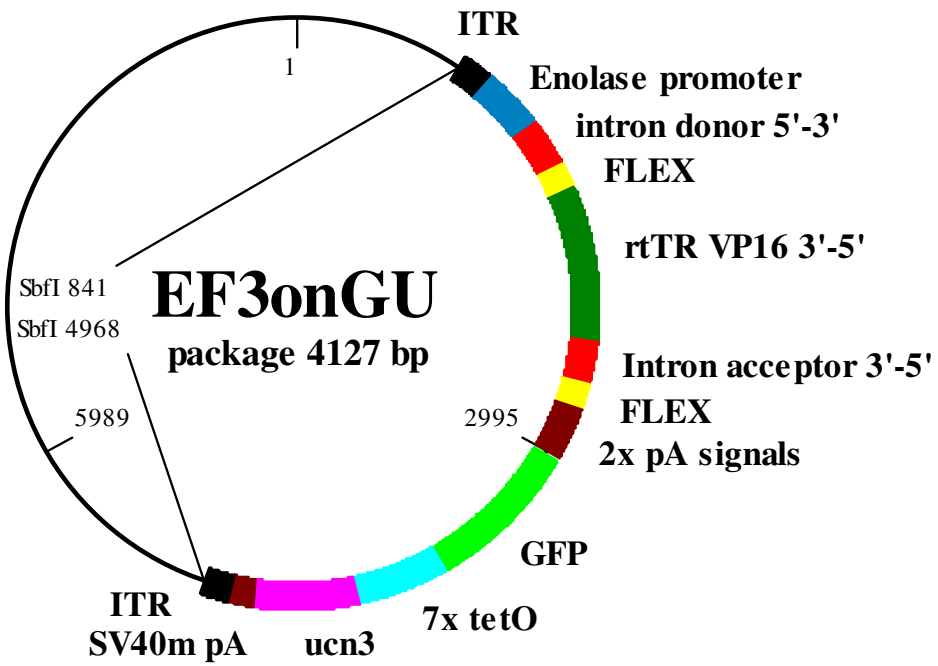

Figure 4-1. The cre and dox dependent Ucn 3 overexpressing vector. This viral vector allows for cell-, time-, and site-specific overexpression of Ucn 3. A cre-recognizing FLEX sequence was inserted at both ends of the reverse tetracycline repressor (rtTR) cassette, which was controlled by an enolase promotor. In the presence of cre, cre-mediated recombination of FLEX changes the orientation of rtTR cassette from anti-sense to sense. The expressed rtTR binds and transactivates the tetO operator flanking both Ucn 3 and GFP to transcribe these genes bidirectionally only in the presence of dox. The result is overexpression of Ucn 3 in cre-positive cells under dox treatment.

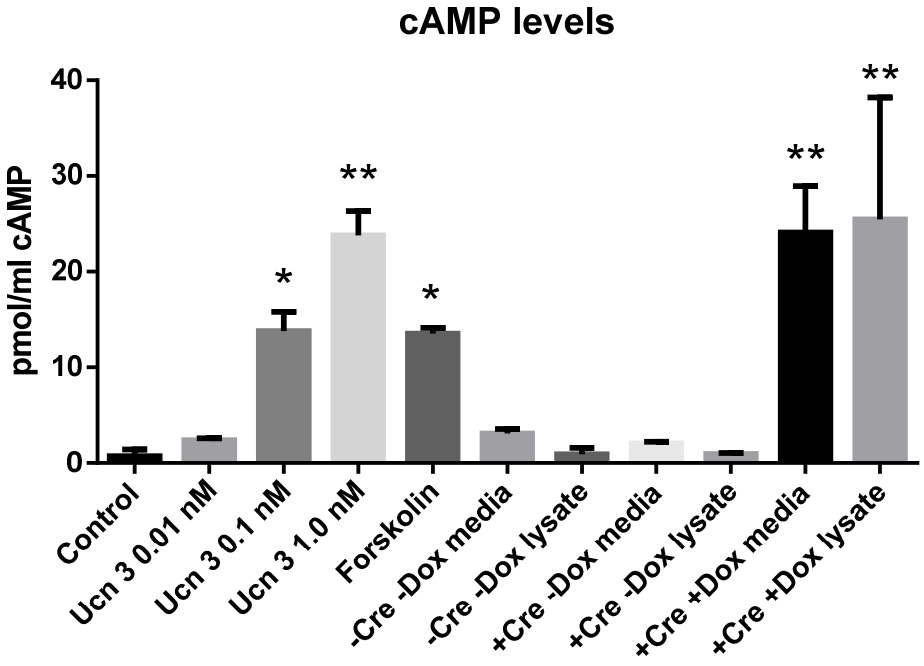

Figure 4-2. *In vitro* validation of Ucn 3 overexpressing viral vector. Intracellular levels of cAMP in CRF_2-expressing cells were measured after treatment with media and lysate from cells transfected with the Ucn 3 o/e vector. Only media and lysates from cells expressing cre and treated with dox induced a signfiant increase in cAMP production in the CRF_2-expressing cells. *$p<0.05$, **$p<0.01$ with one way ANOVA with Dunnett's multiple post hoc comparisons.

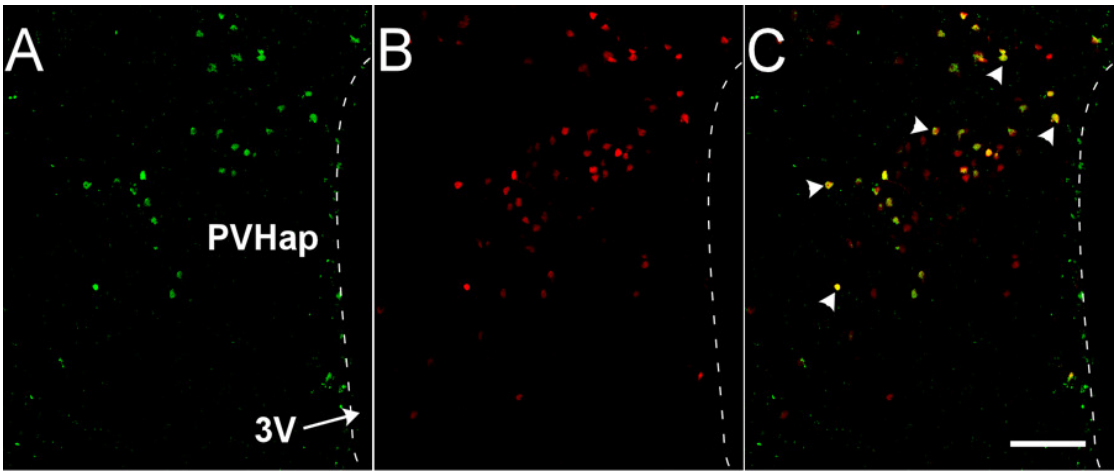

Figure 4-3. *In vivo* validation of Ucn 3 overexpressing viral vector through GFP and mCherry immunofluoresence. Representative confocal images showing GFP immunofluorescence (A) and mCherry (B) in the PVHap area of a Ucn 3-cre-mCherry mice injected with the Ucn 3 overexpressing viral vector and fed with dox chow. The merged image (C) of A and B shows that many double labeled cells were found in the PVHap area. 3V: third ventricle, PVHap: anterior parvicellular part of the paraventricular nucleus of the hypothalamus. Scale bar = 50 μm.

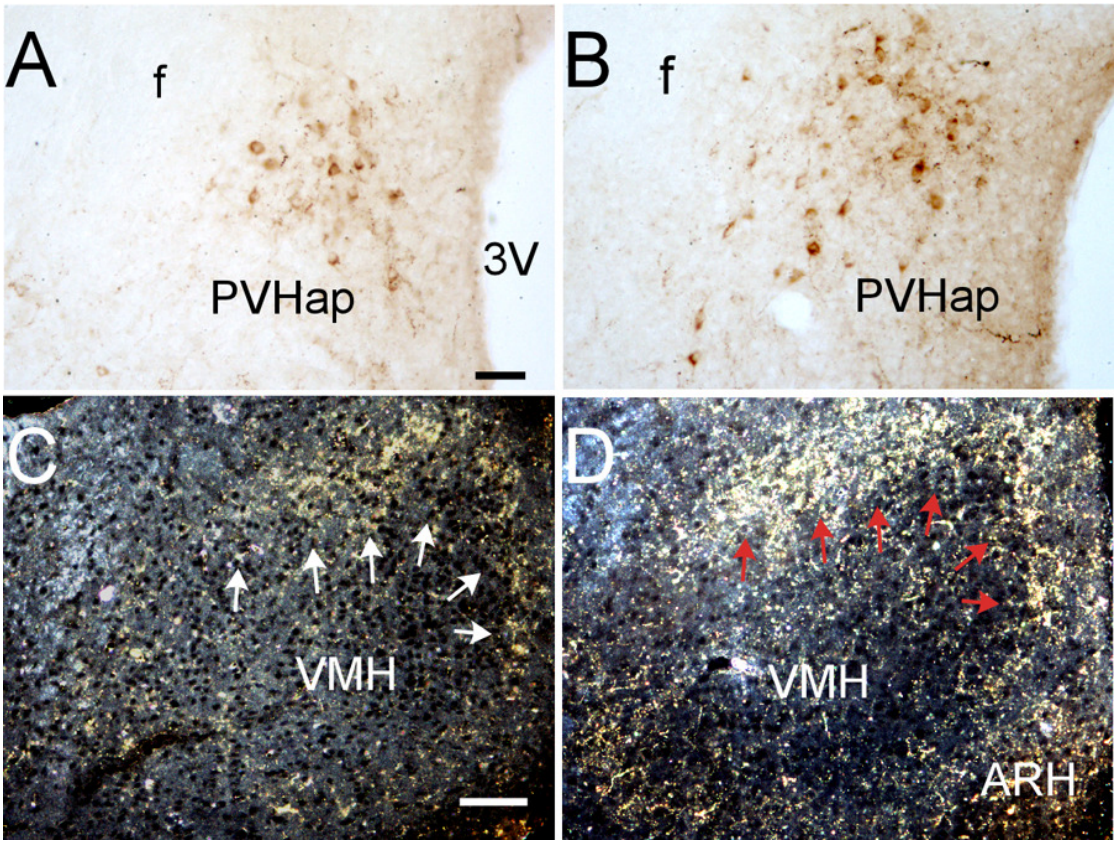

Figure 4-4. *In vivo* validation of Ucn 3 overexpressing viral vector through Ucn 3 immunohistochemistry. Representative photomicrographs showing the PVHap (A, B) and the VMH (C, D) of Ucn 3 overexpressing viral vector-injected mice fed with either control (A, C) or dox chow (B, D) for two weeks. More apparent Ucn 3 immunoreactive cells (identified by brown precipitates) were found in the PVHap of dox fed mice (B) compared to that in control fed mice (A). More abundant Ucn 3 nerve fibers and terminals (gold color staining) were observed in the VMH of dox chow fed mice (D, indicated by red arrows) compared to that in control mice (C, indicated by white arrows). 3V: third ventricle, ARH: arcuate nucleus of the hypothalamus, f: fornix, PVHap: anterior parvicellular part of the paraventricular nucleus of the hypothalamus, VMH: ventromedial hypothalamus. Scale bar = 50 μm.

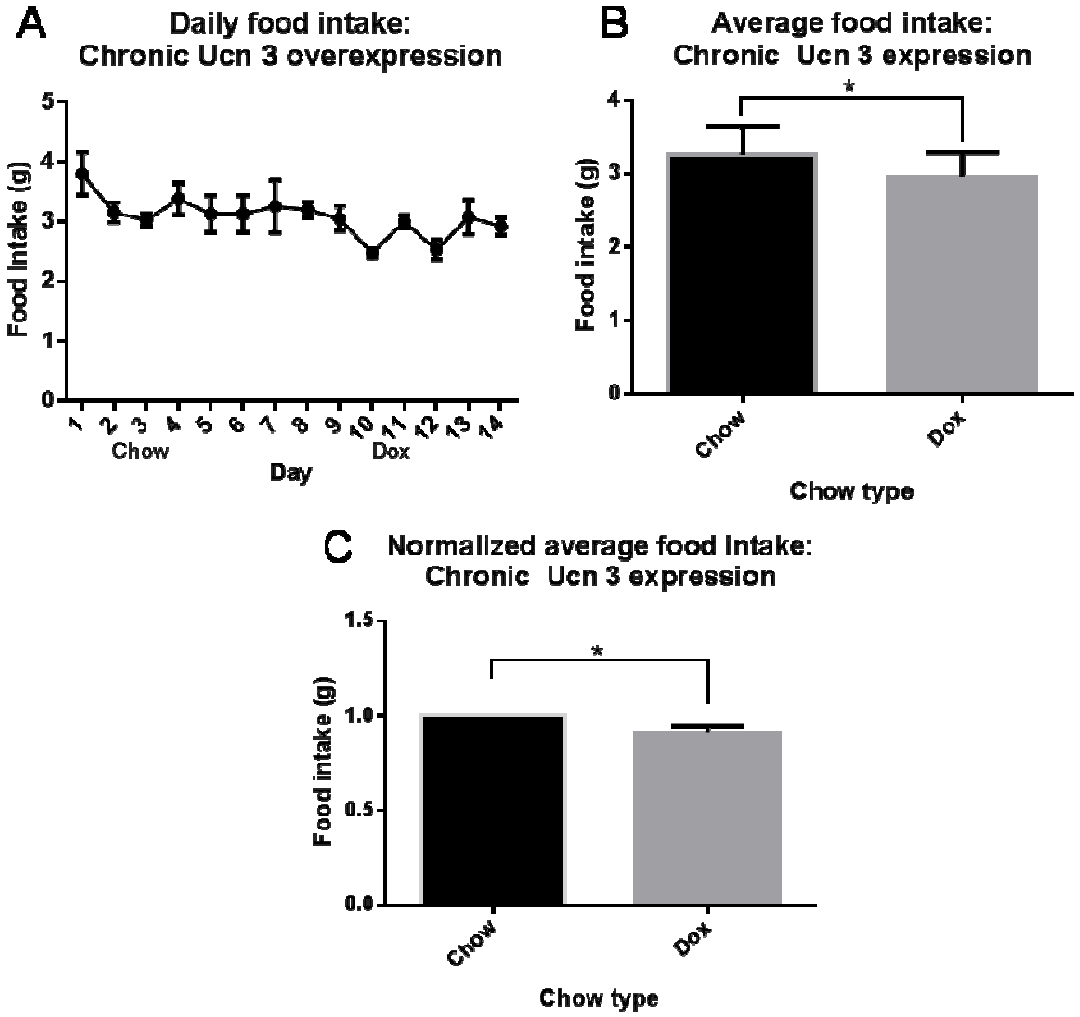

Figure 4-5. Daily basal food intake under chronic Ucn 3 overexpression. Mice (n=4) injected with the Ucn 3 o/e virus were fed control chow (Chow) for seven days to establish baseline food intake and then were fed with dox (Dox) chow for seven days. Daily food intake was monitored (A). Average daily food intake was significantly decreased when mice were fed dox chow compared to control chow, *p<0.05 (B). Daily dox chow intake normalized to control chow intake was reduced by about 10%, *p<0.05 (C).

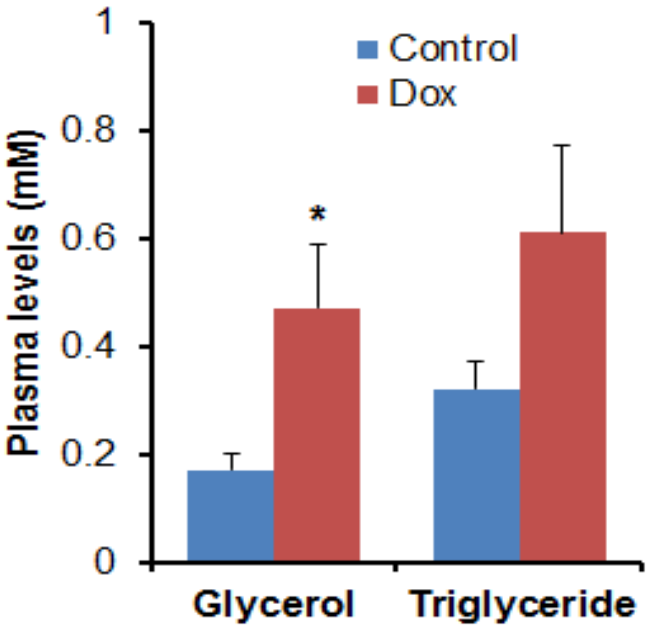

Figure 4-6. Plasma glycerol and triglyceride levels in virally-injected Ucn 3-cre mice fed with control or dox chow (n=5/group). Glycerol levels were significantly elevated in mice fed with dox chow compared to that in mice fed control chow. Triglyceride levels also showed a trend toward increase in dox chow fed mice, although the difference failed to reach statistically significant levels. *$p<0.05$.

Discussion

Ucn 3 plays a critical role in the brain in regulating energy homeostasis (Chen et al., 2010; Fekete et al., 2006; Jamieson et al., 2006; Ohata and Shibasaki, 2004; Pelleymounter et al., 2004; Telegdy et al., 2006) and, like other members of the CRF family, Ucn 3 expression in the brain is regulated by stress (Jamieson et al., 2006; Venihaki et al., 2004). Our previous studies determined that the Ucn 3 mRNA levels in the PVHap were greatly elevated in response to acute restraint stress (van-Hover and Li, 2015) and that Ucn 3 neurons in the PVHap project selectively to the median eminence and the VMH, which modulates energy balance and sympathetic outflow (Chen et al., 2011; Chen et al., 2012a; King, 2006). This raises the possibility that stress stimulates Ucn 3 cells in the PVHap, which in turn activate CRF_2-positive cells in the VMH to modulate energy homeostasis in response to stress. In order to test this hypothesis, we have developed a viral-mediated approach to pharmacogenetically enhance Ucn 3 input in selective brain areas. This approach allows us to determine the functional consequence of chronically enhanced Ucn 3 input into the VMH without repeatedly injecting Ucn 3 into the brain.

Our *in vitro* studies indicate that the viral vector expresses Ucn 3 only in cre-positive cells under dox treatment, as only media and lysate from vector- infected cells expressing cre and treated with dox were able to greatly increase cAMP production in CRF_2-expressing cells. Vector-infected cells without cre and/or not treated with dox did not activate CRF_2 and thus presumably did not produce Ucn 3. That specifically the media and not just the lysate from cre-expressing, dox treated cells was able to activate CRF_2 to stimulate cAMP production indicates that Ucn 3 was present in the media,

suggesting that the peptide is released from virally-infected cells expressing cre and treated with dox.

Our *in vivo* tests further confirmed the utility of the viral vector in animals. Ucn 3-cre-mCherry mice, which express cre and mCherry in Ucn 3-positive cells, were injected with the Ucn 3 o/e virus, which expresses GFP as well as Ucn 3 under the control of dox. GFP was only observed in mCherry neurons, indicating that the virus was selectively expressed in cre-positive cells. Furthermore, Ucn 3 immunoreactivity was more intense in both the PVHap and VMH of mice fed with dox chow compared to that in control mice, indicating that the virus increased levels of Ucn 3 immunoreactivity under dox conditions. This result is particularly interesting because not only were protein levels elevated in the cell bodies where Ucn 3 is produced, they were also elevated at terminals in the VMH. In the present study, we did not determine if release of Ucn 3 in the VMH is also enhanced in virus-injected mice fed with dox chow; elevated cytoplasmic Ucn 3 does not necessarily mean that more Ucn 3 is released from the terminals. Though elevated levels of Ucn 3 in the VMH does not mean that more Ucn 3 is being released, it indicates that Ucn 3 is at least being transported to the neuron terminals rather than being degraded in the soma.

There are several possible ways to determine Ucn 3 secretion at target brain areas. We predict that more Ucn 3 is released in the VMH under dox chow treatment, and Ucn 3 release in the VMH can potentially be measured with microdialysis. While microdialysis to measure Ucn 3 levels specifically has not been performed in mice, microdialysis has been shown to be feasible in mice (Patterson et al., 2015) and has been used to determine CRF levels in the bed nucleus of the stria terminalis of rats using a competitive enzyme

immunoassay kit (Ide et al., 2013). There are limitations to this approach, as an exquisitely sensitive immunoassay for Ucn 3 is a necessary prerequisite. Alternatively, *Fos* immunohistochemistry can be performed to measure functional activation of VMH cells. Though primarily used to measure activation of cells after acute stimulation, *Fos* has been used as a measure for chronic stimulation as well (Viau and Sawchenko, 2002). If the Ucn 3 o/e virus is causing release of more Ucn 3 from PVHap neurons, it is conceivable that there would be more *Fos*-positive cells in the VMH of mice fed with dox chow than those fed with control diet. Another method to measure functional activation of VMH neurons receiving input from Ucn 3 o/e neurons is electrophysiology. Measuring activity of CRF_2-expressing neurons treated with CRF_2 agonists has been shown to stimulate both spontaneous excitatory postsynaptic currents (Silberman and Winder, 2013) and long term potentiation (Guan et al., 2010). Activity of VMH neurons in brain slices from mice injected with the Ucn 3 o/e virus and fed a diet of dox chow or control chow could be similarly measured and may reveal higher levels of spontaneous excitatory postsynaptic currents or channel activity in mice with overexpression of Ucn 3 in the PVHap.

VMH neurons play an important role in regulating feeding and peripheral energy mobilization, as stimulation of the VMH results in suppression of appetite and enhanced lipolysis in fat tissues through increased sympathetic outflow (Nishizawa and Bray, 1978; Ruffin and Nicolaidis, 1999; Takahashi and Shimazu, 1981). Our preliminary studies indicate that Ucn 3 o/e virus-injected, dox treated mice ate less and had higher levels of plasma glycerol. Therefore, although Ucn 3 secretion at target brains areas must still be

examined, our functional study supports the notion that Ucn 3 release in the VMH in dox fed mice was indeed enhanced, leading to alterations in feeding and fat mobilization.

In the present study, virally-injected mice fed with dox showed about a 10% reduction in food intake compared to control chow. Interestingly, a wave-like pattern of food intake was observed during days 10-13 of the dox chow feeding period. It is tempting to speculate that compensatory homeostatic mechanisms were stimulated in response to reduced energy intake in an attempt to return food intake to normal levels during Ucn 3-induced food intake suppression. It has been shown that chronic infusion of an antibody neutralizing the orexigenic peptide Neuropeptide Y resulted in an increase in fasting-induced feeding above control levels (Ishii et al., 2007). In contrast, a single acute injection of the antibody decreases fasting-induced feeding, indicating that continuous suppression of Neuropeptide Y resulted in a compensatory mechanism to increase feeding (Ishii et al., 2007). A similar phenomenon could be happening with chronic overexpression of Ucn 3.

Mice with the activated Ucn 3 o/e virus also showed increased plasma levels of glycerol. Circulating glycerol has been used as an indicator for lipolytic activity. As adipose tissues are the major source of circulating glycerol, we speculate that enhanced Ucn 3 input into the VMH activates sympathetic outflow to fat tissues to enhance lipolysis (Dugan and Kennedy, 2014; Ilias et al., 2014). Interestingly, mice with CRF_2 knockdown in the VMH have decreased glycerol levels and increased adiposity (Chao et al., 2012), meshing nicely with the current results and suggesting that the Ucn 3 pathway from the PVHap to the VMH plays a critical role in regulating lipolysis in adipose tissue.

In conclusion, we have conducted a series of preliminary studies to validate an exciting new tool for studying the functional role of Ucn 3 in different brain areas. In the PVHap, Ucn 3 appears to modestly suppress feeding but plays a significant role in mobilizing fat stores. The Ucn 3 o/e virus offers a less invasive alternative approach than repeated Ucn 3 site specific injections to study the functional role of chronic elevation of Ucn 3 in specific brain areas.

5. Conclusion

Urocortin 3 (Ucn 3) is a member of the corticotropin-releasing factor (CRF) family and is a selective type 2 CRF receptor (CRF_2) ligand. Centrally-injected Ucn 3 suppresses feeding, elevates blood glucose concentration and body temperature, and stimulates the hypothalamic-pituitary-adrenal (HPA) axis (Fekete et al., 2006; Jamieson et al., 2006; Ohata and Shibasaki, 2004; Pelleymounter et al., 2004; Telegdy et al., 2006; Telegdy and Adamik, 2008). Ucn 3 mRNA levels are modulated by leptin, food deprivation, and stress (Jamieson et al., 2006; Yamagata et al., 2013). When considered together, these studies indicate that central Ucn 3 may be involved in regulating energy homeostasis and the stress response. Cell bodies of neurons expressing Ucn 3 are located in the medial amygdala, posterior part of the bed nucleus of the stria terminalis, and hypothalamus. In the hypothalamus, Ucn 3 neurons are found in the anterior parvicellular part of the paraventricular nucleus of the hypothalamus (PVHap), rostral perifornical hypothalamus (rPFH) and median preoptic nucleus (Lewis et al., 2001; Li et al., 2002). Ucn 3 fibers terminate in the ventromedial hypothalamus (VMH), lateral septum, medial amygdala, and bed nucleus of the stria terminalis (Li et al., 2002), where high levels of CRF_2 are found (Chalmers et al., 1995; Van Pett et al., 2000).

The VMH is an important area for modulating the physiological effects of Ucn 3. Injection of the peptide into the VMH results in suppression of feeding and elevation of blood glucose, but not stimulation of the HPA axis (Chen et al., 2010; Fekete et al., 2006). Mice with CRF_2 knocked down in the VMH gain more weight, mostly white fat, than control mice and eat more after overnight fasting, similar to Ucn 3 null mice (Chao et al., 2012). Moreover, mice with CRF_2 deletion in the VMH have been shown to be

resistant to stress-induced hypophagia, indicating that Ucn 3 signaling in the VMH plays a critical role in mediating energy adaptation in response to stress (Chen et al., 2012b). Ucn 3 afferent inputs to the VMH originate primarily from the PVHap, with moderate input from the medial amygdala (Chen et al., 2011). Currently, little is known about Ucn 3 neurons in the PVHap. In my thesis studies, I combined functional and anatomical approaches to characterize these neurons in great detail; three specific aims were proposed to accomplish this goal. In Aim 1, I determined if Ucn 3 neurons in the PVHap were stimulated by restraint stress and which brain areas provided stress-activated input to the PVHap. In Aim 2, I examined the phenotypic characteristics of Ucn 3 neurons in the PVH and identified their efferent targets. In Aim 3, I developed a novel method to chronically and site-specifically overexpress Ucn 3 to evaluate the functional consequence of elevated Ucn 3 output from PVHap neurons.

Results from Aim 1 showed that acute stress rapidly stimulates Ucn 3 expression in the PVHap. A retrograde tracing study identified a number of brain areas that provide stress-activated input into the PVHap area (van-Hover and Li, 2015). In the forebrain, the bed nucleus of the stria terminalis, lateral septal nucleus, the medial amygdala, and a number of nuclei in the hypothalamus including the VMH, the arcuate nucleus, the posterior nucleus, and the ventral premammillary nucleus provided stress-activated input into the PVHap. In the brainstem, stress-sensitive input originated from the periaqueductal gray, the nucleus of the solitary tract, and the ventrolateral medulla. These areas are potentially important in mediating the stress-induced activation of Ucn 3 neurons in the PVHap.

Aim 2 revealed that Ucn 3 neurons in the PVHap do not express oxytocin, CRF, or vasopressin, which are all major neuropeptides expressed in the PVH that regulate energy balance. Ucn 3 neurons in the PVHap project prominently to the VMH, an area important for feeding and sympathetic outflow. I also determined that the PVHap Ucn 3 cells project to the external zone of the median eminence (MEex), where neuropeptides are released from nerve terminals into the portal blood system to influence release of hormones from the pituitary gland. This raises the possibility that PVHap Ucn 3 cells may be involved in neuroendocrine regulation of pituitary function.

Finally, Aim 3 described a novel approach to chronically overexpress Ucn 3 in a temporally and spatially selective manner. Preliminary studies showed that chronic overexpression of Ucn 3 in the PVHap suppresses feeding and increases circulating glycerol levels.

It is noteworthy that the stress-activated input into the PVHap was so widely distributed while the Ucn 3 output from the PVHap was quite selective. Obviously, the technique used in the retrograde tracing study was not Ucn 3-specific, so the brain areas identified are possibly an overrepresentation of the actual areas that provide direct input to Ucn 3 neurons in the PVHap. Cell type-specific tracing techniques are becoming more sophisticated; there is a cre-regulated modified retrograde rabies virus that labels afferent inputs to select cell types (Osakada and Callaway, 2013). As these techniques advance, it will be of great interest to determine if the input to Ucn 3 neurons is truly as widespread as our study suggests or if it is more selective.

The present studies also solidified the existence of two separate clusters of Ucn 3 neurons in the rostral perifornical area consisting of Ucn 3 cells in the PVHap and rPFH. Though these two clusters are often lumped together, we found that they show important phenotypical differences. Acute stress elevated Ucn 3 mRNA levels only in the PVHap, while it had only a modest, non-significant effect on Ucn 3 expression in the rPFH. The Ucn 3-specific efferent tracing study confirmed our previous report that showed differential projection patterns of the PVHap and rPFH Ucn 3 cells. The previous study determined that the PVHap provided input into the VMH, while the rPFH provided Ucn 3 input into the lateral septum (Chen et al., 2011). In the Ucn 3-specific efferent tracing experiment, injections that strayed into the rPFH revealed diffuse fibers that targeted the lateral septum and circumventricular areas. However, tracer injections that were tightly confined to the PVHap only had selective projections to the VMH and MEex. Though anatomically nearby, the Ucn 3 cells in the PVHap and rPFH are differentially regulated by stress and have distinctive projection patterns.

The stress-activated input to the PVHap originated from areas that regulate learning and behavior (lateral septum, bed nucleus of the stria terminalis, amygdala) and autonomic activity (hypothalamus, brainstem). This suggests that during stress, Ucn 3 in the PVHap receives information about the nature of the stress and then initiates behavior and feeding responses by sending signals to the VMH and MEex. As explained above, Ucn 3 in the VMH is known to affect feeding and glucose regulation (Chao et al., 2012; Chen et al., 2010; Fekete et al., 2006). Therefore, stress-activated Ucn 3 neurons in the PVHap may decrease feeding and increase blood glucose levels in response to stress

through the VMH. The role of Ucn 3 in the MEex is less clear, but may be involved in modulating reproductive function in response to stress.

It is interesting that this small population of little-studied Ucn 3 cells in the PVHap project to major regulators of sympathetic outflow and the endocrine gateway yet do not rely on the actions of other peptides by co-releasing with the well known PVH neuropeptides, implying an important functional role for these neurons. However, though Ucn 3 null mice show a subtle elevation of feeding and suppression of circulating insulin levels, they show no other obvious phenotype (Chao et al., 2012; Li et al., 2007). Clearly, the functional role of Ucn 3 in the PVHap and other areas must be studied with a more sophisticated tool than full body knockouts. Rather than invasively injecting Ucn 3 repeatedly into the brain or knocking out all Ucn 3 in the brain and periphery, we have developed a viral-mediated approach that offers a novel and powerful method of studying the effects of chronically overexpressed Ucn 3.

In the present study, enhanced Ucn 3 expression in the PVHap modestly suppressed basal feeding. Mice with the cre-regulated Ucn 3 o/e virus showed a small but significant reduction in food intake when the mice were fed with dox chow as compared to the control diet. This is consistent with an earlier report in which central injection of Ucn 3 decreases food intake in animals under normal fed conditions (Ohata and Shibasaki, 2004). It remains to be determined whether enhanced Ucn 3 in the PVHap can modulate feeding in other conditions such as post-fasting refeeding and high fat diet. As PVHap Ucn 3 cells project predominantly to the VMH, the feeding suppression seen with virally-induced Ucn 3 overexpression is likely mediated by enhanced Ucn 3 signaling through CRF_2 in the VMH. These results are consistent with studies in which injection of Ucn 3

into the VMH decreases feeding (Chen et al., 2010) and knockdown of CRF_2 in the VMH increases feeding (Chao et al., 2012). Chronically overexpressing Ucn 3 may mimic the effect of chronic stress in decreasing food intake, as chronic stress decreases food intake to about 90% of original levels (Jeong et al., 2013). It is also possible that compensatory mechanisms are activated in response to overexpressed Ucn 3, masking the full effect of Ucn 3 on food intake. Thus, it would be interesting to examine the effect of acute Ucn 3 overstimulation to complement the current chronic approach through a Designer Receptors Exclusively Activated by Designer Drugs (DREADD) or optogenetic method (Atasoy et al., 2012; Wess et al., 2013). It is possible that food intake will decrease dramatically under acute Ucn 3 stimulation.

In addition to suppression of feeding, I found that mice fed with dox chow also showed increased plasma levels of glycerol compared to mice fed with control chow. Glycerol is an indicator that fat stores are being mobilized through lipolysis for energy (Chao et al., 2012; Dugan and Kennedy, 2014; Ilias et al., 2014). The elevated circulating glycerol indicates that overexpression of Ucn 3 in the PVHap leads to enhanced lipolysis in white adipose tissue. Interestingly, mice with CRF_2 knockdown in the VMH have decreased glycerol levels (Chao et al., 2012), meshing nicely with the current results and suggesting that Ucn 3 from the PVHap activates CRF_2 in the VMH to stimulate lipolysis. It has been shown that stimulation of the VMH enhances lipolysis in white adipose tissue through sympathetic outflow (Nishizawa and Bray, 1978; Ruffin and Nicolaidis, 1999; Takahashi and Shimazu, 1981), therefore, it is conceivable that a similar mechanism mediates the effect of Ucn 3 in the VMH. Anatomical tracing studies have yielded contrary observations of whether VMH neurons are part of a central neurocircuit that

connects to white adipose tissue. A study using a multi-synaptic pseudorabies viral tracer found that mouse VMH cells are connected to white adipose tissue (Stanley et al., 2010), but a similar tracing approach in siberian hamsters showed that the VMH is not involved the central neurocircuit connecting to peripheral white adipose tissue (Bamshad et al., 1998; Nguyen et al., 2014). Obviously species differences may well explain the discrepancy between the two observations, but more studies are needed to resolve this issue of how the VMH stimulates lipolysis.

While it is likely that both the decreased feeding and increased circulating glycerol seen after Ucn 3 overexpression are modulated by Ucn 3 projections to the VMH, the functional role of PVHap Ucn 3 neuron projection to the MEex remains to be determined. It is possible that the Ucn 3 projection to the MEex is involved in reproductive regulation. Gonadotropes in the anterior pituitary express CRF_2, stimulation of which has been shown to suppress gonadotropin secretion (Kageyama et al., 2003; Nemoto et al., 2010). As Ucn 3 neurons in the PVHap are stimulated by stress, Ucn 3 could act on CRF_2 on gonadotropes during stress to modulate reproductive hormone secretion from the pituitary. An interesting dichotomy with stress and reproduction exists: chronic stress is well known to inhibit luteinizing hormone secretion and consequently reproduction, but acute stress has differential effects. With estrogen priming, as during proestrus, acute restraint stress actually increases luteinizing hormone and follicle-stimulating hormone levels and enhances fertility (Rivier and Rivest, 1991). Conversely, in oviarectomized rats, restraint stress suppresses luteinizing hormone pulsatility and decreases fertility (Li et al., 2004). Studies have shown that the type 1 CRF receptor is involved in the acute stress-induced elevation of luteinizing hormone and follicle-

stimulating hormone secretion in estrogen-primed, oviarectomized rats, while CRF_2 only moderates the follicle-stimulating hormone rise (Traslaviña and Franci, 2012). CRF_2, however, is necessary for the non-estrogen-primed, restraint stress-induced luteinizing hormone inhibition (Li et al., 2005b) and therefore the exact role of each receptor in stress modulation of luteinizing hormone and follicle-stimulating hormone secretion remains to be clarified. It would be interesting to look at how chronically elevated Ucn 3 affects circulating levels of gonadotropins and compare it to models with acute elevation of Ucn 3 signaling.

There are also many studies on how maternal stress affects offspring development; impaired stress responses (Brunton and Russell, 2011), reproductive hormone levels (Pallarés et al., 2012), and cognition (Paris and Frye, 2010), and higher rates of schizophrenia (Limosin, 2014; Ratajczak et al., 2013) are all observed. It would be of great interest to determine the impact of enhanced maternal Ucn 3 signaling on the development of offspring. Elevated Ucn 3 may induce similar effects to stress without the confounding factors of stress handling.

In conclusion, I have determined that stress stimulates Ucn 3 neurons in the PVHap area and traced the neural pathways that convey stress signals to the PVHap to potentially activate Ucn 3 cells. I determined that Ucn 3 in the PVHap is a distinct population of cells that do not colocalize with major PVH neuropeptides. The anterograde anatomical tracing study showed that these Ucn 3 cells in the PVHap project to the VMH and MEex. The VMH projection may modulate feeding behavior and lipolysis in white adipose tissue, which the projection of PVHap Ucn 3 neurons to the MEex suggests that the peptide is involved in neuroendocrine regulation of pituitary

function, potentially modulating reproductive hormone secretion. I have also developed and validated a novel tool for studying the function of Ucn 3 in different brain areas. My study revealed that Ucn 3 in the PVHap is involved in suppressing feeding and mobilizing fat stores and likely plays an important role in energy homeostasis in response to stress. These studies thoroughly characterized Ucn 3 neurons in the PVHap and provide significant insight into the hypothalamic Ucn 3 neurocircuit in regulating stress-associated energy adaptation.

Allen, A.M., O'Callaghan, E.L., Chen, D., Bassi, J.K., 2009. Central Neural Regulation of Cardiovascular Function by Angiotensin: A Focus on the Rostral Ventrolateral Medulla. Neuroendocrinology. 89**,** 361-369.

Allen, A.M., 2011. Role of angiotensin in the rostral ventrolateral medulla in the development and maintenance of hypertension. Current Opinion in Pharmacology. 11**,** 117-123.

Angeles-Castellanos, M., Mendoza, J., Escobar, C., 2007. Restricted feeding schedules phase shift daily rhythms of c-Fos and protein Per1 immunoreactivity in corticolimbic regions in rats. Neuroscience. 144**,** 344-55.

Atasoy, D., Betley, J.N., Su, H.H., Sternson, S.M., 2012. Deconstruction of a neural circuit for hunger. Nature. 488**,** 172-7.

Auvinen, H.E., Romijn, J.A., Biermasz, N.R., Havekes, L.M., Smit, J.W.A., Rensen, P.C.N., Pereira, A.M., 2011. Effects of High Fat Diet on the Basal Activity of the Hypothalamus-Pituitary-Adrenal Axis in Mice: A Systematic Review. Hormone and metabolic research. 43**,** 899.

Bagnol, D., Lu, X.-Y., Kaelin, C.B., Day, H.E.W., Ollmann, M., Gantz, I., Akil, H., Barsh, G.S., Watson, S.J., 1999. Anatomy of an endogenous antagonist: Relationship between agouti-related protein and proopiomelanocortin in brain. Journal of Neuroscience. 19**,** 1-7.

Bale, T.L., Vale, W.W., 2004. CRF and CRF receptors: role in stress responsivity and other behaviors. Annual Review of Pharmacology and Toxicology. 44**,** 525-57.

Balthasar, N., Dalgaard, L.T., Lee, C.E., Yu, J., Funahashi, H., Williams, T., Ferreira, M., Tang, V., McGovern, R.A., Kenny, C.D., Christiansen, L.M., Edelstein, E., Choi, B., Boss, O., Aschkenasi, C., Zhang, C.-y., Mountjoy, K., Kishi, T., Elmquist, J.K., Lowell, B.B., 2005. Divergence of Melanocortin Pathways in the Control of Food Intake and Energy Expenditure. Cell. 123**,** 493-505.

Bamshad, M., Aoki, V.T., Adkison, M.G., Warren, W.S., Bartness, T.J., 1998. Central nervous system origins of the sympathetic nervous system outflow to white adipose tissue. Vol. 275.

Bingham, N.C., Anderson, K.K., Reuter, A.L., Stallings, N.R., Parker, K.L., 2008. Selective Loss of Leptin Receptors in the Ventromedial Hypothalamic Nucleus Results in Increased Adiposity and a Metabolic Syndrome. Endocrinology. 149**,** 2138-2148.

Bochorishvili, G., Nguyen, T., Coates, M.B., Viar, K.E., Stornetta, R.L., Guyenet, P.G., 2014. The orexinergic neurons receive synaptic input from C1 cells in rats. Journal of Comparative Neurology. 522**,** 3834-3846.

Bradbury, M.J., McBurnie, M.I., Denton, D.A., Lee, K.-F., Vale, W.W., 2000. Modulation of Urocortin-Induced Hypophagia and Weight Loss by Corticotropin-Releasing Factor Receptor 1 Deficiency in Mice. Endocrinology. 141**,** 2715-2724.

Bradley, R.M., Grabauskas, G., 1998. Neural Circuits for Taste: Excitation, Inhibition, and Synaptic Plasticity in the Rostral Gustatory Zone of the Nucleus of the Solitary Tracta. Annals of the New York Academy of Sciences. 855**,** 467-474.

Brar, B.K., Stephanou, A., Knight, R., Latchman, D.S., 2002. Activation of Protein Kinase B/Akt by Urocortin is Essential for its Ability to Protect Cardiac Cells Against Hypoxia/Reoxygenation-induced Cell Death. Journal of Molecular and Cellular Cardiology. 34**,** 483-492.

Bray, G.A., 2014. Medical treatment of obesity: The past, the present and the future. Best Practice & Research Clinical Gastroenterology. 28**,** 665-684.

Breu, J., Touma, C., Hölter, S.M., Knapman, A., Wurst, W., Deussing, J.M., 2012. Urocortin 2 modulates aspects of social behaviour in mice. Behavioural Brain Research. 233**,** 331-336.

Brunton, P.J., Russell, J.A., 2011. Neuroendocrine control of maternal stress responses and fetal programming by stress in pregnancy. Progress in Neuro-Psychopharmacology and Biological Psychiatry. 35**,** 1178-1191.

Canteras, N.S., Simerly, R.B., swanson, L.W., 1992. Projections of the ventral premammillary nucleus. Journal of Comparative Neurology. 324**,** 195-212.

Canteras, N.S., Simerly, R.B., Swanson, L.W., 1995. Organization of projections from the medial nucleus of the amygdala: a PHAL study in the rat. Journal of Comparative Neurology. 360**,** 213-45.

Cao, J., Patisaul, H.B., 2011. Sexually dimorphic expression of hypothalamic estrogen receptors alpha and beta and Kiss1 in neonatal male and female rats. J Comp Neurol. 519**,** 2954-77.

Cavalcante, J.C., Bittencourt, J.C., Elias, C.F., 2006. Female odors stimulate CART neurons in the ventral premammillary nucleus of male rats. Physiology & Behavior. 88**,** 160-166.

Cecchi, M., Khoshbouei, H., Javors, M., Morilak, D.A., 2002. Modulatory effects of norepinephrine in the lateral bed nucleus of the stria terminalis on behavioral and neuroendocrine responses to acute stress. Neuroscience. 112**,** 13-21.

Cha, S.H., Wolfgang, M., Tokutake, Y., Chohnan, S., Lane, M.D., 2008. Differential effects of central fructose and glucose on hypothalamic malonyl-CoA and food intake. Proc Natl Acad Sci U S A. 105**,** 16871-5.

Chalmers, D.T., Lovenberg, T.W., De Souza, E.B., 1995. Localization of novel corticotropin-releasing factor receptor (CRF2) mRNA expression to specific subcortical nuclei in rat brain: comparison with CRF1 receptor mRNA expression. Journal of Neuroscience. 15**,** 6340-50.

Chand, D., Lovejoy, D.A., 2011. Stress and reproduction: controversies and challenges. Gen Comp Endocrinol. 171**,** 253-7.

Chao, H., Digruccio, M., Chen, P., Li, C., 2012. Type 2 corticotropin-releasing factor receptor in the ventromedial nucleus of hypothalamus is critical in regulating feeding and lipid metabolism in white adipose tissue. Endocrinology. 153**,** 166-76.

Chen, A., Brar, B., Choi, C.S., Rousso, D., Vaughan, J., Kuperman, Y., Kim, S.N., Donaldson, C., Smith, S.M., Jamieson, P., Li, C., Nagy, T.R., Shulman, G.I., Lee, K.F., Vale, W., 2006. Urocortin 2 modulates glucose utilization and insulin sensitivity in skeletal muscle. Proc Natl Acad Sci U S A. 103**,** 16580-5.

Chen, A.M., Perrin, M.H., Digruccio, M.R., Vaughan, J.M., Brar, B.K., Arias, C.M., Lewis, K.A., Rivier, J.E., Sawchenko, P.E., Vale, W.W., 2005. A soluble mouse brain splice variant of type 2alpha corticotropin-releasing factor (CRF) receptor binds ligands and modulates their activity. Proceedings of the National Academy of Sciences USA. 102**,** 2620-5.

Chen, P., Vaughan, J., Donaldson, C., Vale, W., Li, C., 2010. Injection of Urocortin 3 into the ventromedial hypothalamus modulates feeding, blood glucose levels, and

hypothalamic POMC gene expression but not the HPA axis. American Journal of Physiology - Endocrinology and Metabolism. 298**,** E337-45.

Chen, P., Lin, D., Giesler, J., Li, C., 2011. Identification of urocortin 3 afferent projection to the ventromedial nucleus of the hypothalamus in rat brain. Journal of Comparative Neurology. 519**,** 2023-2042.

Chen, P., Hover, C.V., Lindberg, D., Li, C., 2012a. Central urocortin 3 and type 2 corticotropin-releasing factor receptor in the regulation of energy homeostasis: critical involvement of the ventromedial hypothalamus. Front Endocrinol (Lausanne). 3**,** 180.

Chen, P., Wiltgen, B.J., Li, C., 2012b. Potential role of ventromedial hypothalamic Urocortin 3 signaling in regulating fear conditioning and feeding. In Society for Neuroscience annual meeting. Vol. 281.01, ed.^eds., New Orleans.

Chen, R., Lewis, K., Perrin, M.H., Vale, W., 1993. Expression cloning of a human corticotropin-releasing-factor receptor. Proc Natl Acad Sci U S A. 90**,** 8967-71.

Ciccocioppo, R., Fedeli, A., Economidou, D., Policani, F., Weiss, F., Massi, M., 2003. The Bed Nucleus Is a Neuroanatomical Substrate for the Anorectic Effect of Corticotropin-Releasing Factor and for Its Reversal by Nociceptin/Orphanin FQ. Journal of Neuroscience. 23**,** 9445-9451.

Coolen, L.M., Wood, R.I., 1998. Bidirectional connections of the medial amygdaloid nucleus in the Syrian hamster brain: Simultaneous anterograde and retrograde tract tracing. The Journal of Comparative Neurology. 399**,** 189-209.

Correa, S., Newstrom, D., Cheung, C., Warne, J., Flandin, P., Pierce, A., Xu, A., Rubenstein, J., Ingraham, H., 2013. A Population of Nkx2-1 Neurons in the Ventromedial Hypothalamus (VMH) Mediates Sex-Specific Obesity and Sedentary Behavior in Mice. In Endocrine Review. Vol. 34, ed.^eds.

Coste, S.C., Kesterson, R.A., Heldwein, K.A., Stevens, S.L., Heard, A.D., Hollis, J.H., Murray, S.E., Hill, J.K., Pantely, G.A., Hohimer, A.R., Hatton, D.C., Phillips, T.J., Finn, D.A., Low, M.J., Rittenberg, M.B., Stenzel, P., Stenzel-Poore, M.P., 2000. Abnormal adaptations to stress and impaired cardiovascular function in mice lacking corticotropin-releasing hormone receptor-2. Nature Genetics. 24**,** 403-409.

Cullinan, W.E., Herman, J.P., Battaglia, D.F., Akil, H., Watson, S.J., 1995. Pattern and time course of immediate early gene expression in rat brain following acute stress. Neuroscience. 64**,** 477-505.

Cunningham, E.T., Sawchenko, P.E., 1988. Anatomical specificity of noradrenergic inputs to the paraventricular and supraoptic nuclei of the rat hypothalamus. The Journal of Comparative Neurology. 274**,** 60-76.

Cupples, W.A., 2003. Peptides that regulate food intake. Vol. 284.

Davis, M., Walker, D.L., Lee, Y., 1997. Roles of the Amygdala and Bed Nucleus of the Stria Terminalis in Fear and Anxiety Measured with the Acoustic Startle Reflex. Annals of the New York Academy of Sciences. 821**,** 305-331.

de Kloet, E.R., 2013. Lifetime achievement from a brain-adrenal perspective: On the CRF–urocortin–glucocorticoid balance. Journal of Chemical Neuroanatomy. 54**,** 42-49.

Dhillon, H., Zigman, J.M., Ye, C., Lee, C.E., McGovern, R.A., Tang, V., Kenny, C.D., Christiansen, L.M., White, R.D., Edelstein, E.A., Coppari, R., Balthasar, N.,

Cowley, M.A., Chua Jr, S., Elmquist, J.K., Lowell, B.B., 2006. Leptin Directly Activates SF1 Neurons in the VMH, and This Action by Leptin Is Required for Normal Body-Weight Homeostasis. Neuron. 49**,** 191-203.

Dielenberg, R.A., Hunt, G.E., McGregor, I.S., 2001. 'When a rat smells a cat': the distribution of Fos immunoreactivity in rat brain following exposure to a predatory odor. Neuroscience. 104**,** 1085-1097.

Donato, J., Elias, C.F., 2011. The ventral premammillary nucleus links leptin action and reproduction. Front Endocrinol (Lausanne). 2.

Dong, H.-W., Petrovich, G.D., Swanson, L.W., 2001. Topography of projections from amygdala to bed nuclei of the stria terminalis. Brain Research Reviews. 38**,** 192-246.

Dong, H.-W., Swanson, L.W., 2004. Organization of axonal projections from the anterolateral area of the bed nuclei of the stria terminalis. The Journal of Comparative Neurology. 468**,** 277-298.

Dugan, C.E., Kennedy, R.T., 2014. Chapter Eleven - Measurement of Lipolysis Products Secreted by 3T3-L1 Adipocytes Using Microfluidics. In Methods in Enzymology. Vol. Volume 538, A.M. Ormond, ed.^eds. Academic Press, pp. 195-209.

Eferakeya, A., Buñag, R.D., 1974. Adrenomedullary pressor responses during posterior hypothalamic stimulation. American Journal of Physiology. 227**,** 114-8.

Elmquist, J.K., Bjørbæk, C., Ahima, R.S., Flier, J.S., Saper, C.B., 1998. Distributions of leptin receptor mRNA isoforms in the rat brain. The Journal of Comparative Neurology. 395**,** 535-547.

Fekete, E.M., Inoue, K., Zhao, Y., Rivier, J.E., Vale, W.W., Szucs, A., Koob, G.F., Zorrilla, E.P., 2006. Delayed Satiety-Like Actions and Altered Feeding Microstructure by a Selective Type 2 Corticotropin-Releasing Factor Agonist in Rats: Intra-Hypothalamic Urocortin 3 Administration Reduces Food Intake by Prolonging the Post-Meal Interval. Neuropsychopharmacology. 32**,** 1052-1068.

Ferguson, A.V., Latchford, K.J., Samson, W.K., 2008. The paraventricular nucleus of the hypothalamus - a potential target for integrative treatment of autonomic dysfunction. Expert Opin Ther Targets. 12**,** 717-27.

Ferguson, J.N., Aldag, M., Insel, T.R., Young, L.J., 2001. Oxytocin in the Medial Amygdala is Essential for Social Recognition in the Mouse. Journal of Neuroscience. 21**,** 8278-8285.

Flanagan-Cato, L.M., 2011. Sex differences in the neural circuit that mediates female sexual receptivity. Front Neuroendocrinol. 32**,** 124-36.

Flegal, K.M., Carroll, M.D., Kit, B.K., Ogden, C.L., 2012. Prevalence of obesity and trends in the distribution of body mass index among US adults, 1999-2010. JAMA. 307**,** 491-7.

Flores, M.B., Fernandes, M.F., Ropelle, E.R., Faria, M.C., Ueno, M., Velloso, L.A., Saad, M.J., Carvalheira, J.B., 2006. Exercise improves insulin and leptin sensitivity in hypothalamus of Wistar rats. Diabetes. 55**,** 2554-61.

Florio, P., Vale, W., Petraglia, F., 2004. Urocortins in human reproduction. Peptides. 25**,** 1751-1757.

Gardner, J., Rothwell, N., Luheshi, G., 1998. Leptin affects food intake via CRF-receptor-mediated pathways. Nat Neurosci. 1**,** 103.

Gaykema, R.P.A., Chen, C.-C., Goehler, L.E., 2007. Organization of immune-responsive medullary projections to the bed nucleus of the stria terminalis, central amygdala, and paraventricular nucleus of the hypothalamus: Evidence for parallel viscerosensory pathways in the rat brain. Brain Research. 1130**,** 130-145.

Ghamari-Langroudi, M., Srisai, D., Cone, R.D., 2011. Multinodal regulation of the arcuate/paraventricular nucleus circuit by leptin. Proceedings of the National Academy of Sciences. 108**,** 355-360.

Goland, R.S., 1986. High Levels of Corticotropin-Releasing Hormone Immunoactivity in Maternal and Fetal Plasma during Pregnancy. The journal of clinical endocrinology and metabolism. 63**,** 1199-1203.

Gong, Y., Xu, L., Guo, F., Pang, M., Shi, Z., Gao, S., Sun, X., 2013. Effects of ghrelin on gastric distension sensitive neurons and gastric motility in the lateral septum and arcuate nucleus regulation. J Gastroenterol.

Gonzales, K.L., Quadros-Mennella, P., Tetel, M.J., Wagner, C.K., 2012. Anatomically-specific actions of oestrogen receptor in the developing female rat brain: effects of oestradiol and selective oestrogen receptor modulators on progestin receptor expression. J Neuroendocrinol. 24**,** 285-91.

Graham, C.E., Basappa, J., Vetter, D.E., 2010. A Corticotropin-releasing Factor System Expressed in the Cochlea Modulates Hearing Sensitivity and Protects Against Noise-induced Hearing Loss. Neurobiology of disease. 38**,** 246-258.

Grammatopoulos, D.K., 2000. Urocortin, but Not Corticotropin-Releasing Hormone (CRH), Activates the Mitogen-Activated Protein Kinase Signal Transduction Pathway in Human Pregnant Myometrium: An Effect Mediated via R1 and R2 CRH Receptor Subtypes and Stimulation of Gq-Proteins. Molecular endocrinology. 14**,** 2076-2091.

Griffiths, G.M., 1939. A critical review: Some aspects of the structure of the hypothalamus. Journal of Neurology and Psychiatry. 2**,** 154-164.

Guan, X., Wang, L., Chen, C.-L., Guan, Y., Li, S., 2010. Roles of two subtypes of corticotrophin-releasing factor receptor in the corticostriatal long-term potentiation under cocaine withdrawal condition. J Neurochem. 115**,** 795-803.

Guyenet, P.G., Stornetta, R.L., Bochorishvili, G., Depuy, S.D., Burke, P.G., Abbott, S.B., 2013. C1 neurons: the body's EMTs. Am J Physiol Regul Integr Comp Physiol. 305**,** R187-204.

Hashimoto, K., Nishiyama, M., Tanaka, Y., Noguchi, T., Asaba, K., Hossein, P.N., Nishioka, T., Makino, S., 2004. Urocortins and corticotropin releasing factor type 2 receptors in the hypothalamus and the cardiovascular system. Peptides. 25**,** 1711-1721.

Hatalski, C.G., Guirguis, C., Baram, T.Z., 1998. Corticotropin Releasing Factor mRNA Expression in the Hypothalamic Paraventricular Nucleus and the Central Nucleus of the Amygdala is Modulated by Repeated Acute Stress in the Immature Rat. Journal of Neuroendocrinology. 10**,** 663-669.

Herman, J., Flak, J., Jankord, R., 2008. Chronic stress plasticity in the hypothalamic paraventricular nucleus. 170**,** 353-364.

Hou, S., Duale, H., Cameron, A.A., Abshire, S.M., Lyttle, T.S., Rabchevsky, A.G., 2008. Plasticity of lumbosacral propriospinal neurons is associated with the

development of autonomic dysreflexia after thoracic spinal cord transection. The Journal of Comparative Neurology. 509**,** 382-399.

Hsu, S.Y., Hsueh, A.J., 2001. Human stresscopin and stresscopin-related peptide are selective ligands for the type 2 corticotropin-releasing hormone receptor. Nature Medicine. 7**,** 605-11.

Huang, Q., Timofeeva, E., Richard, D., 2006. Regulation of corticotropin-releasing factor and its types 1 and 2 receptors by leptin in rats subjected to treadmill running-induced stress. J Endocrinol. 191**,** 179-88.

Ide, S., Hara, T., Ohno, A., Tamano, R., Koseki, K., Naka, T., Maruyama, C., Kaneda, K., Yoshioka, M., Minami, M., 2013. Opposing roles of corticotropin-releasing factor and neuropeptide Y within the dorsolateral bed nucleus of the stria terminalis in the negative affective component of pain in rats. J Neurosci. 33**,** 5881-94.

Ilias, I., Vassiliadi, D.A., Theodorakopoulou, M., Boutati, E., Maratou, E., Mitrou, P., Nikitas, N., Apollonatou, S., Dimitriadis, G., Armaganidis, A., Dimopoulou, I., 2014. Adipose tissue lipolysis and circulating lipids in acute and subacute critical illness: Effects of shock and treatment. Journal of Critical Care. 29**,** 1130.e5-1130.e9.

Ishii, T., Muranaka, R., Tashiro, O., Nishimura, M., 2007. Chronic intracerebroventricular administration of anti-neuropeptide Y antibody stimulates starvation-induced feeding via compensatory responses in the hypothalamus. Brain Research. 1144**,** 91-100.

Jamieson, P.M., Li, C., Kukura, C., Vaughan, J., Vale, W., 2006. Urocortin 3 modulates the neuroendocrine stress response and is regulated in rat amygdala and hypothalamus by stress and glucocorticoids. Endocrinology. 147**,** 4578-88.

Jennings, J.H., Ung, R.L., Resendez, S.L., Stamatakis, A.M., Taylor, J.G., Huang, J., Veleta, K., Kantak, P.A., Aita, M., Shilling-Scrivo, K., Ramakrishnan, C., Deisseroth, K., Otte, S., Stuber, G.D., 2015. Visualizing hypothalamic network dynamics for appetitive and consummatory behaviors. Cell. 160**,** 516-27.

Jeong, J.Y., Lee, D.H., Kang, S.S., 2013. Effects of Chronic Restraint Stress on Body Weight, Food Intake, and Hypothalamic Gene Expressions in Mice. Endocrinology and Metabolism. 28**,** 288-296.

Kageyama, K., Li, C., Vale, W.W., 2003. Corticotropin-releasing factor receptor type 2 messenger ribonucleic acid in rat pituitary: localization and regulation by immune challenge, restraint stress, and glucocorticoids. Endocrinology. 144**,** 1524-32.

Kanno, T., 1999. Corticotropin-Releasing Factor Modulation of [Ca.sup.2] Influx in Rat Pancreatic [Beta]-Cells. Diabetes (New York, N.Y.). 48**,** 1741.

Katsurada, K., Maejima, Y., Nakata, M., Kodaira, M., Suyama, S., Iwasaki, Y., Kario, K., Yada, T., 2014. Endogenous GLP-1 acts on paraventricular nucleus to suppress feeding: Projection from nucleus tractus solitarius and activation of corticotropin-releasing hormone, nesfatin-1 and oxytocin neurons. Biochemical and Biophysical Research Communications. 451**,** 276-281.

Keller, A., Litzelman, K., Wisk, L.E., Maddox, T., Cheng, E.R., Creswell, P.D., Witt, W.P., 2012. Does the Perception that Stress Affects Health Matter? The Association with Health and Mortality. Health psychology : official journal of the

Division of Health Psychology, American Psychological Association. 31**,** 677-684.

Keshavarzi, S., Sullivan, R.K., Ianno, D.J., Sah, P., 2014. Functional properties and projections of neurons in the medial amygdala. J Neurosci. 34**,** 8699-715.

Khoshbouei, H., Cecchi, M., Morilak, D.A., 2002. Modulatory Effects of Galanin in the Lateral Bed Nucleus of the Stria Terminalis on Behavioral and Neuroendocrine Responses to Acute Stress. Neuropsychopharmacology. 27**,** 25-34.

Kiang, J.G., 1997. Corticotropin-releasing factor-like peptides increase cytosolic [Ca2+] in human epidermoid A-431 cells. European Journal of Pharmacology. 329**,** 237-244.

Kincheski, G.C., Mota-Ortiz, S.R., Pavesi, E., Canteras, N.S., Carobrez, A.P., 2012. The Dorsolateral Periaqueductal Gray and Its Role in Mediating Fear Learning to Life Threatening Events. PLoS One. 7**,** e50361.

King, B.M., 2006. The rise, fall, and resurrection of the ventromedial hypothalamus in the regulation of feeding behavior and body weight. Physiol Behav. 87**,** 221-44.

Kishi, T., Aschkenasi, C.J., Lee, C.E., Mountjoy, K.G., Saper, C.B., Elmquist, J.K., 2003. Expression of melanocortin 4 receptor mRNA in the central nervous system of the rat. The Journal of Comparative Neurology. 457**,** 213-235.

Klockener, T., Hess, S., Belgardt, B.F., Paeger, L., Verhagen, L.A., Husch, A., Sohn, J.W., Hampel, B., Dhillon, H., Zigman, J.M., Lowell, B.B., Williams, K.W., Elmquist, J.K., Horvath, T.L., Kloppenburg, P., Bruning, J.C., 2011. High-fat feeding promotes obesity via insulin receptor/PI3K-dependent inhibition of SF-1 VMH neurons. Nature Neuroscience. 14**,** 911-8.

Kocho-Schellenberg, M., Lezak, K.R., Harris, O.M., Roelke, E., Gick, N., Choi, I., Edwards, S., Wasserman, E., Toufexis, D.J., Braas, K.M., May, V., Hammack, S.E., 2014. Pituitary Adenylate Cyclase Activating Peptide (PACAP) in the Bed Nucleus of the Stria Terminalis (BNST) Produces Anorexia and Weight Loss in Male and Female Rats. Neuropsychopharmacology.

Koob, G.F., Heinrichs, S.C., 1999. A role for corticotropin releasing factor and urocortin in behavioral responses to stressors. Brain Research. 848**,** 141-152.

Koppell, S., Sodetz, F., 1972. Septal ablation in the rat and bar pressing under appetitive and aversive control. J Comp Physiol Psychol. 81**,** 274-80.

Kostich, W.A., Chen, A., Sperle, K., Largent, B.L., 1998. Molecular Identification and Analysis of a Novel Human Corticotropin-Releasing Factor (CRF) Receptor: The CRF2γ Receptor. Molecular endocrinology. 12**,** 1077-1085.

Kovacs, K.J., Miklos, I.H., Bali, B., 2004. GABAergic Mechanisms Constraining the Activity of the Hypothalamo-Pituitary-Adrenocortical Axis. Annals of the New York Academy of Sciences. 1018**,** 466-476.

Kuperman, Y., Chen, A., 2008. Urocortins: emerging metabolic and energy homeostasis perspectives. Trends in Endocrinology & Metabolism. 19**,** 122-129.

Kuperman, Y., Issler, O., Regev, L., Musseri, I., Navon, I., Neufeld-Cohen, A., Gil, S., Chen, A., 2010. Perifornical Urocortin-3 mediates the link between stress-induced anxiety and energy homeostasis. Proc Natl Acad Sci U S A. 107**,** 8393-8.

Langhans, W., Delprete, E., Scharrer, E., 1991. Mechanisms of vasopressin's anorectic effect. Physiology & Behavior. 49**,** 169-176.

Latchman, D.S., 2002. Urocortin. The International Journal of Biochemistry & Cell Biology. 34**,** 907-910.

Lau, B.K., Vaughan, C.W., 2014. Descending modulation of pain: the GABA disinhibition hypothesis of analgesia. Current Opinion in Neurobiology. 29**,** 159-164.

Lehman, M.N., Winans, S.S., Powers, J.B., 1980. Medial Nucleus of the Amygdala Mediates Chemosensory Control of Male Hamster Sexual Behavior. Science. 210**,** 557-560.

Lewis, K., Li, C., Perrin, M.H., Blount, A., Kunitake, K., Donaldson, C., Vaughan, J., Reyes, T.M., Gulyas, J., Fischer, W., Bilezikjian, L., Rivier, J., Sawchenko, P.E., Vale, W.W., 2001. Identification of urocortin III, an additional member of the corticotropin-releasing factor (CRF) family with high affinity for the CRF2 receptor. Proceedings of the National Academy of Sciences USA. 98**,** 7570-5.

Li, C.-S., Cho, Y.K., 2006. Efferent projection from the bed nucleus of the stria terminalis suppresses activity of taste-responsive neurons in the hamster parabrachial nuclei. Am J Physiol Regul Integr Comp Physiol. 291**,** R914-R926.

Li, C., Chen, P., Smith, M.S., 1999a. Neuropeptide Y and Tuberoinfundibular Dopamine Activities Are Altered during Lactation: Role of Prolactin. Endocrinology. 140**,** 118-123.

Li, C., Chen, P., Smith, M.S., 1999b. Identification of neuronal input to the arcuate nucleus (ARH) activated during lactation: implications in the activation of neuropeptide Y neurons. Brain Research. 824**,** 267-276.

Li, C., Chen, P., Smith, M.S., 2000. Corticotropin releasing hormone neurons in the paraventricular nucleus are direct targets for neuropeptide Y neurons in the arcuate nucleus: an anterograde tracing study. Brain Research. 854**,** 122-129.

Li, C., Vaughan, J., Sawchenko, P.E., Vale, W.W., 2002. Urocortin III-Immunoreactive Projections in Rat Brain: Partial Overlap with Sites of Type 2 Corticotrophin-Releasing Factor Receptor Expression. Journal of Neuroscience. 22**,** 991-1001.

Li, C., Chen, P., Vaughan, J., Lee, K.F., Vale, W., 2007. Urocortin 3 regulates glucose-stimulated insulin secretion and energy homeostasis. Proceedings of the National Academy of Sciences USA. 104**,** 4206-11.

Li, X.F., Edward, J., Mitchell, J.C., Shao, B., Bowes, J.E., Coen, C.W., Lightman, S.L., O'Byrne, K.T., 2004. Differential Effects of Repeated Restraint Stress on Pulsatile Lutenizing Hormone Secretion in Female Fischer, Lewis and Wistar Rats. Journal of Neuroendocrinology. 16**,** 620-627.

Li, X.F., Bowe, J.E., Lightman, S.L., O'Byrn, K.T., 2005a. Role of Corticotropin-Releasing Factor Receptor-2 in Stress-Induced Suppression of Pulsatile Luteinizing Hormone Secretion in the Rat. Endocrinology. 146**,** 318-322.

Li, X.F., Bowe, J.E., Lightman, S.L., O'Byrne, K.T., 2005b. Role of Corticotropin-Releasing Factor Receptor-2 in Stress-Induced Suppression of Pulsatile Luteinizing Hormone Secretion in the Rat. Endocrinology. 146**,** 318-322.

Limosin, F., 2014. Neurodevelopmental and environmental hypotheses of negative symptoms of schizophrenia. BMC Psychiatry. 14**,** 88-88.

Lin, D., Boyle, M.P., Dollar, P., Lee, H., Lein, E.S., Perona, P., Anderson, D.J., 2011a. Functional identification of an aggression locus in the mouse hypothalamus. Nature. 470**,** 221-6.

Lin, Y., Hall, R.A., Kuhar, M.J., 2011b. CART Peptide Stimulation of G Protein-Mediated Signaling in Differentiated PC12 Cells: Identification of PACAP 6-38 as a CART Receptor Antagonist. Neuropeptides. 45**,** 351-358.

Lindberg, D., Chen, P., Li, C., 2013. Conditional viral tracing reveals that steroidogenic factor 1-positive neurons of the dorsomedial subdivision of the ventromedial hypothalamus project to autonomic centers of the hypothalamus and hindbrain. J Comp Neurol. 521**,** 3167-90.

Lovenberg, T.W., Liaw, C.W., Grigoriadis, D.E., Clevenger, W., Chalmers, D.T., De Souza, E.B., Oltersdorf, T., 1995. Cloning and characterization of a functionally distinct corticotropin-releasing factor receptor subtype from rat brain. Proc Natl Acad Sci U S A. 92**,** 836-840.

Lucas, M., Chen, A., Richter-Levin, G., 2013. Hypothalamic Corticotropin-Releasing Factor is Centrally Involved in Learning Under Moderate Stress. Neuropsychopharmacology. 38**,** 1825-1832.

Magoul, R., Ciofi, P., Tramu, G., 1994. Visualization of an efferent projection route of the hypothalamic rat arcuate nucleus through the stria terminalis after labeling with carbocyanine dye (DiI) or proopiomelanocortin-immunohistochemistry. Neuroscience Letters. 172**,** 134-138.

Makino, S., Nishiyama, M., Asaba, K., Gold, P., Hashimoto, K., 1998. Altered expression of type 2 CRH receptor mRNA in the VMH by glucocorticoids and starvation. American Journal of Physiology. 275**,** 1138-45.

Maniscalco, J.W., Kreisler, A.D., Rinaman, L., 2013. Satiation and stress-induced hypophagia: examining the role of hindbrain neurons expressing prolactin-releasing peptide (PrRP) or glucagon-like peptide 1 (GLP-1). Front Neurosci. 6.

Martin, J.R., Beinfeld, M.C., Westfall, T.C., 1988. Blood pressure increases after injection of neuropeptide Y into posterior hypothalamic nucleus. Vol. 254.

Martinez de Morentin, P.B., Gonzalez-Garcia, I., Martins, L., Lage, R., Fernandez-Mallo, D., Martinez-Sanchez, N., Ruiz-Pino, F., Liu, J., Morgan, D.A., Pinilla, L., Gallego, R., Saha, A.K., Kalsbeek, A., Fliers, E., Bisschop, P.H., Dieguez, C., Nogueiras, R., Rahmouni, K., Tena-Sempere, M., Lopez, M., 2014. Estradiol regulates brown adipose tissue thermogenesis via hypothalamic AMPK. Cell Metab. 20**,** 41-53.

Martinez, R.C., Carvalho-Netto, E.F., Ribeiro-Barbosa, É.R., Baldo, M.V.C., Canteras, N.S., 2011. Amygdalar roles during exposure to a live predator and to a predator-associated context. Neuroscience. 172**,** 314-328.

McGregor, I.S., Callaghan, P.D., Hunt, G.E., 2008. From ultrasocial to antisocial: a role for oxytocin in the acute reinforcing effects and long-term adverse consequences of drug use? Br J Pharmacol. 154**,** 358-368.

Millington, G.W., 2007. The role of proopiomelanocortin (POMC) neurones in feeding behaviour. Nutr Metab (Lond). 4**,** 18.

Mitra, A., Lenglos, C., Martin, J., Mbende, N., Gagne, A., Timofeeva, E., 2011. Sucrose modifies c-fos mRNA expression in the brain of rats maintained on feeding schedules. Neuroscience. 192**,** 459-74.

Motta, S.C., Guimarães, C.C., Furigo, I.C., Sukikara, M.H., Baldo, M.V.C., Lonstein, J.S., Canteras, N.S., 2013. Ventral premammillary nucleus as a critical sensory

relay to the maternal aggression network. Proceedings of the National Academy of Sciences. 110**,** 14438-14443.

Nemoto, T., Iwasaki-Sekino, A., Yamauchi, N., Shibasaki, T., 2010. Role of urocortin 2 secreted by the pituitary in the stress-induced suppression of luteinizing hormone secretion in rats. Vol. 299.

Neumann, I.D., Landgraf, R., 2012. Balance of brain oxytocin and vasopressin: implications for anxiety, depression, and social behaviors. Trends Neurosci. 35**,** 649-59.

Nguyen, N., Randall, J., Banfield, B., Bartness, T., 2014. Central sympathetic innervations to visceral and subcutaneous white adipose tissue. Am J Physiol Regul Integr Comp Physiol. 306**,** R375-86.

NIMH, 2015. Adult Stress Factsheet. Vol., ed.^eds., http://www.nimh.nih.gov/health/publications/stress/index.shtml.

Nishiyama, M., Makion, S., Asaba, K., Hasimoto, K., 1999. Leptin Effects on the Expression of Type-2 CRH Receptor mRNA in the Ventromedial Hypothalamus in the Rat. Journal of Neuroendocrinology. 11**,** 307-314.

Nishizawa, Y., Bray, G.A., 1978. Ventromedial Hypothalamic Lesions and the Mobilization of Fatty Acids. Journal of Clinical Investigation. 61**,** 714-721.

Ohata, H., Shibasaki, T., 2004. Effects of urocortin 2 and 3 on motor activity and food intake in rats. Peptides. 25**,** 1703-1709.

Ohata, H., Shibasaki, T., 2011. Involvement of CRF2 receptor in the brain regions in restraint-induced anorexia. Neuroreport. 22**,** 494-8.

Olshansky, S.J., Passaro, D.J., Hershow, R.C., Layden, J., Carnes, B.A., Brody, J., Hayflick, L., Butler, R.N., Allison, D.B., Ludwig, D.S., 2005. A Potential Decline in Life Expectancy in the United States in the 21st Century. New England Journal of Medicine. 352**,** 1138-1145.

Osakada, F., Callaway, E.M., 2013. Design and generation of recombinant rabies virus vectors. Nature protocols. 8**,** 1583-1601.

Padula, W.V., Allen, R.R., Nair, K.V., 2014. Determining the cost of obesity and its common comorbidities from a commercial claims database. Clinical Obesity. 4**,** 53-58.

Pallarés, M.E., Adrover, E., Baier, C.J., Bourguignon, N.S., Monteleone, M.C., Brocco, M.A., González-Calvar, S.I., Antonelli, M.C., 2012. Prenatal maternal restraint stress exposure alters the reproductive hormone profile and testis development of the rat male offspring. Stress. 16**,** 429-440.

Pan, W., Kastin, A.J., 2008. Urocortin and the Brain. Progress in neurobiology. 84**,** 148-156.

Paris, J.J., Frye, C.A., 2010. Juvenile offspring of rats exposed to restraint stress in late gestation have impaired cognitive performance and dysregulated progestogen formation. Stress. 14**,** 23-32.

Patterson, C.M., Wong, J.-M.T., Leinninger, G.M., Allison, M.B., Mabrouk, O.S., Kasper, C.L., Gonzalez, I.E., Mackenzie, A., Jones, J.C., Kennedy, R.T., Jr, M.G.M., 2015. Ventral tegmental area neurotensin signaling links the lateral hypothalamus to locomotor activity and striatal dopamine efflux in male mice. Endocrinology.

Peelman, F., Zabeau, L., Moharana, K., Savvides, S.N., Tavernier, J., 2014. 20 years of leptin: insights into signaling assemblies of the leptin receptor. J Endocrinol. 223**,** T9-23.

Pelleymounter, M., Joppa, M., Carmouche, M., Cullen, M., Brown, B., Murphy, B., Grigoriadis, D., Ling, N., Foster, A., 2000. Role of corticotropin-releasing factor (CRF) receptors in the anorexic syndrome induced by CRF. Journal of Pharmacology and Experimental Therapeutics. 293**,** 799-806.

Pelleymounter, M.A., Joppa, M., Ling, N., Foster, A.C., 2004. Behavioral and neuroendocrine effects of the selective CRF2 receptor agonists urocortin II and urocortin III. Peptides. 25**,** 659-666.

Pelosi, G.G., Tavares, R.F., Busnardo, C., Corrêa, F.M.A., 2009. Paraventricular nucleus mediates pressor response to noradrenaline injection into the dorsal periaqueductal gray area. Autonomic Neuroscience. 151**,** 74-81.

Perrin, M.H., Vale, W.W., 1999. Corticotropin releasing factor receptors and their ligand family. Annals of the New York Academy of Sciences. 885**,** 312-328.

Pilowsky, P.M., Abbott, S.B., Burke, P.G.R., Farnham, M.M.J., Hildreth, C.M., Kumar, N.N., Li, Q., Lonergan, T., McMullan, S., Spirovski, D., Goodchild, A.K., 2008. Metabotropic neurotransmission and integration of sympathetic nerve activity by the rostral ventrolateral medulla in the rat. Clinical and Experimental Pharmacology and Physiology. 35**,** 508-511.

Ratajczak, P., Wozniak, A., Nowakowska, E., 2013. Animal models of schizophrenia: Developmental preparation in rats. Acta Neurobiol Exp. 73**,** 472-484.

Reyes, B.A.S., Valentino, R.J., Xu, G., Van Bockstaele, E.J., 2005. Hypothalamic projections to locus coeruleus neurons in rat brain. European Journal of Neuroscience. 22**,** 93-106.

Reyes, T.M., Lewis, K., Perrin, M.H., Kunitake, K.S., Vaughan, J., Arias, C.A., Hogenesch, J.B., Gulyas, J., Rivier, J., Vale, W.W., Sawchenko, P.E., 2001. Urocortin II: a member of the corticotropin-releasing factor (CRF) neuropeptide family that is selectively bound by type 2 CRF receptors. Proc Natl Acad Sci U S A. 98**,** 2843-8.

Rinaman, L., Hoffman, G.E., Dohanics, J., Le, W.W., Stricker, E.M., Verbalis, J.G., 1995. Cholecystokinin activates catecholaminergic neurons in the caudal medulla that innervate the paraventricular nucleus of the hypothalamus in rats. The Journal of Comparative Neurology. 360**,** 246-256.

Rinaman, L., 2010. Ascending projections from the caudal visceral nucleus of the solitary tract to brain regions involved in food intake and energy expenditure. Brain Research. 1350**,** 18-34.

Risold, P.Y., Swanson, L.W., 1997. Connections of the rat lateral septal complex. Brain Research Reviews. 24**,** 115-195.

Rivier, C., Rivest, S., 1991. Effect of stress on the activity of the hypothalamic-pituitary-gonadal axis: peripheral and central mechanisms. Biology of Reproduction. 45**,** 523-532.

Rodaros, D., Caruana, D.A., Amir, S., Stewart, J., 2007. Corticotropin-releasing factor projections from limbic forebrain and paraventricular nucleus of the hypothalamus to the region of the ventral tegmental area. Neuroscience. 150**,** 8-13.

Rodriguez, E.M., Blazquez, J.L., Guerra, M., 2010. The design of barriers in the hypothalamus allows the median eminence and the arcuate nucleus to enjoy private milieus: the former opens to the portal blood and the latter to the cerebrospinal fluid. Peptides. 31**,** 757-76.

Rollins, B.L., King, B.M., 2000. Amydala-lesion obesity: What is the role of the various amydaloid nuclei. Am J Physiol Regul Integr Comp Physiol. 279**,** R1348-R1356.

Roman, C.W., Lezak, K.R., Kocho-Schellenberg, M., Garret, M.A., Braas, K., May, V., Hammack, S.E., 2012. Excitotoxic lesions of the bed nucleus of the stria terminalis (BNST) attenuate the effects of repeated stress on weight gain: evidence for the recruitment of BNST activity by repeated, but not acute, stress. Behav Brain Res. 227**,** 300-4.

Ruffin, M.-P., Nicolaidis, S., 1999. Electrical stimulation of the ventromedial hypothalamus enhances both fat utilization and metabolic rate that precede and parallel the inhibition of feeding behavior. Brain Research. 846**,** 23-29.

Ryabinin, A.E., Tsoory, M.M., Kozicz, T., Thiele, T.E., Neufeld-Cohen, A., Chen, A., Lowery-Gionta, E.G., Giardino, W.J., Kaur, S., 2012. Urocortins: CRF's siblings and their potential role in anxiety, depression and alcohol drinking behavior. Alcohol. 46**,** 349-357.

Saito, Y., Maruyama, K., 2006. Identification of melanin-concentrating hormone receptor and its impact on drug discovery. Journal of Experimental Zoology Part A: Comparative Experimental Biology. 305A**,** 761-768.

Sarnyai, Z., Kovács, G.L., 2014. Oxytocin in learning and addiction: From early discoveries to the present. Pharmacology Biochemistry and Behavior. 119**,** 3-9.

Sasaki, T., Kitamura, T., 2010. Roles of FoxO1 and Sirt1 in the central regulation of food intake. Endocrine Journal. 57**,** 939-46.

Scallet, A.C., Olney, J.W., 1986. Components of hypothalamic obesity: bipiperidyl-mustard lesions add hyperphagia to monosodium glutamate-induced hyperinsulinemia. Brain Research. 374**,** 380-384.

Schenberg, L.C., Schimitel, F.G., Armini, R.d.S., Bernabé, C.S., Rosa, C.A., Tufik, S., Müller, C.J.T., Quintino-dos-Santos, J.W., 2014. Translational approach to studying panic disorder in rats: Hits and misses. Neuroscience & Biobehavioral Reviews.

Schnutgen, F., Doerflinger, N., Calleja, C., Wendling, O., Chambon, P., Ghyselinck, N.B., 2003. A directional strategy for monitoring Cre-mediated recombination at the cellular level in the mouse. Nat Biotech. 21**,** 562-565.

Schnütgen, F., Ghyselinck, N., 2007. Adopting the good reFLEXes when generating conditional alterations in the mouse genome. Transgenic Research. 16**,** 405-413.

Schulz, C., Paulus, K., Lobmann, R., Dallman, M., Lehnert, H., 2010. Endogenous ACTH, not only α-melanocyte-stimulating hormone, reduces food intake mediated by hypothalamic mechanisms. Vol. 298.

Schwartz, M.W., Woods, S.C., Porte Jr, D., Seeley, R.J., Baskin, D.G., 2000. Central nervous system control of food intake. Nature. 404**,** 661-671.

Scopinho, A.A., Resstel, L.B., Correa, F.M., 2008. alpha(1)-Adrenoceptors in the lateral septal area modulate food intake behaviour in rats. Br J Pharmacol. 155**,** 752-6.

Selye, H., 1936. A syndrome produced by diverse nocuous agents. Nature. 138**,** 32.

Selye, H., 1950. Stress and the General Adaptation Syndrome. British Medical Journal. 1**,** 1383-1392.

Selye, H., 1976. Forty years of stress research: principal remaining problems and misconceptions. Canadian Medical Association Journal. 115**,** 53-56.

Shiuchi, T., Haque, M.S., Okamoto, S., Inoue, T., Kageyama, H., Lee, S., Toda, C., Suzuki, A., Bachman, E.S., Kim, Y.B., Sakurai, T., Yanagisawa, M., Shioda, S., Imoto, K., Minokoshi, Y., 2009. Hypothalamic orexin stimulates feeding-associated glucose utilization in skeletal muscle via sympathetic nervous system. Cell Metabolism. 10**,** 466-80.

Silberman, Y., Winder, D.G., 2013. Corticotropin releasing factor and catecholamines enhance glutamatergic neurotransmission in the lateral subdivision of the central amygdala. Neuropharmacology. 70**,** 316-323.

Silverman, A.J., Hoffman, D.L., Zimmerman, E.A., 1981. The descending afferent connections of the paraventricular nucleus of the hypothalamus (PVN). Brain Research Bulletin. 6**,** 47-61.

Simerly, R.B., Chang, C., Muramatsu, M., Swanson, L.W., 1990. Distribution of androgen and estrogen receptor mRNA-containing cells in the rat brain: An in situ hybridization study. Journal of Comparative Neurology. 294**,** 76-95.

Sobrino Crespo, C., Perianes Cachero, A., Puebla Jimenez, L., Barrios, V., Arilla Ferreiro, E., 2014. Peptides and food intake. Front Endocrinol (Lausanne). 5**,** 58.

Spina, M., Merlo-pich, E., Basso, A.M., Rivier, J., Vale, W., Koob, G.F., 1996. Appetite-Suppressing Effects of Urocortin, a CRF-Related Neuropeptide. Science. 273**,** 1561-1564.

Stanley, S., Pinto, S., Segal, J., Perez, C.A., Viale, A., DeFalco, J., Cai, X., Heisler, L.K., Friedman, J.M., 2010. Identification of neuronal subpopulations that project from hypothalamus to both liver and adipose tissue polysynaptically. Proc Natl Acad Sci U S A. 107**,** 7024-9.

Stengel, A., Tache, Y., 2009. Neuroendocrine control of the gut during stress: corticotropin-releasing factor signaling pathways in the spotlight. Annu Rev Physiol. 71**,** 219-39.

Stengel, A., Taché, Y., 2014. CRF and urocortin peptides as modulators of energy balance and feeding behavior during stress. Front Neurosci. 8**,** 52.

Swanson, L.W., Sawchenko, P.E., Rivier, J., Vale, W., 1983. Organization of ovine corticotropin-releasing factor immunoreactive cells and fibers in the rat brain: an immunohistochemical study. Neuroendocrinology. 36**,** 165-86.

Szabo, S., Tache, Y., Somogyi, A., 2012. The legacy of Hans Selye and the origins of stress research: A retrospective 75 years after his landmark brief “Letter” to the Editor of Nature. Stress. 15**,** 472-478.

Tabarin, A., Diz-Chaves, Y., Consoli, D., Monsaingeon, M., Bale, T.L., Culler, M.D., Datta, R., Drago, F., Vale, W.W., Koob, G.F., Zorrilla, E.P., Contarino, A., 2007. Role of the corticotropin-releasing factor receptor type 2 in the control of food intake in mice: a meal pattern analysis. Eur J Neurosci. 26**,** 2303-14.

Taché, Y., Brunnhuber, S., 2008. From Hans Selye's Discovery of Biological Stress to the Identification of Corticotropin- Releasing Factor Signaling Pathways. Annals of the New York Academy of Sciences. 1148**,** 29-41.

Takahashi, A., Shimazu, T., 1981. Hypothalamic regulation of lipid metabolism in the rat: Effect of hypothalamic stimulation on lipolysis. Journal of the Autonomic Nervous System. 4**,** 195-206.

Telegdy, G., Adamik, A., Tóth, G., 2006. The action of urocortins on body temperature in rats. Peptides. 27**,** 2289-2294.

Telegdy, G., Adamik, A., 2008. Involvement of CRH receptors in urocortin-induced hyperthermia. Peptides. 29**,** 1937-42.

Traslaviña, G.A.A., Franci, C.R., 2012. Divergent Roles of the CRH Receptors in the Control of Gonadotropin Secretion Induced by Acute Restraint Stress at Proestrus. Endocrinology. 153**,** 4838-4848.

Vale, W.W., Spiess, J., Rivier, C., Rivier, J., 1981. Characterization of a 41-Residue Ovine Hypothalamic Peptide that Stimulates Secretion of Corticotropin and β-endorphin. Science. 213**,** 1394-1397.

van-Hover, C., Li, C., 2015. Stress-activated afferent inputs into the anterior parvicellular part of the paraventricular nucleus of the hypothalamus: Insights into urocortin 3 neuron activation. Brain Research.

Van Pett, K., Viau, V., Bittencourt, J.C., Chan, R.K.W., Li, H.-Y., Arias, C., Prins, G.S., Perrin, M., Vale, W., Sawchenko, P.E., 2000. Distribution of mRNAs encoding CRF receptors in brain and pituitary of rat and mouse. Journal of Comparative Neurology. 428**,** 191-212.

Vaughan, J.M., Donaldson, C., Bittencourt, J., Perrin, M.H., Lewis, K., Sutton, S., Chan, R., Turnbull, A., Lovejoy, D., Rivier, C., Rivier, J., Sawchenko, P.E., Vale, W., 1995. Urocortin, a mammalian neuropeptide related to fish urotensin I and to corticotropin-releasing factor. Nature. 378**,** 287–292.

Venihaki, M., Sakihara, S., Subramanian, S., Dikkes, P., Weninger, S.C., Liapakis, G., Graf, T., Majzoub, J.A., 2004. Urocortin III, A Brain Neuropeptide of the Corticotropin-Releasing Hormone Family: Modulation by Stress and Attenuation of Some Anxiety-Like Behaviours. Journal of Neuroendocrinology. 16**,** 411-422.

Verberne, A.J., Sabetghadam, A., Korim, W.S., 2014. Neural pathways that control the glucose counterregulatory response. Front Neurosci. 8**,** 38.

Vetter, D.E., Li, C., Zhao, L., Contarino, A., Liberman, M.C., Smith, G.W., Marchuk, Y., Koob, G.F., Heinemann, S.F., Vale, W., Lee, K.F., 2002. Urocortin-deficient mice show hearing impairment and increased anxiety-like behavior. Nat Genet. 31**,** 363-9.

Viau, V., Sawchenko, P.E., 2002. Hypophysiotropic neurons of the paraventricular nucleus respond in spatially, temporally, and phenotypically differentiated manners to acute vs. repeated restraint stress: Rapid publication. The Journal of Comparative Neurology. 445**,** 293-307.

Wang, C., Kotz, C.M., 2002. Urocortin in the lateral septal area modulates feeding induced by orexin A in the lateral hypothalamus. Am J Physiol Regul Integr Comp Physiol. 283**,** R358-67.

Wess, J., Nakajima, K., Jain, S., 2013. Novel designer receptors to probe GPCR signaling and physiology. Trends Pharmacol Sci. 34**,** 385-92.

Wittmann, G., Füzesi, T., Liposits, Z., Lechan, R.M., Fekete, C., 2009a. Distribution and axonal projections of neurons coexpressing thyrotropin-releasing hormone and urocortin 3 in the rat brain. The Journal of Comparative Neurology. 517**,** 825-840.

Wittmann, G., Fuzesi, T., Singru, P.S., Liposits, Z., Lechan, R.M., Fekete, C., 2009b. Efferent projections of thyrotropin-releasing hormone-synthesizing neurons residing in the anterior parvocellular subdivision of the hypothalamic paraventricular nucleus. The Journal of Comparative Neurology. 515**,** 313-30.

Woulfe, J.M., Flumerfelt, B.A., Hrycyshyn, A.W., 1990. Efferent connections of the A1 noradrenergic cell group: A DBH immunohistochemical and PHA-L anterograde tracing study. Experimental Neurology. 109**,** 308-322.

Xi, D., Gandhi, N., Lai, M., Kublaoui, B.M., 2012. Ablation of Sim1 neurons causes obesity through hyperphagia and reduced energy expenditure. PLoS One. 7**,** e36453.

Yamagata, S., Kageyama, K., Akimoto, K., Watanuki, Y., Suda, T., Daimon, M., 2013. Regulation of corticotropin-releasing factor and urocortin 2/3 mRNA by leptin in hypothalamic N39 cells. Peptides. 50**,** 1-7.

Yang, L.-Z., Tovote, P., Rayner, M., Kockskämper, J., Pieske, B., Spiess, J., 2010. Corticotropin-releasing factor receptors and urocortins, links between the brain and the heart. European Journal of Pharmacology. 632**,** 1-6.

Yin, W., Gore, A.C., 2010. The hypothalamic median eminence and its role in reproductive aging. Ann N Y Acad Sci. 1204**,** 113-22.

Young, C.K., Whishaw, I.Q., Bland, B.H., 2011. Posterior hypothalamic nucleus deep brain stimulation restores locomotion in rats with haloperidol-induced akinesia but not skilled forelimb use in pellet reaching and lever pressing. Neuroscience. 192**,** 452-458.

Zhang, W., Mifflin, S., 2010. Plasticity of GABAergic mechanisms within the nucleus of the solitary tract in hypertension. Hypertension. 55**,** 201-6.

Zigman, J.M., 2003. Minireview: From Anorexia to Obesity--The Yin and Yang of Body Weight Control. Endocrinology. 144**,** 3749-3756.

Zoccal, D.B., Furuya, W.I., Bassi, M., Colombari, D.S.A., Colombari, E., 2014. The Nucleus of the Solitary Tract and the coordination of respiratory and sympathetic activities. Frontiers in Physiology. 5.